2018

WHY DOES DROUGHT KILL TREES? INTERACTIONS BETWEEN WATER, CARBON, AND FUNGAL SYMBIONTS

Gerard Sapes de Moreta
University of Montana, Missoula

WHY DOES DROUGHT KILL TREES?

INTERACTIONS BETWEEN WATER, CARBON, AND FUNGAL SYMBIONTS

By

GERARD SAPES DE MORETA

B.S., Universitat Autònoma de Barcelona, Cerdanyola del Vallès, Spain, 2012
M.S., Universitat Autònoma de Barcelona, Cerdanyola del Vallès, Spain, 2013

Dissertation presented in partial fulfillment of the requirements for the degree of

Doctorate in Philosophy

The University of Montana
Missoula, MT

December 2018

Approved by:

Scott Whittenburg, Dean of The Graduate School
Graduate School

Anna Sala, Chair
Organismal Biology, Ecology, and Evolution

Solomon Dobrowski
W.A. Franke College of Forestry & Conservation

Arthur Woods
Organismal Biology, Ecology, and Evolution

Ragan Callaway
Organismal Biology, Ecology, and Evolution

Craig Brodersen
Yale School of Forestry & Environmental Studies

Why Does Drought Kill Trees? Interactions between Water, Carbon, and Fungal Symbionts

Chairperson: Anna Sala

One of the global causes of forest die-off is climate-change induced drought. Drought kills trees by reducing water supply and non-structural carbohydrate (NSC) availability and by increasing susceptibility to negative biotic interactions. However, we lack an understanding of how water, NSC, and biotic agents interact. As a result, we still cannot accurately predict drought-induced mortality. The overarching goal of my dissertation is to increase our understanding of the interacting mechanisms leading to drought-induced mortality (DIM) and to identify physiological variables that accurately predict risk of DIM. Via greenhouse experiments with *Pinus ponderosa* (ponderosa pine) seedlings, I addressed three overarching research questions: (1) which physiological variables are good predictors of DIM?, (2) What is the role of NSC on plant water relations and DIM?, and (3) Do fungal symbionts affect plant water relations by altering host NSC during periods of carbon deficit? I first show that plant water content integrates the negative effects of reduced water supply and NSC availability under drought and it accurately predicts DIM risk. Further, plant water content shows a threshold at which DIM risk increases. I also provide evidence that plants use NSC to retain water in living tissues and maintain plant water content above critical mortality thresholds. Next, I show that plant water content is a good predictor of DIM risk across populations of ponderosa pine despite differences in morphology, physiology, and drought strategies. The integrative nature of plant water content is relevant because it can be detected remotely, which may allow large-scale assessments of mortality risk. Lastly, I show that fungal symbionts connecting multiple plant hosts can become parasitic and deplete NSC in some hosts. Such a depletion impairs plant water relations, which could increase host vulnerability to drought. My dissertation provides insight on physiological mechanisms leading to DIM and identifies simple physiological variables useful for monitoring DIM risk.

ACKNOWLEDGEMENTS

I could not have completed this dissertation without the help and support of many people. First, I would like to thank Anna Sala for her advice, time, and help. Your commitment to your students is admirable. I would not have made it this far without your insight, patience, and support both scientifically and emotionally. You have made me think big and in depth and have taught me how to be (a bit more) humble. I also thank Solomon Dobrowski, Art Woods, Ray Callaway, and Craig Brodersen for serving on my committee. You always were there to work with me and help me grow as a scientist. Thank you so much for believing in my decisions and always being so flexible. It was only through Francisco Lloret's encouragement that I decided to pursue a PhD in this country, and for that I will always be grateful. This dissertation is the result of continuous collaborations with people without whom this would not have been possible. Thanks to Patrick Demaree most of all, as well as Beth Roskilly, Elliott Conrad, Laura Thornton and Dylan Budke. I also want to thank everyone who has given me a space and materials to work: Ylva Lekberg, Maury Valett, Creagh Breuner, and Marco Maneta. A special thanks to Lila Fishman for letting me occupy half of her greenhouse space for four years and for many hours of unofficial committee member advice. Funding for this work was provided by the National Science Foundation grant BCS 1461576, NSF Experimental Program to Stimulate Competitive Research (EPSCoR) Track-1 EPS-1101342 (INSTEP 3) and NSF EPSCoR RII Track 1 award number IIA-1443108, and University of Montana scholarships. Lastly, I thank my wonderful partner Alex Sugiri, my family, and my friends for their endless support and patience with me through this process. I want to dedicate my dissertation to my uncle Santi who transmitted his passion for plants and fungi to me. This work is as yours as it is mine.

CONTENTS

INTRODUCTION

One of the big questions in biology is 'how species distributions will respond to future changes in climate'. To answer this question, we must understand how changes in abiotic and biotic conditions will affect species distributions. In plants, one of the global causes of shifts in species distributions is climate-change induced drought. During the last fifty years, extreme drought events have become more frequent and intense [1]. As a result, forests around the world - including wet regions- are dying [2]. These die-off events have instigated a lot of research to understand why trees are dying and to predict how this will affect the distribution of species and forests themselves.

In 2008, McDowell proposed a mechanistic framework based on two physiological drivers of drought-induced mortality (DIM): water and carbon [3]. This framework suggested that intense and short droughts may kill plants by disrupting transport of water through their vascular system (i.e., hydraulic failure). Alternatively, mild and long droughts may kill plants by forcing them to consume their carbohydrate reserves and starve to death. This framework also acknowledged that, sometimes, drought may kill plants through an interaction between both water and carbon. However, the framework did not stress this interaction. The McDowell framework also suggested that biotic agents may amplify hydraulic failure or carbon depletion thus leading to early death. This framework has been cited nearly 2,000 times and led to an intense search for hydraulic failure or carbon depletion. However, after ten years of research and despite having a mechanistic framework of DIM, we still cannot accurately predict DIM. The question is 'why not?'.

1- We do not fully understand how hydraulic failure and carbon depletion interact. Recent studies indicate that, in most DIM cases, hydraulic failure killed plants but carbon depletion played an important role [4]. This suggests that water and carbon interact in ways that we do not fully understand [5]. Therefore, we must understand the mechanisms underlying this interaction to model and predict DIM, and foresee its effects on species distributions. However, it is very difficult to study how water and carbon interact under drought because water deficit (i.e., drought) reduces both water and carbon availability. Thus, correlations between variables related to water and carbon do not imply causation because such correlations could simply result from water deficit.

2- We cannot tell when trees actually die. Contrary to animals, plants do not show clear indicators of death such as sudden lack of heartbeat, respiration, motion, etc. Thus, it is very difficult to determine the exact moment when a tree dies [6]. Accurately distinguishing dead trees from live trees is critical to determine the physiological processes that lead to death and to find accurate predictors of DIM.

3- We lack large-scale predictors applicable to different plant types. A species can vary substantially in morphology, physiology, and drought strategies across populations within its distribution. This variation can lead to different responses to drought among populations and, therefore, predictors of DIM [7]. Finding a variable that only predicts DIM in a specific population barely increases our capacity to predict distribution shifts. Consequently, we must find variables that accurately predict DIM risk regardless of spatial variation in morphology, physiology, and drought strategies. Additionally, these variables should be measurable at large scales (e.g., through remote sensing) to facilitate monitoring of species distributions over time.

4- We must understand the interaction between drivers of DIM before studying biotic agents. Biotic factors may be as important as abiotic factors. Plant parasites may be more prevalent in future climates as a result of higher temperatures. These parasites may feed on resources from their plant hosts such as water or carbon and amplify hydraulic failure or carbon depletion. Alternatively, plant symbionts such as mycorrhizal fungi may provide resources to their hosts and ameliorate hydraulic failure or carbon depletion. However, it is difficult to study how biotic agents interact with hydraulic failure and carbon depletion without having a clear understanding of how water and carbon interact on their own. Before studying how biotic agents influence DIM, first we must i) find a way to accurately classify dead and live trees and ii) understand how water and carbon interact. Then, we can assess how biotic agents influence these two components and infer how they may affect species distributions under future climates.

Studying whole distributions is a herculean task. Alternatively, studying individual physiology is feasible and allows us to understand fundamental processes that ultimately drive distribution shifts (e.g., seedling mortality). With this in mind, my dissertation has consisted of a series of greenhouse experiments with ponderosa pine seedlings that address the four gaps of knowledge described above. In chapter 1, I explore the interaction between water and carbon through plant water relations (Gap 1), design a method that distinguishes dead and live plants (Gap 2), and identify predictors of DIM. In chapter 2, we assess different predictors of DIM risk

across populations with varying traits and discuss their large-scale capabilities (Gap 3). In chapter 3, we assess how mycorrhizal symbionts influence plant water relations during periods of carbon limitation and its implications under drought (Gap 4). The overarching goals of my dissertation were to i) increase basic scientific understanding of the physiological processes leading to DIM, ii) provide tools to monitor current DIM risk across large scales, and iii) provide data to parameterize mechanistic models that can predict future DIM risk based on water, carbon, and biotic agents.

REFERENCES

1. Stocker, T. F. *et al.* Summary for Policymakers. In: Climate Change 2013: The Physical Science Basis. Contribution of Working Group I to the Fifth Assessment Report of the Intergovernmental Panel on Climate Change. *CEUR Workshop Proc.* **1542,** 33–36 (2015).
2. Greenwood, S. *et al.* Tree mortality across biomes is promoted by drought intensity, lower wood density and higher specific leaf area. *Ecol. Lett.* **20,** 539–553 (2017).
3. McDowell, N. *et al.* Mechanisms of plant survival and mortality during drought: why do some plants survive while others succumb to drought? *New Phytol.* **178,** 719–39 (2008).
4. Adams, H. D. *et al.* A multi-species synthesis of physiological mechanisms in drought-induced tree mortality. *Nat. Ecol. Evol.* **1,** 1285–1291 (2017).
5. Mencuccini, M., Minunno, F., Salmon, Y., Martínez-Vilalta, J. & Hölttä, T. Coordination of physiological traits involved in drought-induced mortality of woody plants. *New Phytol.* **208,** 396–409 (2015).
6. Anderegg, W. R. L., Berry, J. A. & Field, C. B. Linking definitions, mechanisms, and modeling of drought-induced tree death. *Trends Plant Sci.* **17,** 693–700 (2012).
7. Anderegg, W. R. L. Spatial and temporal variation in plant hydraulic traits and their relevance for climate change impacts on vegetation. *New Phytol.* **205,** 1008–1014 (2015).

CHAPTER 1: PLANT WATER CONTENT IS A USEFUL INDICATOR OF POPULATION-LEVEL DROUGHT-INDUCED SEEDLING MORTALITY

ABSTRACT

Widespread drought-induced forest mortality (DIM) is expected to increase with climate change and drought, with major impacts on carbon and water cycles. For large scale assessment and management, it is critical to identify physiological thresholds that signal risk of drought mortality and that can be assessed at landscape scales. To identify thresholds of DIM risk, we subjected *Pinus ponderosa* seedlings to experimental drought using a point of no return experimental design. Periodically during the drought, independent sets of seedlings were sampled to measure physiological state (volumetric water content [*VWC*], percent loss of conductivity [*PLC*] and non-structural carbohydrates) and to estimate population-level probability of mortality through re-watering. We show that plant *VWC* and *PLC* are good predictors of population-level DIM risk. However, *VWC* exhibits a threshold-type relationship with mortality risk that distinguishes plants at no risk from those at increasing risk of mortality. Further, plant *VWC* integrates the effects of hydraulic failure and carbon depletion across organs, two mechanisms involved in individual tree death. We show for the first time that *VWC*, a variable that can be remotely sensed, is a robust indicator of population-level DIM risk. Our results offer promise for landscape level monitoring of DIM risk.

INTRODUCTION

Episodes of drought-induced forest mortality (DIM) (Lewis, Brando, Phillips, van der Heijden & Nepstad 2011; Williams *et al.* 2013; Rowland *et al.* 2015) are expected to increase with climate change (Allen, Breshears & McDowell 2015; Stocker *et al.* 2015), and to have profound consequences for global water and carbon cycles and vegetation-climate feedbacks. For monitoring and management purposes, there is a critical need to identify reliable plant variables that provide early warning signals of DIM risk at the population level (defined as percentage of dead individuals within a stand or area at a given point in time) and that can potentially be monitored at large spatial scales (Hartmann *et al.* 2018). Intense research in the past decade on the mechanisms of mortality at the individual level has identified hydraulic failure (i.e., loss of

water transport capacity in the xylem) as a dominant mechanism of DIM, with non-structural carbohydrate (*NSC*) depletion often playing a significant, interacting role (Adams *et al.* 2017). While complete hydraulic failure under persistent drought will always lead to death, measures of hydraulic deterioration, often quantified at the individual level as loss of percent hydraulic conductivity (*PLC*), are difficult to monitor continuously in a given plot or stand, thus hindering our ability to monitor mortality risk it at larger scales. Here, we explore whether plant water content, a variable that can be measured remotely (Ceccato, Flasse, Tarantola, Jacquemoud & Grégoire 2001; Ullah, Skidmore, Naeem & Schlerf 2012; Konings *et al.* 2016), is a useful indicator of drought- induced mortality risk.

Regardless of the specific mechanisms involved, mortality under drought occurs due to progressive dehydration leading to irreversible loss of turgor (Tyree *et al.* 2003) – when living cells lose function. How living plant cells sense dehydration is still under debate (Sack, John & Buckley 2018), but it involves changes in cell volume, cell turgor, and osmolyte concentration (Zhu 2016; Sack *et al.* 2018), which in most plants eventually leads to membrane dysfunction (Wang *et al.* 2008; Chaturvedi, Patel, Mishra, Tiwari & Jha 2014) and death (Guadagno *et al.* 2017). Plants must maintain a given pool of water to generate turgor in living cells and this must be done by balancing water supply and demand. Survival under drought, therefore, could be ultimately related to maintenance of plant water content above a minimum threshold leading to permanent turgor loss. Under drought, when stomata close to minimize water loss, the water balance of plants depends in large part on the balance between water supply and water retention capacity in living cells. Water supply to living cells depends on hydraulic conductance, which decreases under drought due to xylem embolism potentially leading to hydraulic failure (Tyree & Sperry 1989). Water retention in living cells depends on their ability to decrease their water potential to match that of the adjacent xylem, which occurs by concentrating solutes. Otherwise, cells will unavoidably lose water to the xylem. *NSC* depletion may lead to loss of water retention capacity and turgor loss via reductions of organic solutes and their osmotic or energetic roles (Brodersen, McElrone, Choat, Matthews & Shackel 2010; Sevanto, McDowell, Dickman, Pangle & Pockman 2014).

A water balance approach (Fig. 1) suggests that water content may be a useful early-warning indicator of mortality risk for several reasons. First, while hydraulic failure appears to be the dominant mechanism of drought mortality, NSC depletion is thought to play a role (Adams et al. 2017) and the two mechanisms often interact (McDowell 2011; Sala, Woodruff & Meinzer 2012; Meir, Mencuccini & Dewar 2015). However, the nature of this interaction is not well understood and is difficult to model (Mencuccini, Minunno, Salmon, Martínez-Vilalta & Hölttä 2015). The water balance approach under drought mechanistically captures this interaction and integrates it into a single variable – water content. Second, and critical for an indicator variable, just as turgor loss shows a threshold response (from sufficient turgor pressure to maintain cell function to irreversible turgor loss and loss of cell function) water content is also likely to mirror such a threshold response and to distinguish plants at no risk of DIM from those at risk as drought proceeds (i.e., to detect incipient risk of mortality). Third, and particularly relevant for the purposes of large scale monitoring, water content can be measured remotely (Ceccato *et al.* 2001; Ullah *et al.* 2012; Konings *et al.* 2016). Indeed, recent remote sensing studies show that progressive declines in canopy water content are associated with subsequent increases of tree mortality (Saatchi *et al.* 2013; Asner *et al.* 2015). Although these data suggest that water content may successfully predict DIM, so far, experimental evidence is limited (Kursar *et al.* 2009). In summary, water content may prove a useful indicator of drought mortality risk because it is likely to integrate the mechanisms of drought mortality and to show a threshold response that signals incipient risk of mortality. If so, and because it can be measured remotely, water content offers significant potential for monitoring drought mortality risk at larger scales.

Most studies of individual DIM physiological thresholds have focused on measurements of dead or nearly-dead plants based on visual cues, including browning, defoliation, and branch die-off (Anderegg *et al.* 2015; Dickman *et al.* 2015; Adams *et al.* 2017; Hoffmann *et al.* 2011; Anderegg *et al.* 2012b; Anderegg & Anderegg 2013; O'Brien *et al.* 2014; Pratt *et al.* 2014; Rowland *et al.* 2015; Garcia-Forner *et al.* 2016). This can be problematic because visual symptoms of plant death generally occur well after plants have crossed the point of no return (the point beyond which plants can no longer survive; Anderegg *et al.* 2012b), thus potentially missing early-warning physiological signals. Furthermore, for some species, measurements at the

leaf or branch level may not be representative of whole plant level mortality processes. Thus, identifying physiological states at the whole plant level that are indicative of DIM risk, particularly incipient DIM risk thresholds, requires experimental designs based on the point of no return. That is, it requires concurrent multi-organ/whole-plant level measurements of potential physiological indicators (*PLC*, *NSC*, water content) at different stages of drought regardless of symptoms and of probability of mortality (e.g., by re-watering and subsequent assessment of mortality). Because whole plant measurements are usually destructive, physiological measurements must be independent of mortality assessment. Such an approach entails pairing independent measurements of physiological state and of probability of mortality progressively during drought to identify the physiological states at which population-level mortality risk increases as drought progresses. To our knowledge, only Barigah *et al.* (2013) and Kursar *et al.* (2009) used such a design. However, Barigah *et al.* (2013) did not measure water content and neither study focused on thresholds for incipient mortality risk, which is a critical feature for a useful indicator with monitoring purposes.

We performed a greenhouse drought experiment with two-year-old ponderosa pine (*Pinus ponderosa* Douglas ex C. Lawson) seedlings to identify physiological predictors of DIM risk at the population level based on the point of no return. We focused on thresholds signaling incipient DIM risk. We sampled independent sets of seedlings periodically during the experimental drought to: 1) measure their physiological state (e.g. volumetric water content, *PLC* and *NSC*) and 2) estimate the probability of mortality once re-watered. We hypothesized that i) tissue water content is related to loss of hydraulic conductivity and *NSC* availability at both tissue and whole-plant levels; ii) *PLC*, *NSC* and water content explain DIM risk, though their respective predictive power will vary (Fig. 1); and iii) both *PLC* and water content show a threshold-like response distinguishing healthy plants from those at risk of DIM. The focus on water content as a useful indicator is because, as opposed to other indicators, it can be measured remotely and, as such, it offers significant potential for large scale applications.

MATERIALS AND METHODS

Study Design. The experiment took place at the University of Montana greenhouse facilities. On August 2nd 2015 we obtained 165 two-year-old *Pinus ponderosa* seedlings in soil

plugs from the Coeur D'Alene Nursery (USDA Forest Service) and planted them in 7.6 cm diameter x 43 cm tall pots using a homogeneous soil mixture consisting of 3:1:1 sand, peat moss, and top soil, respectively. Seedlings were ca. 20 cm tall from the base to the tip of the stem and soil plugs were similar in length. Pots were randomized on a bench at regular distances from each other and left to acclimate for a month under well-watered conditions (i.e. field capacity, when the soil is saturated). Soil field capacity corresponded to soil volumetric water content values (VWC_s) of ca. 20%. Based on preliminary experiments and for the purpose of timing consecutive samplings, we monitored changes in VWC_s using Decagon 5TE sensors placed in five representative seedlings 10 cm above the bottom of the pots. Sensors were inserted through a hole drilled on the side of the pots to minimize disturbance and root damage, which had reached 40 cm in depth by the end of the experiment.

From September 2nd to October 1st, seedlings underwent four drought pre-conditioning cycles to allow plants to acclimate to drought stress. During the first three cycles, we let pots dry down to 50% of their field capacity (VWC_s = 10%) after which we watered again to field capacity. On the last cycle, pots were dried to 25% of their field capacity (VWC_s = 5%), which corresponds to a soil water potential of -0.7 MPa based on an empirical soil characteristic curve (see below), and then watered again to field capacity. From October 1st to December 1st, we stopped watering all but five seedlings (controls). Drought-treated seedlings were left un-watered for the rest of the experiment while control seedlings were kept at field capacity (Fig. 2). Based on a preliminary drought experiment to assess symptoms of mortality as a function of soil drought and to optimize sampling times and sample size, we started measurements 34 days after the beginning of the drought treatment.

Sampling procedure. We assessed soil water potential, seedling physiology, and mortality risk on six weekly samplings at days 0, 34, 41, 48, 55, and 62. At each sampling, we measured midday VWC_s in five randomly chosen seedlings. VWC_s sensors were installed 24h prior to measurement to reach equilibrium with soil conditions. VWC_s was then used to estimate the soil water potential at which each seedling was exposed to at the time of sampling. To do so, we converted VWC_s values to soil water potential based on an empirical soil characteristic curve, describing the relationship between VWC_s and soil water potential as a soil dries (Fredlund & Xing 1994). To generate this curve, we dried a pot with the same soil used in the experiment at a

constant temperature (ca. 40 ºC). A VWC_s sensor (Decagon 5TE) and a soil water potential sensor (Decagon MPS-6) were placed at the same height in the center of the pot. This process was repeated twice with the same pot to reduce variability due to measurement error.

We also measured leaf water potentials. However, these measurements were not reliable because needles became dry and brittle as the drought intensified thus breaking during measurements or becoming hydraulically disconnected from the rest of the plant. We note, however, that this did not prevent us from assessing hydraulic failure, carbon depletion, and plant water content, which was the main goal of this experiment. Although plant water status is usually assessed with plant water potential, plant water content and *PLC* are also indicators of drought stress. At every sampling date, the same five seedlings in which VWC_s was measured were then harvested and kept in zip-lock bags with a moist paper towel in a cooler to prevent further water loss (Garcia-Forner *et al.* 2016). We did not measure stem water potential to prevent artifacts on subsequent measurements of stem *PLC* and *VWC*. Samples were transported to the laboratory within two hours for physiological measurements (below). Because physiological measurements were destructive, at each sampling event during the drought a second independent subset of randomly sampled seedlings was used to assess mortality risk.

Mortality assessment. To estimate the probability of mortality at the population level over time, at each sampling event, 15% of the total pool of drought-treated seedlings were randomly chosen, re-watered to field capacity, and kept well-watered for at least 39 days (until January 8th) to assess mortality. This method ensures accurate classification of both live and dead plants at every sampling event regardless of visual symptoms. We classified seedlings as dead only if their canopy and phloem were completely brown and dry (Cregg 1994) and no subsequent buds appeared (dead seedlings were left in the greenhouse for two additional months). Notice that early re-watering groups were re-watered for longer periods of time due to the nature of the experimental design. However, seedlings removed at the later stages of the drought were completely dry and brittle with no subsequent signs of recovery. Because the total pool of drought-treated seedlings was reduced every time when mortality probability was assessed, a 15% of the total pool of drought-treated seedlings represented a different number of individuals at each sampling event (max:32 – min: 14). To make estimates of mortality comparable across sampling events in terms of sample size, we estimated mortality using only 13 plants randomly subsampled from the pool of plants chosen to estimate mortality at each

sampling date. This subsampling procedure was repeated a thousand times using a bootstrapping scheme, and the thousand values of mortality generated per sampling event were averaged to generate a proxy for population-level probability of mortality at each sampling event. Note that in our design, physiological measurements during drought were done in individual plants and averaged, while mortality measurements were conducted at the population level.

Tissue Volumetric Water Content. Upon arrival to the laboratory we separated roots, stems, and needles of each seedling to measure their volumetric water content (*VWC*) based on fresh and dry weights as: ((Fresh weight-Dry weight)/ Fresh Volume)*100. We measured volume with the water displacement method in a reservoir of deionized water (Olesen 1971; Hughes 2005). Dry weights were measured after hydraulic conductivity measurements (see below). We focused on VWC because this variable can be directly related to variables measured through remote sensing (Yilmaz, Hunt & Jackson 2008; Mirzaie *et al.* 2014; Veysi, Naseri, Hamzeh & Bartholomeus 2017). We calculated whole plant *VWC* weighed by tissue fraction biomass (proportion of each tissue dry mass fraction multiplied by their respective VWC). For consistency, root *VWC* was measured before any other tissue to avoid changes in *VWC* or hydraulic conductivity due to cleaning procedures and exposure to dry air. After a very quick immersion in water to minimize water absorption, we immediately blotted tissues with paper towels until no surface water was left. Stems and root systems were returned to Ziploc bags and the cooler immediately after measurements of fresh weight and volume, prior to hydraulic conductivity measurements.

Stem and Root Hydraulics. We measured stem hydraulic conductivity and root hydraulic conductance using the gravimetric method (Sperry, Donnelly & Tyree 1988) immediately after fresh volume measurements of tissues. We used a modification of the hydraulic apparatus described in Sperry (1988) that allowed us to measure hydraulic conductance of whole root systems in addition to stems. In our system, a micro-flow sensor (Sensirion SLI-0430) was placed upstream from the stem (instead of a scale) to record water flow. This sensor measures flow every 70 ms with a precision of 1 µL/min thus allowing precise measurements in plants with low hydraulic conductivity. Stem segments previously used for *VWC* measurements were immersed in deionized water for 20 minutes to relax xylem tensions that could artificially alter conductivity values (Trifilo, Barbera, Raimondo, Nardini & Gullo 2014). After relaxation, stems were placed on the hydraulic apparatus and each end was recut twice at a distance of 1 mm

from the tips (total of 2 mm per side) to remove any potential emboli resulting from previous cuts, transport, and relocation (Torres-Ruiz *et al.* 2015). Stems were then connected to the hydraulic apparatus while under water, with their terminal ends facing downstream flow. The stems were then raised out of the water and the connections were checked to ensure that there were no leaks.

First, initial background flow was measured to account for the flow existing under no pressure, which can vary depending on the degree of dryness of the measured tissue (Hacke *et al.* 2000; Torres-Ruiz, Sperry & Fernández 2012; Blackman *et al.* 2016). Second, a pressure gradient of 5-8 kPa was applied to run water through the stem and pressurized flow was measured. This small pressure gradient prevented embolism removal from the samples while ensuring flow. Lastly, final background flow was measured, initial and final background flows were averaged, and net flow was calculated as the difference between pressurized flow and average background flow. Native specific hydraulic conductivity (*K*) was estimated in stems as the (net) flow divided by the pressure gradient used and standardized by xylem area and length. Xylem length was measured using a caliper and xylem area was calculated from stem diameter assuming a circular area.

The configuration of the apparatus was then changed to measure whole root system hydraulic conductance using the same gravimetric principle. This approach requires the water to flow backwards through the roots. Such backwards flow has been proven to have no significant effect on hydraulic measurements (Kolb & Robberecht 1996; Tyree *et al.* 2003). We ensured that both configurations of the apparatus were comparable by measuring stems using both arrangements and we found no significant differences between them (t= 0.7854, p-value= 0.4761). As in stems, roots were also relaxed in deionized water for 20 minutes to relax xylem tensions that could artificially alter conductivity values (Trifilo *et al.* 2014). Flow, including initial and final background flow, was measured as above and whole root native hydraulic conductance (*k*) was estimated as the (net) flow divided by the pressure gradient used and standardized by xylem area at the root collar.

Maximum stem hydraulic conductivity (*Kmax*) and root hydraulic conductance (*kmax*) were estimated as the average stem *K* and root *k* of the well-watered seedlings measured at day 62 after the onset of the drought and used to calculate *PLC* in all measured seedlings. Such a population approach was chosen because 1) destructive measurements in these small seedlings

prevented multiple successive measurements of *K* and water potentials on the same individuals, and 2) flushing and vacuum infiltration techniques to obtain *Kmax* from embolized tissues can generate artifacts and overestimate *Kmax* (Cochard *et al.* 2013). Percent loss of stem conductivity and percent loss of root conductance (PLC) were estimated for each measured seedling as *100**(*Kmax-K)/Kmax* and *100**(*kmax-k)/kmax*, respectively. Note that slightly negative *PLC* values may occur if *K* or *k* in a given sample is larger than *Kmax* estimated as the average *K* of controls. We calculated whole-plant PLC weighted by the proportion of each tissue fraction. Root and stem *PLC* can be averaged together because they are unit-less indexes that represent the *relative* loss of water transport capacity of their respective tissues. Because we did not measure *PLC* in needles, whole-plant *PLC* represents the overall hydraulic integrity of the stem and root systems. A solution of water with 10 mM KCl degassed at 3 kPa for at least 8 hours was used for all hydraulic measurements (Espino & Schenk 2011). We developed an R code (see Methods S1 in Supporting Information) that automatically calculates pressurized and background flows once flow stabilizes. We excluded hydraulic measurements taken at days 0 and 34 since the onset of drought (see Fig. 3b) because a leakage was detected in our apparatus leading to artificial values. However, this did not prevent us from obtaining *PLC* values across the full range of observed mortality, including values close to 0.

Non-structural Carbohydrates (*NSC*). After hydraulic measurements, needle, stem, and root samples were microwaved for 180 seconds at 900 Watts in three cycles of 60 seconds to stop any metabolic activity. Tissues were subsequently oven-dried at 70 ºC until constant mass. Samples were weighed and ground to a fine powder. Approximately 11 mg of needle tissue and 13 mg of stem or root tissue were used to analyze *NSC* dry mass content following the enzymatic digestion method (McCleary, Gibson & Mugford 1997). We calculated the total pool of *NSCs*, starch, soluble sugars, and glucose or fructose in each tissue by multiplying the corresponding concentration per dry mass by the dry weight. Concentrations (total *NSC* and each individual component) were scaled up to the whole-plant by weighting by tissue fraction as above.

Statistical analyses. We developed five models to evaluate trends in drought intensity, whole-plant physiological status, and population-level mortality over time. All models had days since the onset of drought as their predictor variable and one of the following variables as the response variable: (1) Soil Water Potential, (2) total *NSC* concentrations, (3) *VWC*, (4) *PLC*, or (5) Probability of Mortality. Linear models were used for the first three cases given that response

variables could be transformed to meet model assumptions. Generalized linear models with binomial error distribution (logit link) were used in the last two instances. *PLC* and probability of mortality were expressed on a decimal fraction basis following requirements of models with binomial distributions.

To test whether *NSC* concentrations, loss of hydraulic conductivity (*PLC*), and *VWC* at each sampling time predicted population level probability of mortality we used six linear models at the whole plant level with the probability of mortality as the response variable. Predictor variables for each model were: (1) starch and soluble sugar concentrations; (2) total *NSC* concentrations; (3) *PLC*; (4) *VWC*; (5) starch and soluble concentrations and *PLC*; and (6) total *NSC* and *PLC* as the explanatory variables. We ran these last two models to test whether the combined predictive capacity of hydraulic and carbohydrate variables was similar to the predictive capacity of *VWC* alone given that *VWC* should integrate both hydraulic failure and carbon depletion. *VWC* was log-transformed to achieve normality. We used Differential Akaike Information Criterion (ΔAIC) and adjusted R-square values (R^2_{adj}) to rank the models in terms of simplicity and predictive power.

We used segmented linear models using the segmented function from R package *segmented* (Muggeo 2008) to explore potential threshold-type relationships between *NSC*, *PLC* or *VWC* and population-level probability of mortality. Given a linear regression model, this function tries to estimate a new model with a segmented relationship (the linear function is divided into two segments, each with different slope, starting from an initial inflection point provided by the user and then identifies the actual inflection point at which the change of slope occurs). The model simultaneously optimizes the slopes and inflection point through several iterations until a local optima is achieved (Muggeo 2003). As suggested by package instructions, initial inflection points were determined by visually inspecting the relationship between mortality risk and the variables of interest. We emphasize that thresholds are not meant to distinguish dead from living plants, but rather, values of a given explanatory variable above or below which the risk of mortality at the population level is no longer zero (incipient mortality risk). We used ΔAIC to justify the use of segmented models instead of simple linear models. Only segmented models with a ΔAIC equal or greater than 10 were considered to provide a better fit for the data (Burnham & Anderson 2004). In those cases, thresholds among tissues and

whole-plant were considered significantly different when the confidence intervals of the threshold values did not overlap.

To test whether loss of hydraulic conductivity explained plant water content, we performed tissue-level and plant-level linear models with *VWC* as the response variable and stem *PLC*, root *PLC*, or plant *PLC* as predictors. We also assessed the relationship between *NSC* and *VWC*. Because under drought and minimal carbon supply, consumption of *NSC* storage for metabolic demands is expected, a positive relationship between *NSC* and *VWC* could simply reflect that both variables independently responded to drought. To test whether *NSC* concentrations directly affected tissue or plant water content, we first performed two sets of tissue and plant-level linear models with *VWC* and *NSC* as the response variables and soil water potential as predictor. Then, we tested whether the residuals from the relationships of *VWC* vs soil water potential were related to those from the relationship of *NSC* vs soil water potential, thus removing the direct effect of drought on each variable.

RESULTS

Soil water potential decreased with time in drought-stressed seedlings (Fig. 3a, R^2_{adj} = 0.82, $p < 0.001$, Table S1). The first signs of DIM did not appear until day 34 after the onset of drought (Fig. 3a), after which the probability of mortality increased over time ($p = 0.005$, Table S1). Whole-plant percent loss of conductivity (*PLC*) was still low at day 40 but increased sharply over time in drought-stressed seedlings (Fig. 3b, $p = 0.028$, Table S1) with plants reaching 50% loss of conductivity by approximately day 50. Both whole-plant total *NSC* concentrations and *VWC* decreased over time ($R^2_{adj} = 0.09$, $p = 0.044$ and $R^2_{adj} = 0.74$, $p < 0.001$ respectively, Table S1). *NSC* declined linearly over time (Fig. 3c) while *VWC* declined non/linearly (Fig. 3d). The observed decrease in *NSC* was driven by a decline in starch (plant: $R^2_{adj} = 0.33$, $p < 0.001$; needles: $R^2_{adj} = 0.18$, $p = 0.005$; stem: $R^2_{adj} = 0.47$, $p < 0.001$; roots: $R^2_{adj} = 0.48$, $p < 0.001$; Fig. S1), which offset an increase in soluble sugars (plant: $R^2_{adj} = 0.62$, $p < 0.001$; needles: R^2_{adj} = 0.06, $p = 0.08$; stem: $R^2_{adj} = 0.51$, $p < 0.001$; roots: $R^2_{adj} = 0.53$, $p < 0.001$; Fig. S1).

VWC at each sampling time was negatively related to the probability of mortality (R^2_{adj} = 0.90, $p < 0.001$), both at the whole plant (Fig. 4 main) and organ level (Fig. S2, Table S2 & S3). *PLC* and *NSC* were positively and negatively related, respectively, to the probability of mortality ($R^2_{adj} = 0.82$, $p < 0.001$ and $R^2_{adj} = 0.14$, $p < 0.009$, respectively). However, only *PLC* was a

good predictor of mortality based on R^2_{adj} (Figs. 4 inset, S3 & Table S2). Segmented models identified thresholds for incipient mortality for *VWC* (*VWC* value below which the risk of mortality was no longer zero and started to increase rapidly), but failed to find such thresholds for *PLC* and *NSC* (Fig. 4, Table S3). These results are robust to differences in sample size among explanatory variables and to the uncertainty in PLC estimates generated by using different sets of individuals to measure native and maximum conductivity/conductance (SI Methods S2, S3). When *VWC* was assessed at the organ level, needles and roots also showed a threshold-type response (Fig. S2 & Table S3). Thresholds in needles and roots were not significantly different despite the observed variability among tissues due to differences in *VWC* at full turgor.

PLC increased as soil water potentials decreased (plant: Adjusted $R^2 = 0.39$, $p = 0.002$; stem: $R^2_{adj} = 0.39$, $p = 0.002$; roots: $R^2_{adj} = 0.33$, $p = 0.005$), and *VWC* was strongly related to *PLC* in all organs and at the whole plant level (plant: $R^2_{adj} = 0.74$, $p < 0.001$; stem: $R^2_{adj} = 0.54$, $p < 0.001$; roots: $R^2_{adj} = 0.52$, $p < 0.001$) (Fig. 5, Table S4a). *VWC* was also correlated with *NSC* depletion (Fig. S4), as both decreased with drought. The residuals from the relationship of *VWC* vs soil water potential and those from the relationship of *NSC* vs soil water potential were positively correlated (plant: $R^2 = 0.67$, $p < 0.001$; needles: $R^2 = 0.20$, $p = 0.041$; roots: $R^2 = 0.21$, $p = 0.024$) (Fig. 6b & Table S4a), indicating that *VWC* and *NSC* were related independent of soil water potential (see statistical analyses section for rationale behind this analysis). Contrary to expectations, however, the effect of *NSC* on *VWC* was driven by starch, not by soluble sugars (Fig. 6b & Table S4b) as supported by the lack of a significant relationship between sugar residuals and *VWC* residuals (Fig. 6b).

DISCUSSION

Our experimental design based on the point of no return allowed us to identify *PLC* and *VWC*, both at the whole plant (Fig. 4 main) and organ levels (Fig. S2, Table S2 & S3), as excellent indicators of DIM risk. While *PLC* indicates mortality risk (see below), the ability of *VWC* to predict incipient mortality risk is particularly relevant because *VWC* can be measured remotely (Mirzaie *et al.* 2014; Veysi *et al.* 2017), which opens a promising avenue for monitoring DIM risk at large spatial scales.

The threshold-like response of *VWC* (Fig. 4 main and Fig S2) or other water content-related variables is expected based on physiological principles: DIM risk is low over ranges of

water content sufficient to maintain turgor, but may increase substantially as tissue water contents decrease below values leading to turgor loss. Although plants can recover from temporary turgor loss, continued decreases of water content below turgor loss may increase the risk of irreversible turgor loss due to cellular damage. Because widespread and permanent loss of turgor in living cells unavoidably leads to tissue or plant death, variables related to water pools have the potential to signal incipient DIM risk thresholds across species (Martínez-Vilalta et al. *in review),* a much-needed feature for mortality risk assessment across communities (Hartmann *et al.* 2018).

A critical advantage of adding water content in our toolkit and current framework for assessing DIM is that it can be measured across scales ranging from organs to ecosystems via remote sensing (Saatchi & Moghaddam 2000; Ceccato *et al.* 2001; Ullah *et al.* 2014; Ma *et al.* 2016; Fang *et al.* 2017; Konings *et al.* 2017). Remotely-sensed water content has been linked to forest mortality across diverse forest types (Saatchi *et al.* 2013; Asner *et al.* 2015). In contrast, *PLC* is more difficult to measure at large spatial scales, and values leading to mortality are variable across organs and species (Tyree *et al.* 2003; Brodribb & Cochard 2009; Choat *et al.* 2012; Urli *et al.* 2013). Therefore, water content may offer improved potential for monitoring DIM risk across scales, especially if water content thresholds leading to DIM risk prove to be consistent across species and plant types.

PLC has also been shown to cause a DIM threshold-like response at the individual (Brodribb & Cochard 2009; Urli *et al.* 2013) and population levels (Barigah *et al.* 2013). However, in our study *PLC* did not signal incipient mortality risk (i.e., the relationship between *PLC* and probability of mortality was linear rather than showing an inflection point that distinguishes healthy from at-risk plants) (Fig. 4, Table S3). Caution is needed before drawing conclusions based on our data because the removal of faulty *PLC* values at days 0 and 34 and estimations of *PLC* based on population-level *Kmax* could have biased the results. However, our sensitivity analysis indicate that our results are robust to differences in sample size among explanatory variables and to the uncertainty in *PLC* estimates generated by using different sets of individuals to measure *Kmax* (SI Methods S2, S3). Additionally, the lack of an incipient *PLC* threshold is unlikely to be caused by variability in *PLC* among individuals given that such variability also exists in *VWC*. Yet, segmented regressions detected a mortality threshold for *VWC,* even after removing *VWC* values at days 0 and 34 of drought (the period with no *PLC*

measurements; see methods S2). These results tentatively suggest that water content-related variables have threshold-type responses and may be good indicators of incipient mortality risk. It is important to note that while our sensitivity analyses did not support a threshold response for *PLC*, *PLC* thresholds may occur at other life stages, populations, or species as suggested by the results in Barigah *et al.(* 2013). The critical point is not which variables are or are not good indicators of incipient mortality risk, but which are more useful and for what purpose. While others have shown that water content is linked to drought mortality (Kursar et al. 2009), this study is the first to show that water content can distinguish populations at no risk of drought mortality from those at risk (i.e. incipient mortality risk), a critical property for monitoring purposes. Because water content can be measured remotely at large scales, if corroborated in other species, our results in ponderosa pine have important implications for large scale applications if corroborated in other species.

Our results also support that water content integrates the diverse mechanisms leading to drought mortality. When stomata close under drought, plant water content depends on losses via cuticular conductance and stomatal leakiness, along with the water supply through the vascular system (Blackman *et al.* 2016). Consistently, *VWC* was strongly related to *PLC* in all organs and at the whole plant level (Fig. 5, Table S4a). *VWC* also decreased significantly with *NSC* depletion (Fig. S4), which occurred as the drought intensified and starch concentration decreased, likely as a result of decreased supply via photosynthesis (Fig. S1). In contrast, soluble sugars, the osmotically active component of *NSC*, increased during drought (Fig. S1), a common response (Martinez-Vilalta *et al.* 2016). Critically, *VWC* residuals and *NSC* residuals were tightly related indicating that *NSC* storage is involved directly or indirectly in tissue water retention capacity independent of direct drought effects on both variables. Contrary to expectations, however, the effect of *NSC* on *VWC* was driven by starch, not by soluble sugars (Fig. 6b & Table S4b). Such a response was unexpected if the role of *NSC* on water relations is via the supply of compatible solutes for osmotic adjustment. It could be that the actual osmotic components are not the compounds we measured (glucose, fructose and sucrose) and were conflated with starch by the digestion method. This can occur because amyloglucosidase does not specifically target starch but rather glucose chains regardless of chain length. Thus, small molecules containing glucose units such as trioses (which have significant osmotic potential) could be partially or fully

digested during the starch digestion step and misclassified as starch. Alternatively, *NSC* could serve as an energy source for the active accumulation of inorganic solutes (White & Broadley 2001; Plett & Møller 2010). Overall, our results at the whole plant and tissue level show that metrics of water content accurately capture the progressive dehydration leading to desiccation that occurs during the process of DIM (Tyree *et al.* 2003; Saiki, Ishida, Yoshimura & Yazaki 2017). Plants regulate water content by preventing loss of hydraulic conductivity or *PLC*, enhancing retention (including capacitance), and reducing water loss (Meinzer, Clearwater & Goldstein 2001) (Fig. 1). We find that both water supply (*PLC*) and *NSC* influence *VWC*, and that failure to maintain water content above certain thresholds increases risk of death (Fig. 1). The incorporation of water content-related variables advances our current conceptual framework for predicting DIM based on hydraulic failure and carbon starvation (Mcdowell *et al.* 2008): water content integrates important aspects of the two mechanisms (Figs. 5 & 6) and provides a metric to which living cells respond directly (Zhu 2016; Sack *et al.* 2018). Consistent with recent evidence (Adams *et al.* 2017), our results show that hydraulic failure (i.e., the water supply) has a dominant effect on DIM relative to *NSC* storage depletion (i.e., water retention capacity) (Fig. 4 inset; Fig. S3 &Table S2). The degree to which hydraulic failure and *NSC* depletion contribute to changes in plant water balance likely varies across species but such variability is potentially captured by water content variables. Thus, water content variables may provide more consistent relationships with mortality risk across species than *PLC* or *NSC* alone because they integrate the two.

The expected increase in DIM under climate change has large ecological, economic, and social implications (Stocker *et al.* 2015). Despite intense research, the lack of physiological indicators with incipient DIM thresholds measurable at large scales, and our limited understanding of the interaction between hydraulic failure and carbon depletion have hindered our ability to accurately model and monitor DIM risk (Hartmann *et al.* 2018). We provide experimental evidence that plant water content, a variable scalable from organs to the whole plant and detectable through remote sensing (Saatchi *et al.* 2013; Asner *et al.* 2015; Konings *et al.* 2017), is a good indicator of DIM risk and shows a threshold response (i.e. detects incipient mortality risk). We also provide evidence that water content integrates the mechanisms of mortality. While our results have important implications for large scale monitoring of DIM risk,

much research is needed to: i) corroborate our results in other species; ii) test the consistency of incipient mortality thresholds in water content variables such as relative water content, which standardizes differences in *VWC* across species, iii) examine similar thresholds from remotely sensed data concurrent with drought mortality data, and iv) integrate dynamics of vegetation water content in systems with multiple species and plant growth strategies. We hope our results will motivate such work.

ACKNOWLEDGEMENTS

This work was supported by a National Science Foundation grant to SD, MM and AS (BCS 1461576). The authors also thank Elliott Conrad, Dylan Budke, and Aurora Bayless-Edwards for their assistance in data collection; Zack Holden for his feedback on the experimental design; and Douglas Emlen, Art Woods, Ray Callaway, and Nate McDowell and several anonymous reviewers for insightful comments and suggestions on early versions of this manuscript. GS received funding from the NSF Experimental Program to Stimulate Competitive Research (EPSCoR) Track-1 EPS-1101342 (INSTEP 3).

REFERENCES

Adams H.D., Zeppel M.J.B., Anderegg W.R.L., Hartmann H., Landhäusser S.M., Tissue D.T., … McDowell N.G. (2017) A multi-species synthesis of physiological mechanisms in drought-induced tree mortality. *Nature Ecology & Evolution* **1**, 1285–1291.

Allen C.D., Breshears D.D. & McDowell N.G. (2015) On underestimation of global vulnerability to tree mortality and forest die-off from hotter drought in the Anthropocene. *Ecosphere* **6**, 1–55.

Anderegg W.R.L. & Anderegg L.D.L. (2013) Hydraulic and carbohydrate changes in experimental drought-induced mortality of saplings in two conifer species. *Tree Physiology* **33**, 252–260.

Anderegg W.R.L., Berry J. a, Smith D.D., Sperry J.S., Anderegg L.D.L. & Field C.B. (2012a) The roles of hydraulic and carbon stress in a widespread climate-induced forest die-off. *Proceedings of the National Academy of Sciences of the United States of America* **109**, 233–7.

Anderegg W.R.L., Berry J.A. & Field C.B. (2012b) Linking definitions, mechanisms, and modeling of drought-induced tree death. *Trends in Plant Science* **17**, 693–700.

Anderegg W.R.L., Flint A., Huang C., Flint L., Berry J. a., Davis F.W., … Field C.B. (2015) Tree mortality predicted from drought-induced vascular damage. *Nature Geoscience*, 1–5.

Asner G.P., Brodrick P.G., Anderson C.B., Vaughn N., Knapp D.E. & Martin R.E. (2015) Progressive forest canopy water loss during the 2012–2015 California drought. *Proceedings of the National Academy of Sciences* **2015**, 201523397.

Barigah T.S., Charrier O., Douris M., Bonhomme M., Herbette S., Améglio T., … Cochard H. (2013) Water stress-induced xylem hydraulic failure is a causal factor of tree mortality in beech and poplar. *Annals of Botany* **112**, 1431–1437.

Blackman C.J., Pfautsch S., Choat B., Delzon S., Gleason S.M. & Duursma R.A. (2016) Toward an index of desiccation time to tree mortality under drought. *Plant Cell and Environment* **39**, 2342–2345.

Brodersen C.R., McElrone a. J., Choat B., Matthews M. a. & Shackel K. a. (2010) The Dynamics of Embolism Repair in Xylem: In Vivo Visualizations Using High-Resolution Computed Tomography. *Plant Physiology* **154**, 1088–1095.

Brodribb T.J. & Cochard H. (2009) Hydraulic failure defines the recovery and point of death in water-stressed conifers. *Plant physiology* **149**, 575–84.

Burnham K.P. & Anderson D.R. (2004) Multimodel inference: Understanding AIC and BIC in model selection. *Sociological Methods and Research* **33**, 261–304.

Ceccato P., Flasse S., Tarantola S., Jacquemoud S. & Grégoire J.M. (2001) Detecting vegetation leaf water content using reflectance in the optical domain. *Remote Sensing of Environment* **77**, 22–33.

Chaturvedi A.K., Patel M.K., Mishra A., Tiwari V. & Jha B. (2014) The SbMT-2Gene from a halophyte confers abiotic stress tolerance and modulates ROS scavenging in transgenic tobacco. *PLoS ONE* **9**.

Choat B., Jansen S., Brodribb T.J., Cochard H., Delzon S., Bhaskar R., … Zanne A.E. (2012) Global convergence in the vulnerability of forests to drought. *Nature* **491**, 752–755.

Cochard H., Badel E., Herbette S., Delzon S., Choat B. & Jansen S. (2013) Methods for measuring plant vulnerability to cavitation: a critical review. *Journal of Experimental Botany* **64**, 4779–4791.

Cregg B.M. (1994) Carbon allocation, gas exchange, and needle morphology of Pinus ponderosa genotypes known to differ in growth and survival under imposed drought. *Tree Physiology*

14, 883–898.

Dickman L.T., Mcdowell N.G., Sevanto S., Pangle R.E. & Pockman W.T. (2015) Carbohydrate dynamics and mortality in a piñon-juniper woodland under three future precipitation scenarios. *Plant, Cell and Environment* **38**, 729–739.

Espino S. & Schenk H.J. (2011) Mind the bubbles: Achieving stable measurements of maximum hydraulic conductivity through woody plant samples. *Journal of Experimental Botany* **62**, 1119–1132.

Fang M., Ju W., Zhan W., Cheng T., Qiu F. & Wang J. (2017) A new spectral similarity water index for the estimation of leaf water content from hyperspectral data of leaves. *Remote Sensing of Environment* **196**, 13–27.

Fredlund D.G. & Xing A. (1994) Equations for the soil-water characteristic curve. *Canadian Geotechnical Journal* **31**, 521–532.

Garcia-Forner N., Sala A., Biel C., Savé R. & Martínez-Vilalta J. (2016) Individual traits as determinants of time to death under extreme drought in Pinus sylvestris L. *Tree Physiology* **36**, 1196–1209.

Guadagno C.R., Ewers B.E., Speckman H.N., Aston T.L., Huhn B.J., DeVore S.B., … Weinig C. (2017) Dead or alive? Using membrane failure and chlorophyll fluorescence to predict mortality from drought. *Plant Physiology* **175**, 223–234.

Hacke U.G., Sperry J.S., Ewers B.E., Ellsworth D.S., Schäfer K.V.R. & Oren R. (2000) Influence of soil porosity on water use in Pinus taeda. *Oecologia* **124**, 495–505.

Hartmann H., Moura C.F., Anderegg W.R.L., Ruehr N.K., Salmon Y., Allen C.D., … O'Brien M. (2018) Research frontiers for improving our understanding of drought-induced tree and forest mortality. *New Phytologist* **218**, 15–28.

Hoffmann W. a., Marchin R.M., Abit P. & Lau on L. (2011) Hydraulic failure and tree dieback are associated with high wood density in a temperate forest under extreme drought. *Global Change Biology* **17**, 2731–2742.

Hughes S.W. (2005) Archimedes revisited: A faster, better, cheaper method of accurately measuring the volume of small objects. *Physics Education* **40**, 468–474.

Kolb P.F. & Robberecht R. (1996) High temperature and drought stress effects on survival of Pinus ponderosa seedlings. *Tree Physiology* **16**, 665–672.

Konings A.G., Piles M., Rötzer K., McColl K.A., Chan S.K. & Entekhabi D. (2016) Vegetation

optical depth and scattering albedo retrieval using time series of dual-polarized L-band radiometer observations. *Remote Sensing of Environment* **172**, 178–189.

Konings A.G., Yu Y., Xu L., Yang Y., Schimel D.S. & Saatchi S.S. (2017) Active microwave observations of diurnal and seasonal variations of canopy water content across the humid African tropical forests. *Geophysical Research Letters* **44**, 2290–2299.

Kursar T. a., Engelbrecht B.M.J., Burke A., Tyree M.T., El Omari B. & Giraldo J.P. (2009) Tolerance to low leaf water status of tropical tree seedlings is related to drought performance and distribution. *Functional Ecology* **23**, 93–102.

Lewis S.L., Brando P.M., Phillips O.L., van der Heijden G.M.F. & Nepstad D. (2011) The 2010 Amazon drought. *Science (New York, N.Y.)* **331**, 554.

Ma B., Xu A., Zhang S. & Wu L. (2016) Retrieval of Leaf Water Content for Maize Seedlings in Visible Near Infrared and Thermal Infrared Spectra. 6930–6933.

Martinez-Vilalta J., Sala A., Asensio D., Galiano L., Hoch G., Palacio S., … Lloret F. (2016) Dynamics of non-structural carbohydrates in terrestrial plants: A global synthesis. *Ecological Monographs* **86**, 495–516.

McCleary B. V., Gibson T.S. & Mugford D.C. (1997) Measurement of Total Starch in Cereal Products by Amyloglucosidase-α-Amylase Method: Collaborative Study. *Journal of AOAC International* **80**, 571–579.

Mcdowell N., Pockman W.T., Allen C.D., David D., Cobb N., Kolb T., … Yepez E.A. (2008) Mechanisms of plant survival and mortality during drought: why do some plants survive while others succumb to drought? *New Phytologist* **178**, 719–739.

McDowell N.G. (2011) Mechanisms linking drought, hydraulics, carbon metabolism, and vegetation mortality. *Plant physiology* **155**, 1051–1059.

Meinzer F.C., Clearwater M.J. & Goldstein G. (2001) Water transport in trees: current perspectives, new insights and some controversies. *Environmental and Experimental Botany* **45**, 239–262.

Meir P., Mencuccini M. & Dewar R.C. (2015) Drought-related tree mortality: addressing the gaps in understanding and prediction. *New Phytologist* **207**, 28–33.

Mencuccini M., Minunno F., Salmon Y., Martínez-Vilalta J. & Hölttä T. (2015) Coordination of physiological traits involved in drought-induced mortality of woody plants. *New Phytologist* **208**, 396–409.

Mirzaie M., Darvishzadeh R., Shakiba A., Matkan A.A., Atzberger C. & Skidmore A. (2014) Comparative analysis of different uni- and multi-variate methods for estimation of vegetation water content using hyper-spectral measurements. *International Journal of Applied Earth Observation and Geoinformation* **26**, 1–11.

Muggeo V. (2003) Estimating regression models with unknown break-points. *Statistics in Medicine* **22**, 3055–3071.

Muggeo V. (2008) Segmented: an R package to fit regression models with broken-line relationships. *R News* **8**, 20–25.

O'Brien M.J., Leuzinger S., Philipson C.D., Tay J. & Hector A. (2014) Drought survival of tropical tree seedlings enhanced by non-structural carbohydrate levels. *Nature Climate Change* **4**, 1–5.

Olesen P.O. (1971) *Forest tree Improvement Vol. 3: The water displacement method; a fast and accurate method of determining the green volume of wood samples.* Akademisk Forlag.

Plett D.C. & Møller I.S. (2010) Na+ transport in glycophytic plants: What we know and would like to know. *Plant, Cell and Environment* **33**, 612–626.

Pratt R.B., Jacobsen A.L., Ramirez A.R., Helms A.M., Traugh C. a, Tobin M.F., … Davis S.D. (2014) Mortality of resprouting chaparral shrubs after a fire and during a record drought: physiological mechanisms and demographic consequences. *Global change biology* **20**, 893–907.

Rowland L., da Costa A.C.L., Galbraith D.R., Oliveira R.S., Binks O.J., Oliveira A.A.R., … Meir P. (2015) Death from drought in tropical forests is triggered by hydraulics not carbon starvation. *Nature*, 1–13.

Saatchi S., Asefi-Najafabady S., Malhi Y., E. O. C. Aragão L., Anderson L.O., Myneni R.B. & Nemani R. (2013) Persistent effects of a severe drought on Amazonian forest canopy. *Proceedings of the National Academy of Sciences* **110**, 565–570.

Saatchi S.S. & Moghaddam M. (2000) Estimation of crown and stem water content and biomass of boreal forest using polarimetric SAR imagery. *IEEE Transactions on Geoscience and Remote Sensing* **38**, 697–709.

Sack L., John G.P. & Buckley T.N. (2018) ABA accumulation in dehydrating leaves is associated with decline in cell volume not turgor pressure. *Plant Physiology* **176**, 489–493.

Saiki S.T., Ishida A., Yoshimura K. & Yazaki K. (2017) Physiological mechanisms of drought-

induced tree die-off in relation to carbon, hydraulic and respiratory stress in a drought-tolerant woody plant. *Scientific Reports*.

Sala A., Woodruff D.R. & Meinzer F.C. (2012) Carbon dynamics in trees: feast or famine? *Tree physiology* **32**, 764–75.

Sevanto S., McDowell N.G., Dickman L.T., Pangle R. & Pockman W.T. (2014) How do trees die? A test of the hydraulic failure and carbon starvation hypotheses. *Plant, cell & environment* **37**, 153–61.

Sperry J.S., Donnelly J.R. & Tyree M.T. (1988) A method for measuring hydraulic conductivity and embolism in xylem. *Plant, Cell & Environment* **11**, 35–40.

Stocker T.F., D. Qin G.-K., Plattner, Tignor M., Allen S.K., Boschung J., … Midgley P.M. (2015) Summary for Policymakers. In: Climate Change 2013: The Physical Science Basis. Contribution of Working Group I to the Fifth Assessment Report of the Intergovernmental Panel on Climate Change. *CEUR Workshop Proceedings* **1542**, 33–36.

Torres-Ruiz J.M., Jansen S., Choat B., McElrone A.J., Cochard H., Brodribb T.J., … Delzon S. (2015) Direct X-Ray Microtomography Observation Confirms the Induction of Embolism upon Xylem Cutting under Tension. *Plant Physiology* **167**, 40–43.

Torres-Ruiz J.M., Sperry J.S. & Fernández J.E. (2012) Improving xylem hydraulic conductivity measurements by correcting the error caused by passive water uptake. *Physiologia Plantarum* **146**, 129–135.

Trifilo P., Barbera P.M., Raimondo F., Nardini A. & Gullo M. a. L. (2014) Coping with drought-induced xylem cavitation: coordination of embolism repair and ionic effects in three Mediterranean evergreens. *Tree Physiology* **34**, 109–122.

Tyree M.T., Engelbrecht B.M.J., Vargas G., Kursar T. a, States U., Forest A., … Vermont M.T.T. (2003) Desiccation Tolerance of Five Tropical Seedlings in Panama. Relationship to a Field Assessment of Drought Performance. *Plant physiology* **132**, 1439–1447.

Tyree M.T. & Sperry J.S. (1989) Vulnerability of Xylem to Cavitation and Embolism. *Ann. Rev. Plant. Phys. Mol. Bio.* **40**, 19–38.

Ullah S., Skidmore A.K., Naeem M. & Schlerf M. (2012) An accurate retrieval of leaf water content from mid to thermal infrared spectra using continuous wavelet analysis. *Science of the Total Environment* **437**, 145–152.

Ullah S., Skidmore A.K., Ramoelo A., Groen T.A., Naeem M. & Ali A. (2014) Retrieval of leaf

water content spanning the visible to thermal infrared spectra. *ISPRS Journal of Photogrammetry and Remote Sensing* **93**, 56–64.

Urli M., Porté A.J., Cochard H., Guengant Y., Burlett R. & Delzon S. (2013) Xylem embolism threshold for catastrophic hydraulic failure in angiosperm trees. *Tree Physiology* **33**, 672–683.

Veysi S., Naseri A.A., Hamzeh S. & Bartholomeus H. (2017) A satellite based crop water stress index for irrigation scheduling in sugarcane fields. *Agricultural Water Management* **189**, 70–86.

Wang C.-R., Yang A.-F., Yue G.-D., Gao Q., Yin H.-Y. & Zhang J.-R. (2008) Enhanced expression of phospholipase C 1 (ZmPLC1) improves drought tolerance in transgenic maize. *Planta* **227**, 1127–1140.

White P.J. & Broadley M.R. (2001) Chloride in soils and its uptake and movement within the plant: A review. *Annals of Botany* **88**, 967–988.

Williams A., Allen C.D., Macalady A.K., Griffin D., Woodhouse C. a., Meko D.M., … McDowell N.G. (2013) Temperature as a potent driver of regional forest drought stress and tree mortality. *Nature Climate Change* **3**, 292–297.

Yilmaz M.T., Hunt E.R. & Jackson T.J. (2008) Remote sensing of vegetation water content from equivalent water thickness using satellite imagery. *Remote Sensing of Environment* **112**, 2514–2522.

Zhu J.-K. (2016) Abiotic Stress Signaling and Responses in Plants. *Cell* **167**, 313–324.

FIGURES

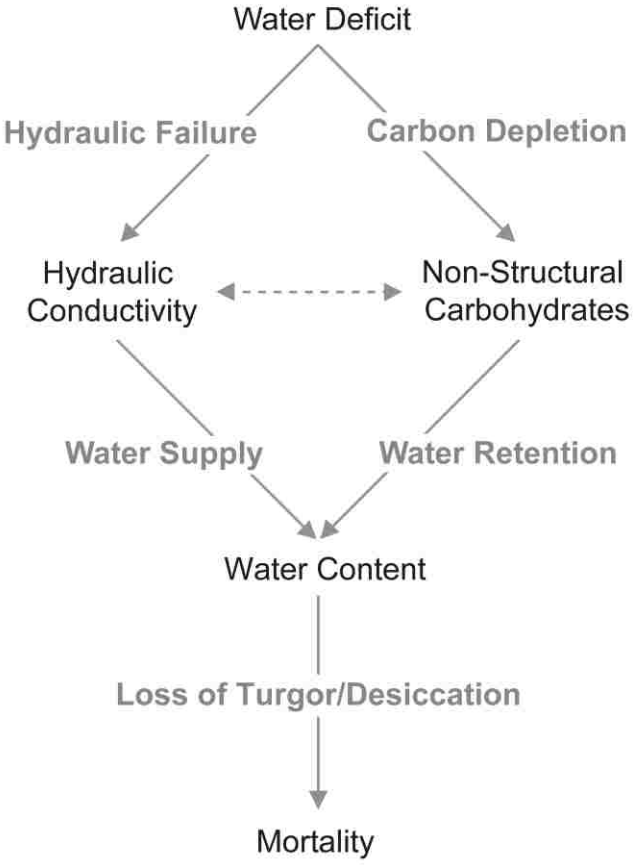

Fig 1. A framework of drought-induced mortality (DIM) focused on plant water content. Plants experience dehydration when water supply is insufficient to replace water loss leading to water deficit. Consequently, xylem tension increases, leading to embolism formation (hydraulic failure). Likewise, stomatal closure eventually leads to carbon depletion during long periods of drought. Loss of hydraulic function and carbon depletion further limit water supply and retention capacity of tissues leading to inability to maintain water balance, loss of turgor/desiccation and death. Black text indicates variables of interest. Grey text indicates DIM mechanisms. Solid arrows link variables within a given mechanism. Dashed arrow indicates potential (but still controversial) interactions between non-structural carbohydrates and hydraulic conductivity (e.g. embolism repair processes).

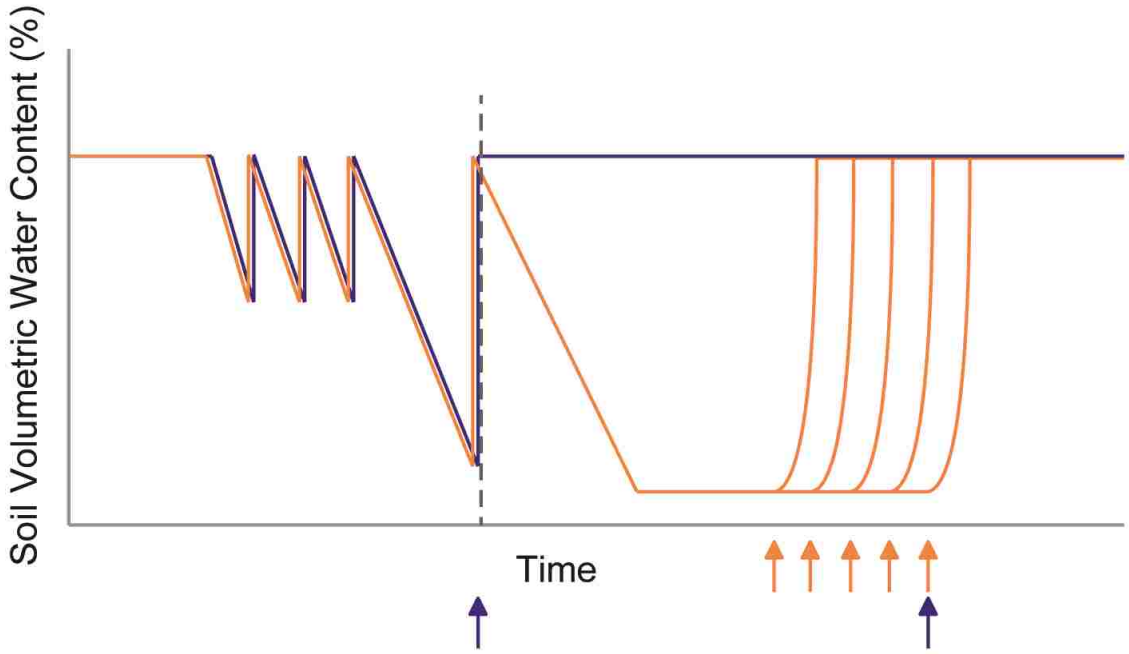

Fig 2. Experimental drought design based on changes in soil volumetric water content (*VWC*$_s$). All seedlings used for the experiment were drought pre-conditioned in four consecutive dry down cycles. The first three lowered the *VWCs* to 50% of field capacity, while the last one to 25% of field capacity. After the last pre-conditioning dry down, five seedlings were kept at field capacity (dark blue) and the rest received no watering (orange). Dark blue represent controls subjected to drought pre-conditioning but kept well-watered through the final dry-down. Orange arrows represent when drought-treated seedlings were measured and the corresponding mortality assessment was conducted (by re-watering a random, independent sample of seedlings). Blue arrows indicate when measurements in control seedlings were done.

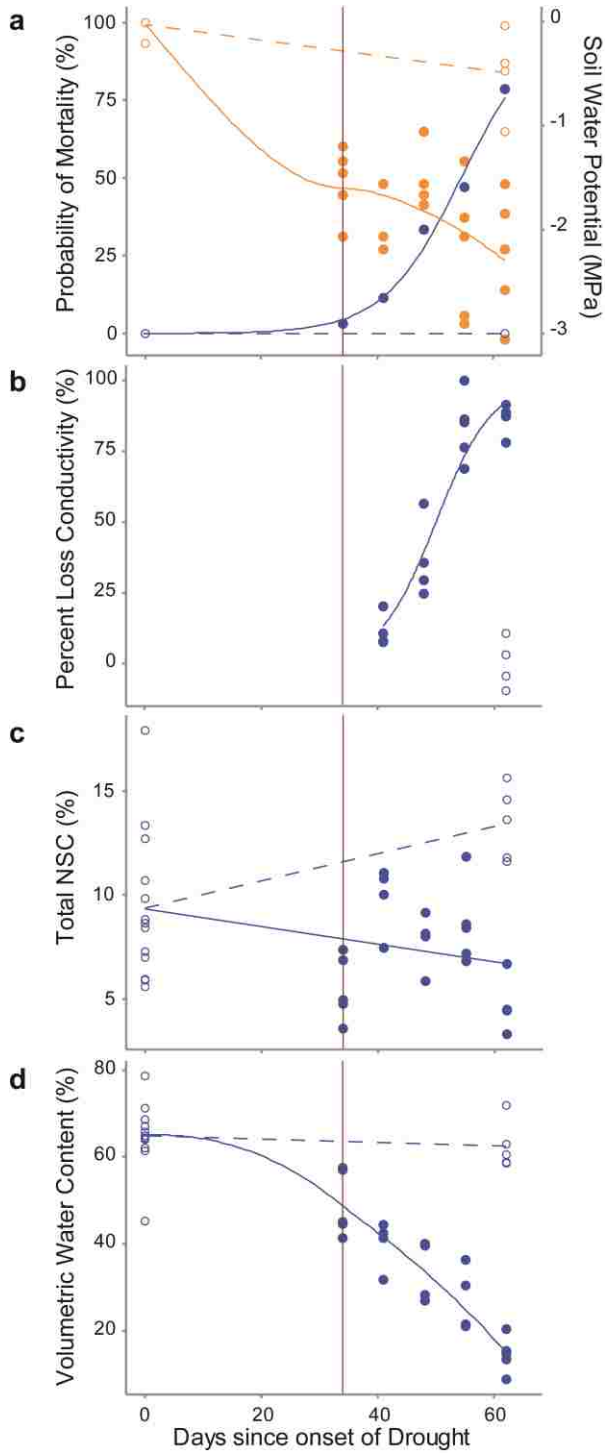

Fig 3. Dynamics of drought intensity, population-level mortality, and whole-plant physiological state over time. Panel A: Probability of mortality (blue) increased after day 34 of drought. Soil water potentials (orange) decreased over time. Panel B: Significant increases of percent loss of conductivity (i.e. *PLC*= 50%) occurred several days after first cases of mortality. Panel C: Non-structural carbohydrate concentrations decreased over time. Panel D: Volumetric

water content experienced a rapid decline once mortality started. Open circles and corresponding dashed lines indicate control groups. Solid regression lines in panels a b and d are loess functions. The regression line in panel c is a linear function. These functions were chosen to best represent the natural behavior of each variable (see Table S1 for statistics). Vertical lines indicate onset of mortality.

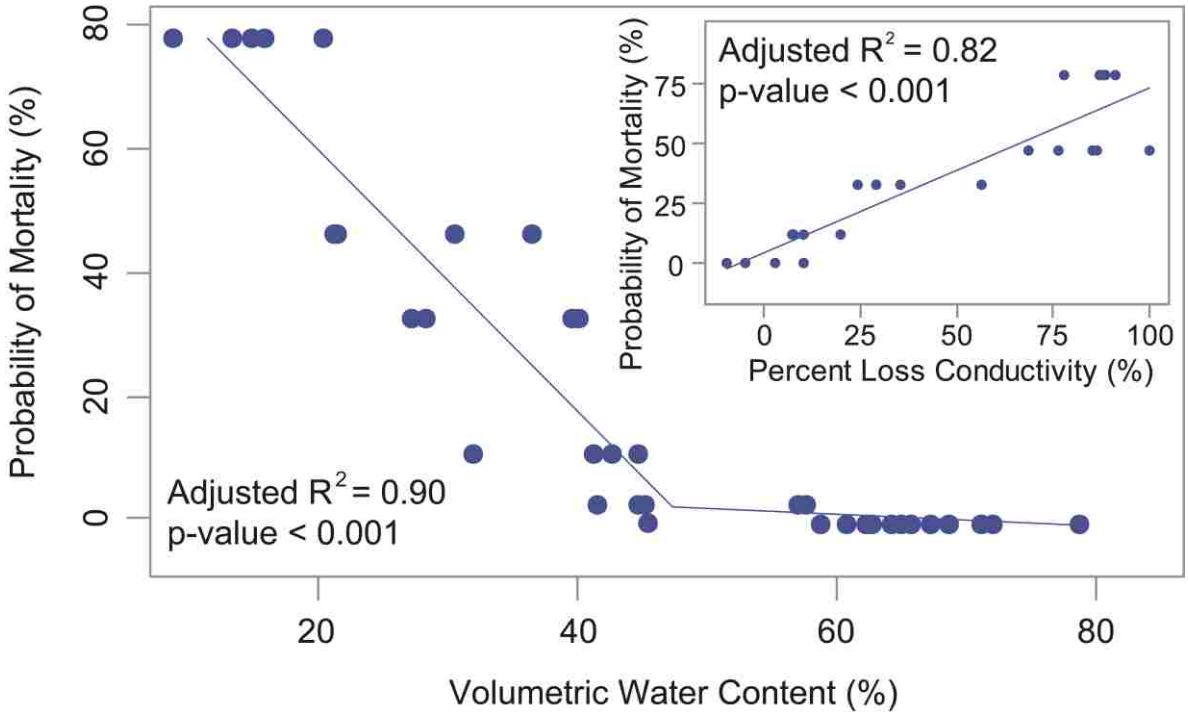

Fig 4. **Plant-level volumetric water content (*VWC*) predicts mortality risk and shows a threshold response (i.e. identifies a threshold of incipient DIM risk) based on segmented linear regression.** Probability of mortality increases sharply after the population reaches *VWC* values above ca. 45%. Percent loss of conductivity (*PLC*) also predicts mortality risk, but in contrast to *VWC*, the response is linear over the full range of *PLC* (inset). Each point corresponds to one plant (n=5 for each probability of mortality with some points overlapping).

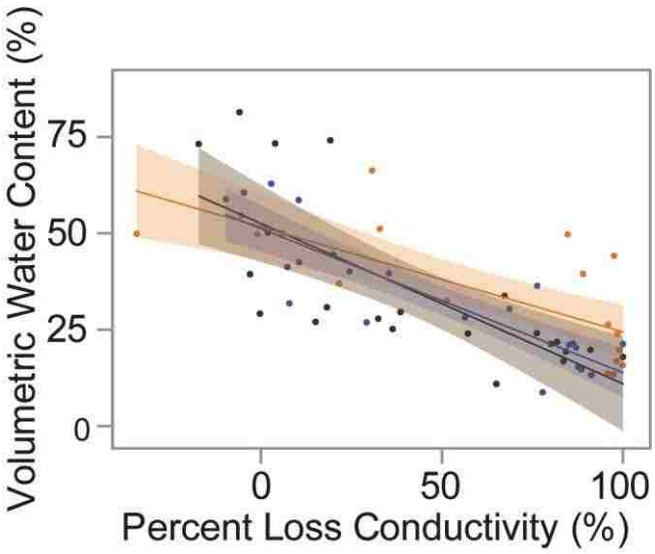

Fig 5. Plant-level volumetric water content (*VWC*) decreases as water supply capacity is lost (measured as the percent loss of conductivity, *PLC*). The response is similar across all measured tissues (stems: orange, roots: brown) and at the whole plant level (blue). Adjusted R^2 values range from 0.52 to 0.74 (Table S4a). Shaded areas represent 95% confidence intervals of the regression lines.

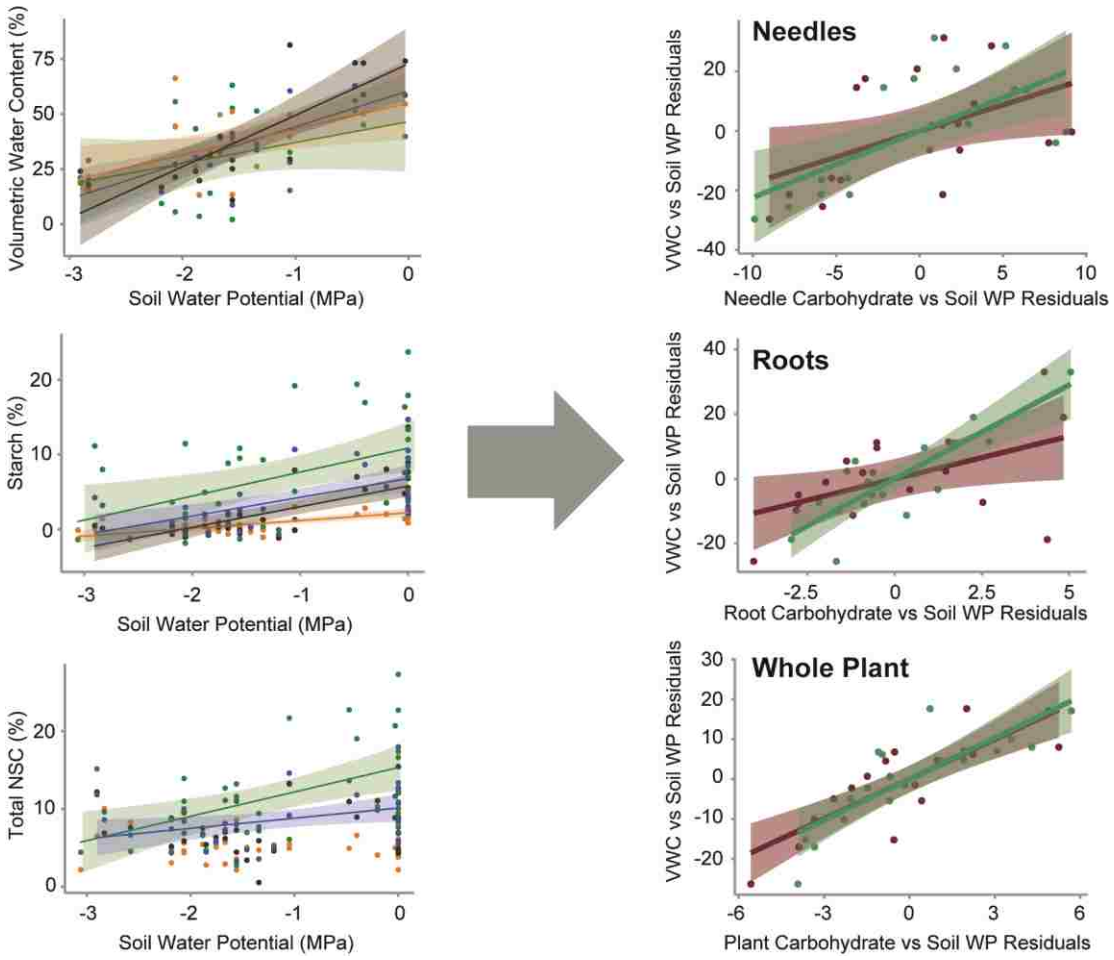

Fig 6. Water retention capacity depends on *NSC* storage. The positive correlation between the residuals of the regression between plant-level volumetric water content (*VWC*) *vs.* soil water potential (WP) and those between non-structural carbohydrates (*NSC*) *vs.* soil water potential indicates that for a given soil WP, if *NSCs* were higher than expected, then *VWC* was also higher than expected. A) Relationship between *VWC* (top), starch concentrations (middle), and Total *NSC* concentrations (bottom) and Soil Water Potential. B) Residuals of the relationship between volumetric water content and Soil Water Potential as a function of residuals of the relationship between *NSC* and Soil Water Potential (purple), and between Starch and Soil Water Potential (dark green) in needles (top), roots (middle) and at the whole plant level (bottom). Carbohydrate contents are represented as percentage of dry mass. Only significant regressions are shown and *NSC* components for which there was no significant relationship (glucose + fructose and sucrose) are not shown. Shaded areas are 95% confidence intervals of the regression lines. P-values in residual analyses ranged between less than 0.001 and 0.04 and adjusted R^2 values ranged between 0.20 and 0.68 (Table S4a & S4b).

SUPPORTING INFORMATION

Methods S1 R code for measuring Hydraulics conductivity and conductance.

```
#########Sensirion SLI-0430 Flow Meter Data Retriever ############

###Author: Gerard Sapes

#####DESCRIPTION:#######
#This program calculates the initial background flow, pressurized flow and
final background flow values needed to
#calculate hydraulic conductivity and conductance. The program also provides
a flow stability criteria based on three measures:
#The change in flow (Delta flow), the change in standard deviation
(DeltaSDflow), and the slope over the last 1200 values (ca.70 seconds).
#You can specify the threshold value at which you consider that the flow is
steady and ready to be recorded.
#The program is built for Sensirion sensors.

#Travels through all the Sensirion CSV datafile. If initial background flow
hasn't been recorded, finds the position
#where the timescale is trunkated, calculates initial background flow as the
mean of the last 300 values and changes the
#initial background flow status to TRUE. If initial background flow has been
calculated but pressurized flow has not,
#the program travels to the next trunkated point and calculates pressurized
flow as the mean of the last 300 values
#and changes pressured flow status to TRUE. If pressurized flow has been
calculated but final background flow has not,
#the program travels to the next trunkated point and calculates final
background flow as the mean of the last 300 values
#and changes final background flow status to TRUE.

######Instructions
#1- Enter the directory path and the name of the files you will create with
the sensors. They should match the name you gave
#them in the sensor interface.
#2-Once, the plant tissue is connected to the apparatus, set the sensors to
RUN and to START logging.
#3-Set valves so that flow only travels through the plant tissue AND without
any pressure coming from the reservoir.
#4-Wait for at least 70 seconds before running the code or you will get an
error message.
#5-Keep running the code to check the stabilization criteria until your
thresholds are met. Then, PAUSE logging to record
#initial background flow.
#6-Open valves so that water flows pressurized from the reservoir to the
plant tissue. Then CONTINUE logging.
#7-Keep running the code to check the stabilization criteria until your
thresholds are met. Then, PAUSE logging to record
#Pressurized flow.
#8-Close valves so that water stops flowing from the reservoir nor the
vertical tubing. Open the loop valves momentarily
#to release the remaining pressure existing between the vertical tube and the
plant tissue. Then close the valves again
```

```
#so that water only flows through the plant tissue at no pressure. Then
CONTINUE logging.
#9-Keep running the code to check the stabilization criteria until your
thresholds are met. Then, PAUSE logging,
#wait for at least a second, and CONTINUE logging again to record final
background flow.

#####Considerations
#The program needs a minimum amount of 1200 values in the CSV file before
correctly reporting stability criteria. Wait a couple
#of minutes from the moment you start loging for the program to start working
properly. If you do not wait enough
#you will receive an error message.

#Because of how I constructed the loop, the results are reported 3 times for
each sensor as the measurements are taken... but
#it's a free software so we can tolerate this right? :)

##Packages
library(ggplot2)
library(Rmisc)

##############Hydroflow Function#############

hydroflow <-
function(data,filename,stable_deltaflow,stable_deltaSDflow,stable_slope.Ymin,
Ymax){

  ##Loading CSV file and preparing data to graph

  colnames(data) <- c('Sample','Time','Flow_rate')
  data$Time <- as.numeric(gsub(",","", data$Time))
  data$Relative_Time <- data$Time-data$Time[1]
  x<- data$Relative_Time
  y<- data$Flow_rate

  SampleID <- paste('Sample ID:', filename)

  ##Initial Checkpoint statuses
  initial_bg_status <- F
  pressured_flow_status <- F
  final_bg_status <- F

  ##Stabilization criteria

  #Calculates change in flow during the last ca. 70 seconds. When delta
approximates 0 flow has stabilized
  # and measurements can be taken. The range of values used to calculate
delta is shown in purple on the graph

  deltaflow <- mean(y[(length(y)-600):length(y)])-mean(y[(length(y)-
1200):(length(y)-600)])

  if (deltaflow >= stable_deltaflow | deltaflow <= -stable_deltaflow){
    deltaflow_status <- 'UNSTABLE'
  } else {
    deltaflow_status <- 'OK'
```

```
  }

  #Calculates change in standard deviation of flow during the last ca. 70
seconds. When delta approximates 0 flow has stabilized
  # and measurements can be taken. The range of values used to calculate
delta is shown in purple on the graph

  deltasdflow <- sd(y[(length(y)-600):length(y)])-sd(y[(length(y)-
1200):(length(y)-600)])

  if (deltasdflow >= stable_deltaSDflow | deltasdflow <= -
stable_deltaSDflow){
    deltaSDflow_status <- 'UNSTABLE'
  } else {
    deltaSDflow_status <- 'OK'
  }
  #Calculates the slope in the graph for the last ca. 70 seconds. When slope
approximates 0 flow has stabilized
  # and measurements can be taken. The range of values used to calculate the
slope is shown in purple on the graph

  slopefile <- data[(length(y)-1200):length(y),]
  n <- nrow(slopefile)
  xy <- x*y

  slope <- (n*sum(xy)-sum(x)*sum(y)) / (n*sum(x^2)-sum(x)^2)

  if (slope >= stable_slope | slope <= -stable_slope){
    slope_status <- 'UNSTABLE'
  } else {
    slope_status <- 'OK'
  }

  #Calculates the average flow in the graph for the last ca. 70 seconds. The
range of values used to calculate the
  #slope is shown in purple on the graph.

  meanflow <- mean(y[(length(y)-1200):length(y)])

  ##Plotting data

  graph<- ggplot(data, aes(x=data[,4], y=data[,3]), environment =
environment()) +
    geom_line(aes(group=1), colour='#33CC00') +
    ylab('Flow rate (ul/min)') +
    xlab('Time (seconds)') +
    theme_bw() +
    theme(panel.border = element_blank(), panel.grid.major = element_blank(),
          panel.grid.minor = element_blank(), axis.line = element_line(colour
= "black"),
          plot.title = element_text(lineheight = .8,face='bold')) +
    ggtitle(filename)

  graph + geom_vline(xintercept = x[length(x)],colour='purple') +
    geom_vline(xintercept = x[length(x)-1200],colour='purple')

  ##Scanning for background and pressured flow values
```

```
  for (i in 2:length(x)){
    if (initial_bg_status == F && x[i]-x[i-1]>= 1){
      initial_bg <- mean(y[i-1]:y[i-301])
      InBGFlow_rows <- paste('Initial Background Flow measured using
rows:',i-301,'-', i-1,'(Light Blue)')
      graph <- graph + coord_cartesian(ylim = c(Ymin, Ymax)) +
geom_vline(xintercept = x[i-301],colour='light blue') +
        geom_vline(xintercept = x[i-1],colour='light blue')

      InBGFlow <- paste('Initial Background Flow is:', initial_bg)

      writeLines(paste('-------------------------------------------','\n---
-----------------------------------------',
                       '\n\n',SampleID,'\n\n','Flow Stabilization criteria
(based on last ca. 70 secs):\n\nDelta Flow is:',
                       deltaflow, '   ', deltaflow_status,'\nDelta SD Flow
is:',deltasdflow, '   ',deltaSDflow_status,
                       '\nSlope is:',slope, '   ',
slope_status,'\n\n','Current flow is:',meanflow,'\n\n','------------RESULTS--
----------',
                       '\n\n', InBGFlow_rows,'\n\n', InBGFlow))

      initial_bg_status <- T
      i<-i+1

    } else if (initial_bg_status == T && pressured_flow_status == F && x[i]-
x[i-1]>= 1){
      pressured_flow <- mean(y[i-1]:y[i-301])
      PFlow_rows <- paste('Pressured Flow measured using rows:',i-301,'-', i-
1,'(Dark Blue)')
      graph<- graph + geom_vline(xintercept = x[i-301],colour='dark blue') +
        geom_vline(xintercept = x[i-1],colour='dark blue')
      PFlow <- paste('Pressured Flow is:',pressured_flow)

      writeLines(paste('-------------------------------------------','\n---
-----------------------------------------',
                       '\n\n',SampleID,'\n\n','Flow Stabilization criteria
(based on last ca. 70 secs):\n\nDelta Flow is:',
                       deltaflow, '   ', deltaflow_status,'\nDelta SD Flow
is:',deltasdflow, '   ',deltaSDflow_status,
                       '\nSlope is:',slope, '   ',
slope_status,'\n\n','Current flow is:',meanflow,'\n\n','------------RESULTS--
----------',
                       '\n\n', InBGFlow_rows,'\n', PFlow_rows,'\n\n',
InBGFlow,'\n', PFlow))

      pressured_flow_status <- T
      i<-i+1

    } else if (pressured_flow_status == T && final_bg_status == F  && x[i]-
x[i-1]>= 1){
      final_bg <- mean(y[i-300]:y[i-1])
      FiBGFlow_rows <- paste('Final Background Flow measured using rows:',i-
300,'-', i-1,'(Light Blue)')
      graph<- graph + geom_vline(xintercept = x[i-300],colour='light blue') +
        geom_vline(xintercept = x[i-1],colour='light blue')
```

```
      FiBGFlow <- paste('Final Background Flow is:',final_bg)

      writeLines(paste('-------------------------------------------','\n---
-----------------------------------------',
                       '\n\n',SampleID,'\n\n','Flow Stabilization criteria
(based on last ca. 70 secs):\n\nDelta Flow is:',
                       deltaflow, '   ', deltaflow_status,'\nDelta SD Flow
is:',deltasdflow, '   ',deltaSDflow_status,
                       '\nSlope is:',slope, '   ',
slope_status,'\n\n','Current flow is:',meanflow,'\n\n','------------RESULTS--
----------',
                       '\n\n', InBGFlow_rows,'\n', PFlow_rows,'\n',
FiBGFlow_rows,'\n\n', InBGFlow,'\n', PFlow,'\n', FiBGFlow))

      final_bg_status <- T
      i<-i+1

    } else if (initial_bg_status == F && i==length(x)){

      writeLines(paste('-------------------------------------------','\n---
-----------------------------------------',
                       '\n\n',SampleID,'\n\n','Flow Stabilization criteria
(based on last ca. 70 secs):\n\nDelta Flow is:',
                       deltaflow, '   ', deltaflow_status,'\nDelta SD Flow
is:',deltasdflow, '   ',deltaSDflow_status,
                       '\nSlope is:',slope, '   ',
slope_status,'\n\n','Current flow is:',meanflow,'\n\n'))

    } else {
      i<-i+1
    }
  }

  graph<-graph + geom_vline(xintercept = x[length(x)],colour='purple') +
    geom_vline(xintercept = x[length(x)-1200],colour='purple')


  return(graph)

}

#####User-defined variables######

##Files
directory <-
'D:/Gerard/University_of_Montana/Thesis/Chapter_1/Sensirion_measurements/'
#Enter the name of the csv file currentlly being created by the Sensirion
sensor

filename_1 <- 'C8_RMR_1260_Roots.csv'
filename_2 <- 'C8_CP_47_Roots.csv'
filename_3 <- 'C8_RMR_180_Roots.csv'
#Y axis size
Ymax <- 10  # Enter the expected maximum value of flow here to better
visualize your graph
Ymin <- -1 # Enter the expected minimum value of flow here to better
visualize your graph
```

```
##Stability Thresholds
stable_deltaflow <- 0.1  # Enter the maximum change in flow over 70 secs.
that you consider acceptable as STABLE
stable_deltaSDflow <- 0.04 # Enter the maximum change in standard deviation
of flow over 70 secs. that you consider acceptable as STABLE
stable_slope <- 0.05  # Enter the minimum slope over 70 secs. that you
consider acceptable as STABLE

#############Program#############
#Loading Data

data_sensor_1 <- read.csv(paste(directory,filename_1,sep=''),header=T,
sep=",", dec='.')
data_sensor_2 <- read.csv(paste(directory,filename_2,sep=''),header=T,
sep=",", dec='.')
data_sensor_3 <- read.csv(paste(directory,filename_3,sep=''),header=T,
sep=",", dec='.')

#Calling function

#interval = 120
#repeat {
#  startTime = Sys.time()
#
sensor_1 <-
hydroflow(data_sensor_1,filename_1,stable_deltaflow,stable_deltaSDflow,stable
_slope.Ymin,Ymax)
sensor_2 <-
hydroflow(data_sensor_2,filename_2,stable_deltaflow,stable_deltaSDflow,stable
_slope.Ymin,Ymax)
sensor_3 <-
hydroflow(data_sensor_3,filename_3,stable_deltaflow,stable_deltaSDflow,stable
_slope.Ymin,Ymax)

#Plotting

if (exists("sensor_1") == T && exists("sensor_2") == T && exists("sensor_3")
== T){
  multiplot(sensor_1,sensor_2,sensor_3,layout=matrix(c(1,2,3,3), nrow=2,
byrow=T))
  } else if (exists("sensor_1") == T && exists("sensor_2") == T &&
exists("sensor_3") == F){
    multiplot(sensor_1,sensor_2,layout=matrix(c(1,1,2,2), nrow=2, byrow=T))
  } else if (exists("sensor_1") == T && exists("sensor_2") == F &&
exists("sensor_3") == T){
    multiplot(sensor_1,sensor_3,layout=matrix(c(1,1,2,2), nrow=2, byrow=T))
  } else if (exists("sensor_1") == F && exists("sensor_2") == T &&
exists("sensor_3") == T){
    multiplot(sensor_2,sensor_3,layout=matrix(c(1,1,2,2), nrow=2, byrow=T))
  } else if (exists("sensor_1") == T && exists("sensor_2") == F &&
exists("sensor_3") == F){
    sensor_1
  } else if (exists("sensor_1") == F && exists("sensor_2") == T &&
exists("sensor_3") == F){
    sensor_2
```

```
  } else if (exists("sensor_1") == F && exists("sensor_2") == F &&
exists("sensor_3") == T){
    sensor_3
  } else {
    writeLines(paste('\n\n','Error: Files not found or minimal time needed
for stabilization routines not met'))
  }
```

Methods S2. Sensitivity analysis assessing the effects of sample size on threshold detectability. We tested the potential effects of sample size on the detection of incipient mortality thresholds in *VWC* by removing *VWC* data of days 0 and 34 and generating a thousand iterations of the segmented regression. We calculated the probability of finding an incipient mortality threshold as the number of times that a threshold was found at *VWC* values associated with mortality risk near zero. These regressions still found an incipient threshold in 530 of the thousand iterations (53 %) that were ran (Panel B). In the other instances, a threshold was still found but at higher mortality. Without removing these data, the incipient threshold was found in 1000 out of a thousand iterations (100 %) (Panel A). We also generated a thousand iterations of the segmented regression between *PLC* and probability of mortality to assess the robustness of our findings. Accordingly, no incipient mortality threshold was found in any of the iterations (0 %) for *PLC* (Panel C).

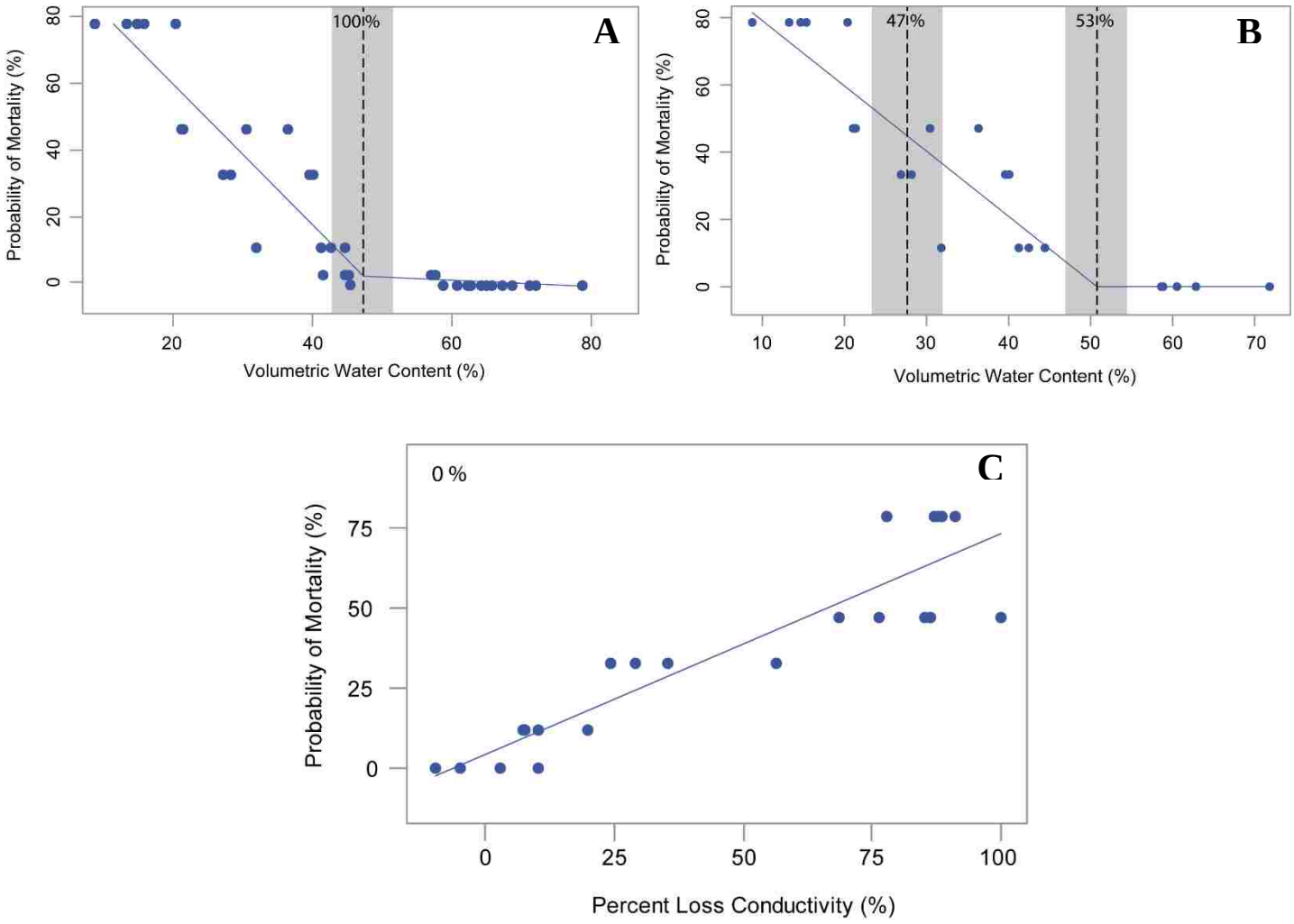

Methods S3. Sensitivity analysis assessing the effects of maximum conductivity on percent loss conductivity values.

We tested the potential effects of *Kmax* on the detection of incipient mortality thresholds in *PLC* by simulating *Kmax* estimates with added uncertainty. We randomly generated a normal distribution of a thousand *Kmax* values with a mean equal to the average *K* of controls and a standard deviation equal to the standard deviation of the mean *K* of controls. Then, we recalculated *PLC* for each individual using each of the generated *Kmax* values (1000 *PLC* estimates per individual were obtained). Finally we run a thousand iterations of the segmented regressions using the thousand different sets of *PLC* values and extracted the distribution of threshold values for *PLC*. This analysis detected an important influence of *Kmax* on low *PLC* values and a threshold around *PLC* = 85, corresponding to 63% probability of mortality (see figure below). However, no threshold was detected below ca. *PLC* = 70 in any of the thousand iterations of the segmented regression despite the effect of *Kmax* on the relationship between *PLC* and mortality at low *PLC* values. Blue points and line indicate actual data. Red points and grey lines indicate simulated data. Dashed line and the gradient around it indicate the mean threshold +/- one standard distribution for simulated data.

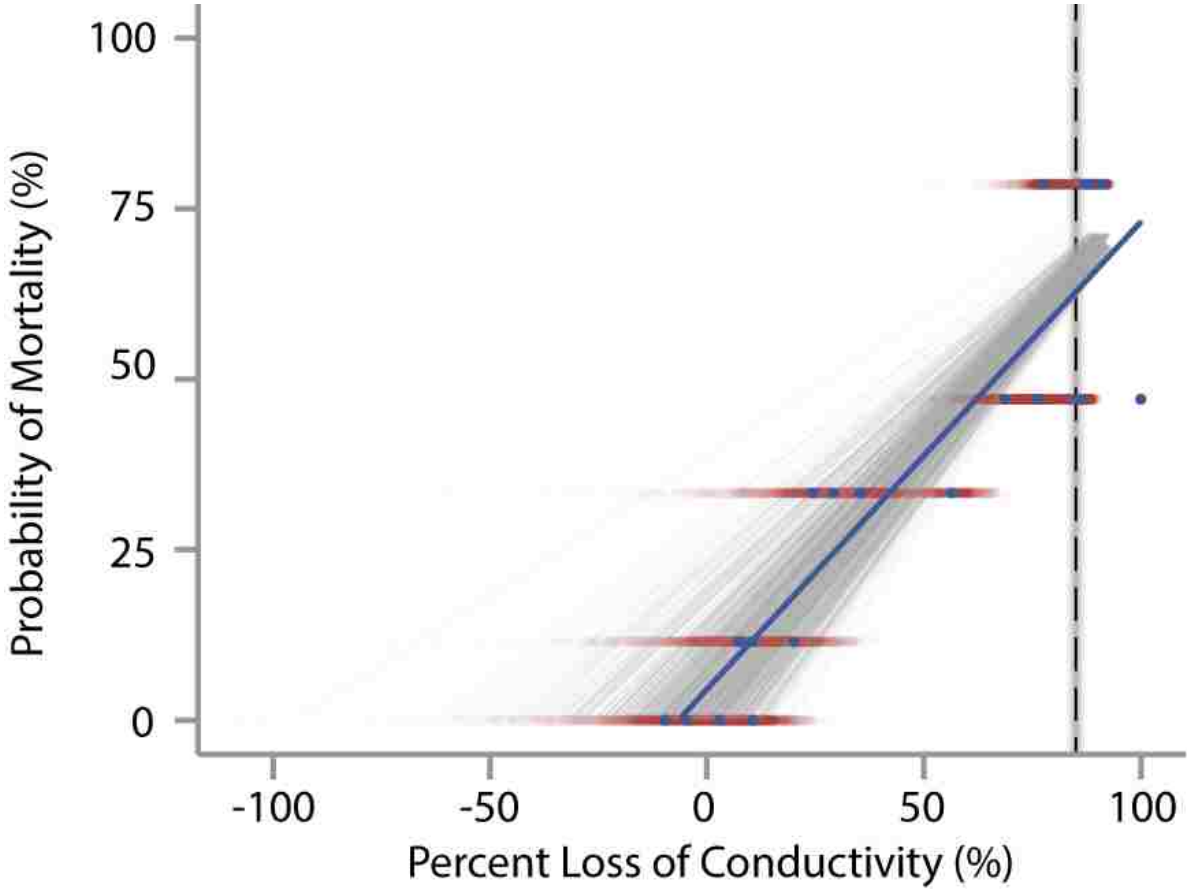

Figure S1. Depletion of NSC pools under drought. Non-structural carbohydrate pools (by component and total) as function of soil water potential in needles (green), stems (orange), roots (brown), and at the whole plant level (blue). Carbohydrate contents are represented as percentage of dry mass. Only significant regressions are shown. Shaded areas are 95% confidence intervals of the regression line. P-values ranged between less than 0.001 and 0.04 and R2 values ranged between 0.13 and 0.73.

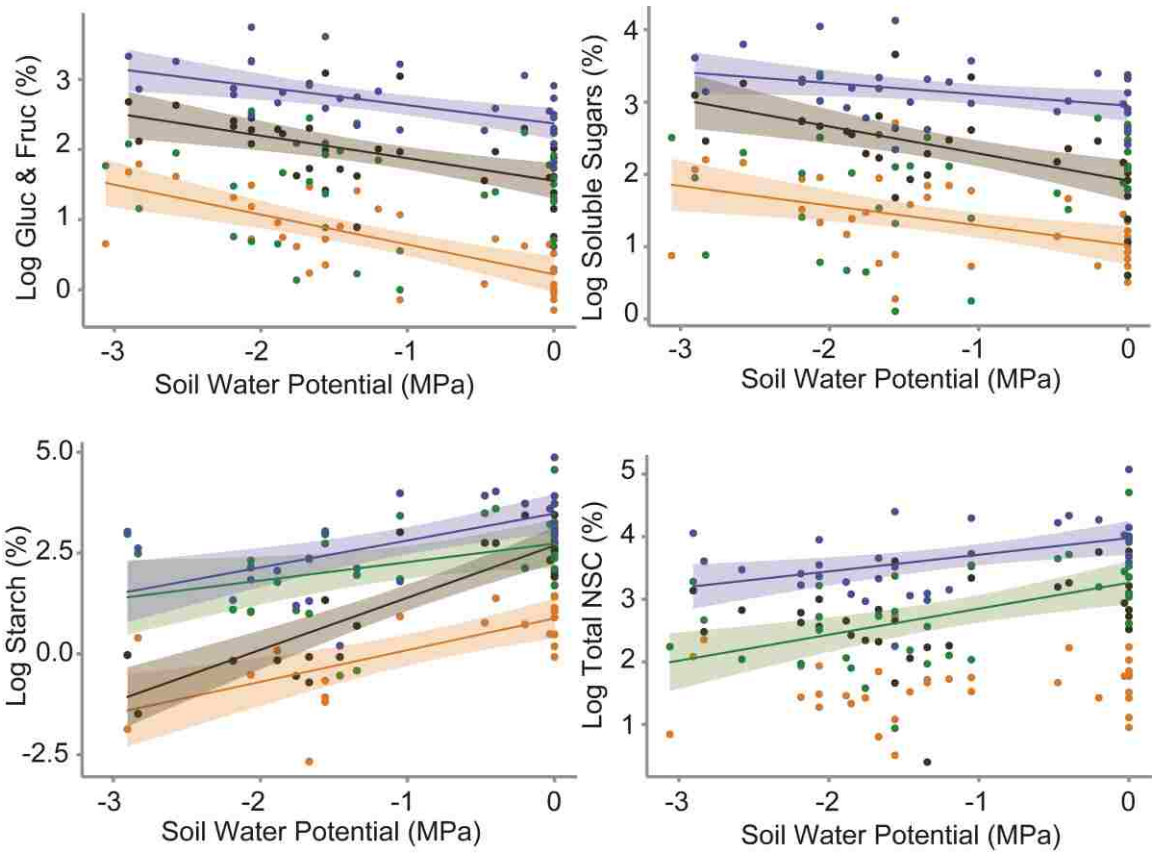

Figure S2. Volumetric water content predicts mortality across needles (green), stems (orange), and roots (brown). Breaking points between mortality and volumetric water content of needles and roots did not significantly differ from each other. All p-values were lower than 0.001 and adjusted R^2 values ranged between 0.69 and 0.78.

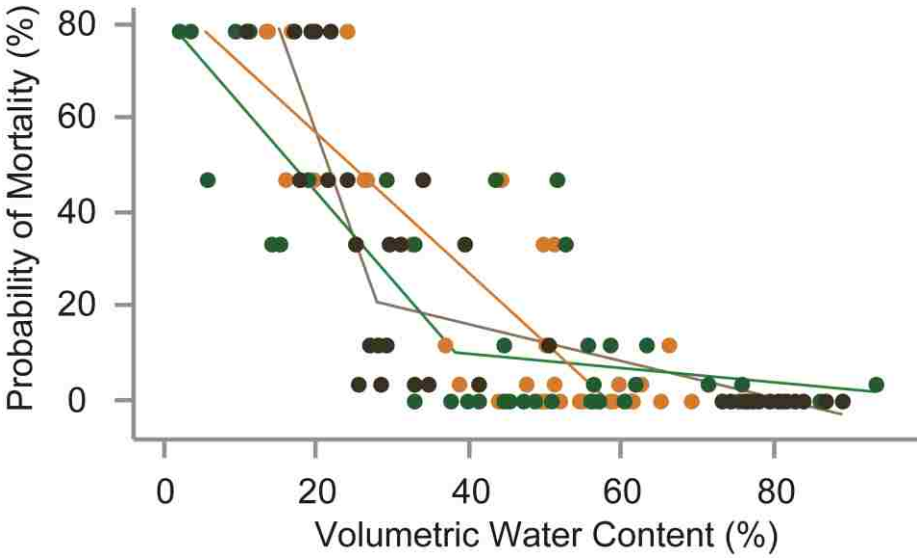

Figure S3. NSC and its components are not good predictors of mortality. Carbohydrate contents are represented as percentage of dry mass. Left panel: Starch concentrations at the whole plant level. Right panel: Total NSC at the whole plant level. Both relationships are significant but show low adjusted R^2 values.

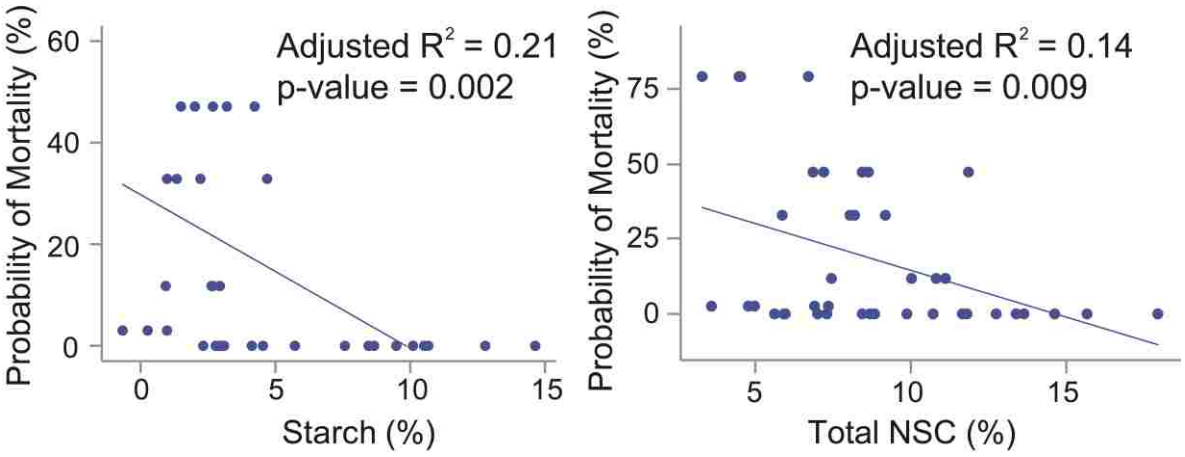

Figure S4. Volumetric water content decreases as non-structural carbohydrates decrease, as shown by the relationships between Volumetric Water Content and NSC components in needles (green), stems (orange), roots (brown), and at the whole plant level (blue). Carbohydrate contents are represented as percentage of dry mass. Regression lines are shown for significant relationships only. Shaded areas are 95% confidence intervals of the regression line. P-values ranged between less than 0.001 and 0.06 and R2 values ranged between 0.10 and 0.58.

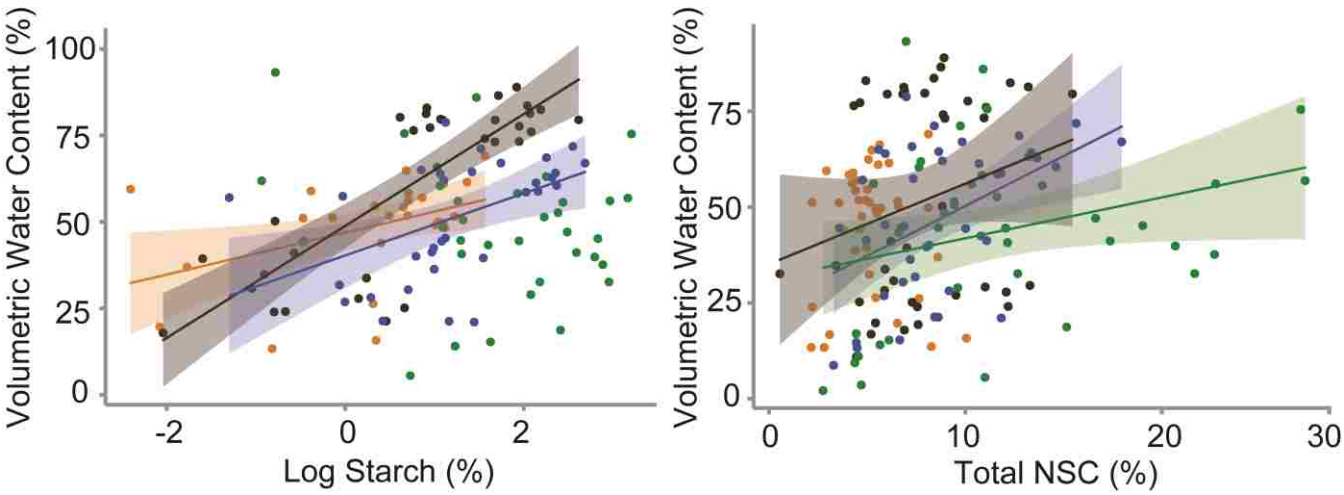

Table S1. Models assessing changes in drought intensity, whole-plant physiological status, and population-level mortality over time. Full models with non-significant variables not shown. Linear models were used for soil water potential, total *NSC*, and *VWC* given that response variables could be transformed to meet model assumptions. Generalized linear models with binomial distribution were used for *PLC* and probability of mortality. *PLC* and probability of mortality where expressed on a per unit basis following requirements of models with binomial distributions.

Model and Factors	**Model type**	**Estimate**	**95% C.I. Estimates**		***p-value***	**d.f. (res.)**	**Adjusted R square**
			2.5%	**97.5%**			
Soil Water Potential =Days since Onset of Drought					**< 0.001**	30	0.82
Intercept	LM	-0.07708	-0.3380643	0.18389813	0.551	-	-
Days since Onset of Drought		-0.03699	-0.0433191	-0.0306578	**< 0.001**	-	-
Plant NSC Concentrations = Days since Onset of Drought					**0.044**	33	0.09
Intercept	LM	9.31706	7.73983095	10.8942943	**< 0.001**	-	-
Days since Onset of Drought		-0.04214	-0.0829767	-0.0013115	**0.044**	-	-
log(Plant VWC) = Days since Onset of Drought					**< 0.001**	34	0.74
Intercept	LM	4.253857	4.09723357	4.41048039	**< 0.001**	-	-
Days since Onset of Drought		-0.01932	-0.0232866	-0.0153490	**< 0.001**	-	-
Plant PLC/100 = Days since Onset of Drought						16	NA
Intercept	GLM	-10.3141	-22.200904	-2.2965819	**0.032**	-	-
Days since Onset of Drought		0.20603	0.05139158	0.4374114	**0.028**	-	-
Probability of Mortality/100 = Days since Onset of Drought						40	NA
Intercept	GLM	-8.17236	-15.365634	-3.7203390	**0.005**	-	-
Days since Onset of Drought		0.15000	0.06799845	0.2805273	**0.005**	-	-

Table S2. Linear models predicting probability of Mortality as function of *PLC*, *NSC* (and its components), and *VWC*. Models are sorted in descending order by best fit and simplicity based on Adjusted R2 and AIC. Full models with non-significant variables (i.e. Starch) not shown.

Model and Factors	Estimate	95% C.I. Estimates		*p-value*	d.f. (res.)	Adjusted R square	AIC
		2.5%	97.5%				
Probability of Mortality = log(Plant VWC)				< **0.001**	39	0.87	-68.84
Intercept	1.95323	1.7363176	2.170149	< **0.001**	-	-	-
log(Plant VWC)	-0.47164	-0.5294125	-0.413869	< **0.001**	-	-	-
Probability of Mortality = Plant PLC + Plant NSC Concentrations				< **0.001**	18	0.91	-37.60
Intercept	0.4664640	0.271083252	0.661844718	< **0.001**	-	-	-
Plant PLC	0.0046814	0.003337284	0.006025493	< **0.001**	-	-	-
Plant NSC Concentrations	-0.0378331	-0.054587488	-0.021078792	< **0.001**	-	-	-
Probability of Mortality = Plant PLC				< **0.001**	20	0.82	-24.46
Intercept	0.0441359	-0.044440599	0.132712302	0.311	-	-	-
Plant PLC	0.0068423	0.005367984	0.008316518	< **0.001**	-	-	-
Probability of Mortality = Plant PLC + Plant Soluble Sugar Concentrations				< **0.001**	18	0.80	-20.79
Intercept	0.0816678	-0.108392585	0.271728185	0.379	-	-	-
Plant PLC	0.0066867	0.005125231	0.008248081	< **0.001**	-	-	-
Plant Soluble Sugar Concentrations	-0.0066286	-0.038449437	0.025192299	0.667	-	-	-
Probability of Mortality = Plant NSC Concentrations				**0.009**	38	0.14	5.01
Intercept	0.46	0.2436815	0.676318147	< **0.001**	-	-	-
Plant NSC Concentrations	-0.03137	-0.0544841	-0.008246711	**0.009**	-	-	-
Probability of Mortality = Plant Soluble Sugar Concentrations				**0.0272**	38	0.10	7.05

Intercept	-0.06602	-0.30213946	0.17009931	0.5747	-	-	-
Plant Soluble Sugar Concentrations	0.05100	0.00606307	0.09593456	**0.0272**	-	-	-

Table S3. Segmented models predicting probability of Mortality as function of *VWC* and their corresponding linear models. Segmented models were only used if their ΔAIC (AIC simple linear model – AIC segmented model) was greater than 10 (see reference 38 in main document). Otherwise, simple linear regressions were applied. Segmented models for *PLC* and *NSC* failed to detect breakpoints (i.e. thresholds) and are not included.

Model and Factors	**Estimate**	***p-value***	**Breakpoint & C.I.**	**d.f. (res.)**	**Adjusted R square**	**ΔAIC**
Probability of Mortality = Plant VWC		**< 0.001**	47.3 ± 7.61	37	0.90	27.39
Intercept	1.021509	**< 0.001**	-	-	-	-
Plant VWC	-0.021226	**< 0.001**	-	-	-	-
U1. Plant VWC	0.020380	NA	-	-	-	-
Probability of Mortality = Needle VWC		**< 0.001**	38.3 ± 11.89	36	0.69	13.85
Intercept	0.819363	**< 0.001**	-	-	-	-
Needle VWC	-0.018840	**< 0.001**	-	-	-	-
U1. Needle VWC	0.017309	NA	-	-	-	-
Probability of Mortality = Stem VWC		**< 0.001**	Not detected	39	0.75	0
Intercept	0.870377	**< 0.001**	-	-	-	-
Stem VWC	-0.014966	**< 0.001**	-	-	-	-
Probability of Mortality = Root VWC		**< 0.001**	27.9 ± 3.67	38	0.78	26.76
Intercept	1.496336	**< 0.001**	-	-	-	-
Root VWC	-0.046331	**< 0.001**	-	-	-	-
U1. Root VWC	0.042396	NA	-	-	-	-

Table S4a. Significant linear models predicting VWC as function of *PLC* and *NSC* for each tissue and at the whole plant level.

Model and Factors	Estimate	95% C.I. Estimates		*p-value*	d.f. (res.)	Adjusted R square
		2.5%	97.5%			
Plant VWC= Plant PLC				**<0.001**	20	0.74
Intercept	51.18226	45.1871346	57.1773949	**<0.001**	-	-
Plant PLC	-0.37327	-0.4730545	-0.2734885	**<0.001**	-	-
Stem VWC = Stem PLC				**<0.001**	19	0.54
Intercept	51.60841	43.0292752	60.1875516	**<0.001**	-	-
Stem PLC	-0.27180	-0.3874893	-0.1561097	**<0.001**	-	-
Root VWC = Root PLC				**<0.001**	20	0.52
Intercept	52.52591	42.5576402	62.4941876	**<0.001**	-	-
Root PLC	-0.41544	-0.5941348	-0.2367427	**<0.001**	-	-
Residuals Plant VWC vs Soil WP = Residuals Plant NSC vs Soil WP				**<0.001**	16	0.67
Intercept	2.758e-16	-3.345780	3.345780	1	-	-
Residuals Plant NSC vs Soil WP	3.318	2.142986	4.493076	**<0.001**	-	-
Residuals Needle VWC vs Soil WP = Residuals Needle NSC vs Soil WP				**0.037**	16	0.20
Intercept	5.267e-16	-8.4602577	8.460258	1	-	-
Residuals Needle NSC vs Soil WP	1.755	0.1189953	3.390435	**0.037**	-	-
Residuals Root VWC vs Soil WP = Residuals Root NSC vs Soil WP				**0.0314**	16	0.21
Intercept	5.270e-17	-6.1267231	6.1267231	1	-	-
Residuals Root NSC vs Soil WP	2.636	0.2663532	5.005323	**0.0314**	-	-

Table S4b. Significant linear models predicting VWC as function of Starch. Soluble sugars did not show a significant relationship with *VWC* in any tissue.

Model and Factors	Estimate	95% C.I. Estimates		*p-value*	d.f. (res.)	Adjusted R square
		2.5%	97.5%			
Residuals Plant VWC vs Soil WP = Residuals Plant Starch vs Soil WP				**<0.001**	16	0.66
Intercept	-3.977e-17	-3.406275	3.406275	1	-	-
Residuals Plant Starch vs Soil WP	3.448	2.194836	4.701916	**<0.001**	-	-
Residuals Needle VWC vs Soil WP = Residuals Needle Starch vs Soil WP				**0.003**	16	0.39
Intercept	3.359e-16	-7.3687150	7.3687150	1	-	-
Residuals Needle Starch vs Soil WP	2.241	0.8642181	3.617169	**0.003**	-	-
Residuals Root VWC vs Soil WP = Residuals Root Starch vs Soil WP				**<0.001**	16	0.68
Intercept	9.866e-17	-3.886078	3.886078	1	-	-
Residuals Root Starch vs Soil WP	5.813	3.803182	7.822944	**<0.001**	-	-

CHAPTER 2: INTRASPECIFIC VARIATION IN MORPHOLOGY AND PHYSIOLOGY INFLUENCES INDICATORS OF DROUGHT-INDUCED MORTALITY RISK

ABSTRACT

Widespread drought-induced forest mortality (DIM) is expected to increase with climate change and drought, with major impacts on carbon and water cycles. Anticipating and predicting the global impacts of DIM requires large-scale assessments of DIM risk but indicators that can accurately predict DIM risk across the landscape are rare. The main challenge that large-scale assessments of DIM risk face is finding indicators that predict DIM risk regardless of variation in morphology and physiology across the landscape. We assessed whether intraspecific variation in morphology and physiology among *Pinus ponderosa* populations translates into variation in incipient mortality thresholds or predictive power of water potential, percent loss of conductivity (PLC), and relative water content (RWC). We found that intraspecific variation can significantly influence incipient mortality thresholds and predictive power in PLC. However, water potential and RWC showed consistent incipient mortality thresholds and high predictive power among populations and across organs. Both water potential and RWC are promising candidates for large-scale assessments of DIM risk. RWC is of special interest because it integrates different physiological drivers of DIM, allows comparisons across species, and can be remotely sensed. Our results offer promise for landscape level monitoring of DIM risk.

INTRODUCTION

Drought-induced forest mortality (DIM) is a major cause of forest die-off and is expected to increase in many regions (both in frequency and intensity) with climate change (Dai 2013; Trenberth *et al.* 2014; Greenwood *et al.* 2017). Increases in DIM are expected to severely impact carbon cycles, species distributions, the economy, and global climate feedbacks (Stocker *et al.* 2013). Anticipating (for the purposes of active management) and predicting the global impacts of DIM requires large-scale monitoring of DIM risk that provide early warning signals. However, large-scale assessments of DIM risk are rare and lack accuracy, in part, because we lack information on the properties of potential indicators (Hartmann *et al.* 2015). Ideally, accurate, large-scale indicators of DIM risk should i) consistently predict DIM risk across plants of

varying morphology, physiology, and drought strategies and ii) distinguish healthy populations (no risk) from those at risk of DIM (i.e., should show an incipient mortality threshold) (Martinez-Vilalta et al. *in review*). Thus, the first step towards accurate large-scale monitoring of DIM risk is identifying which indicators show consistent incipient mortality thresholds and high predictive power.

Mortality thresholds and the predictive power of DIM risk indicators can vary due to morphological and physiological variation within and among species. Under drought, plants avoid lethal desiccation by continuously supplying water to critical living tissues, preventing water loss, or both. Plants can maintain water supply through a variety of strategies including deep root systems (Matías, González-Díaz & Jump 2014), using stored water (i.e., drought-avoidant) (Mcculloh *et al.* 2014), or by developing embolism-resistant xylem that prevents emboli formation and interruption of water transport under water deficit (i.e., drought-tolerant) (Maherali & Pockman 2004). Similarly, plants can prevent water loss by reducing canopy area (Daubenmire 1972) and stomatal conductance (Meinzer *et al.* 2016) or by retaining water under water deficit through osmotic adjustment (Subbarao *et al.* 2000). Given that plants combine multiple strategies to maintain water balance (Wright *et al.* 2004; Mencuccini *et al.* 2015), DIM indicators that do not reflect their combined integrative effect may show less consistent incipient mortality thresholds and predictive power among plants with varying strategies. Further, thresholds and predictive power can also vary among species and populations as a function of individual variation. Species or population thresholds will be clearly distinguishable if all individuals exhibit the same mortality threshold and threshold consistency (or lack of thereof) will be easily detected (Martinez-Vilalta et al. *in review*). In turn, low variation in mortality thresholds among individuals should also result in high predictive power as mortality is expected at similar values for all individuals. Thus, we need to assess individual variability among populations and species to determine whether a given variable is a suitable indicator of DIM risk at large scales.

While the morphological and physiological traits involved in drought survival strategies vary widely both among and within species, research has mostly focused on the importance of variation among species (Bartlett, Scoffoni & Sack 2012; Choat *et al.* 2012). However, studies have shown that mortality rates under drought not only depend on species' traits but also on intraspecific variation in traits and drought strategies (Cregg 1994; Tognetti, Michelozzi &

Giovannelli 1997; Sergent *et al.* 2014; Garcia-Forner *et al.* 2016). Thus, depending on the type of indicator used, intraspecific variation across a species' range may affect the mortality thresholds and predictive power of variables that indicate DIM risk. For this reason, assessments of the relative consistency and predictive power of candidate variables are necessary to identify useful large-scale indicators of DIM risk.

Water potential is a commonly used indicator of DIM (Choat *et al.* 2012) and has been extremely useful to understand water transport across the soil-plant-atmosphere continuum (Sperry & Love 2015) and develop species-specific models of DIM risk (Simeone *et al.* 2018; Venturas *et al.* 2018). Additionally, water potential can detect turgor loss, a process that precedes cellular damage and plant death in many plants (Guadagno *et al.* 2017) (but see resurrection plants). However, species vary widely in their ability to tolerate low water potentials (Bartlett *et al.* 2012; Choat *et al.* 2012) and water potential thresholds for incipient mortality are therefore likely to vary across species. Similarly, just as it occurs among species, lethal water potential thresholds may vary among populations with different morphology, physiology, and drought strategies. For instance, drought-avoidant and drought-tolerant populations may show different lethal water potential thresholds as a result of local adaptation to their respective environments including changes in osmotic adjustment capacity, resistance to embolism, turgor loss point, biomass allocation, etc. However, the extent to which water potential thresholds leading to incipient mortality and predictive power vary within species remains understudied. Given that lethal water potentials vary widely across species, it is critical to assess the extent to which such variation also exists among populations of the same species.

Percent loss of conductivity (PLC) is a useful indicator of DIM risk because of its general consistency across species within broad lineages. Several studies have reported similar PLC thresholds within gymnosperms (~ 50%) and angiosperms (~ 88% in angiosperms) (Choat *et al.* 2012). Thus, PLC mortality thresholds are also likely to be consistent among populations of the same species. However, PLC thresholds reported in the literature are often inferred from dead plants and may represent thresholds leading to 100% DIM risk rather than incipient mortality risk thresholds (Anderegg, Berry & Field 2012; but see Barigah *et al.* 2013). While thresholds leading to 100% DIM tell us when to expect *extensive* regional mortality, incipient DIM thresholds allow us to anticipate mortality based on observations and initiate preventive management. Therefore, PLC holds enormous potential as an indicator of DIM risk but only if

incipient mortality thresholds are consistent within and across species. A potential complication with PLC as a DIM risk indicator is that incipient mortality thresholds and the predictive power of PLC may vary among populations if hydraulic failure is not the sole driver of DIM (Mitchell *et al.* 2013). For instance, plants may show both high and low mortality risk at low PLC in populations if other factors (e.g., carbon depletion) kill individuals before they reach 50% or 80% PLC (depending on lineage). In this case, the predictive power of PLC might be low and incipient mortality thresholds might be less clear due to other factors increasing mortality risk at low PLC values. Exploring the extent to which PLC is the prevalent driver of DIM and the consistency of its incipient mortality thresholds among populations is critical to determine the potential of PLC as a large-scale indicator of DIM risk.

Plant water content is a direct measurement of desiccation status and could be a strong candidate indicator of DIM risk at large scales because it integrates the multiple strategies that plants use to maintain water balance. As opposed to PLC, a clear advantage of water content as a large scale indicator of DIM is that it can be measured from organs to ecosystems via remote sensing (Ullah *et al.* 2012; Wang & Li 2012; Mirzaie *et al.* 2014). Indeed, several remote sensing studies have observed substantial decreases in canopy water content which were followed by increased drought mortality (Saatchi *et al.* 2013; Asner *et al.* 2015). Consistently, Sapes et al., *in review* have shown that plant volumetric water content (VWC): i) predicts DIM risk with high accuracy, ii) shows incipient mortality thresholds, and iii) integrates water supply, retention, and loss. Relative water content (RWC) is of special interest because it is highly correlated to VWC but it reflects the amount of water present in a plant or organ relative to its maximum water content (i.e., desiccation status) (Barrs & Weatherley 1962). Thus, it standardizes differences among individuals or species with different maximum water contents due to varying anatomy. Accordingly, Bartlett *et al.* 2012 showed that turgor loss occurs at similar RWC values (but different water potential) across species from different biomes which inherently vary in morphology and physiology. The fact that RWC, like water potential, can detect turgor loss is critical given its link to cellular damage and plant death (Guadagno *et al.* 2017). Because RWC is a relative measure and it detects turgor loss (a process that may become irreversible and lead to death if drought persists), it is possible that incipient mortality thresholds for RWC and predictive power are relatively consistent across plants with varying morphology and physiology. The potential for consistency and the fact that water content can be remotely sensed, place RWC

as a potentially useful candidate for large-scale assessments of DIM risk. However, note that RWC thresholds and predictive power could vary if populations and their individuals differ in tolerance to desiccation or turgor loss.

Good indicators of DIM risk should also show consistent mortality thresholds and predictive power across plant organs of varying morphology and physiology. Under drought, plants often shed certain organs to reduce water loss. For instance, drought-deciduous trees shed leaves or even branches to reduce canopy area and increase their survival during periods of drought stress (Daubenmire 1972). In extreme cases, some species can re-sprout from their roots if all above-ground organs desiccate and perish (Hastings, Oechel & Sionit 1989). Clearly, DIM risk should be assessed in live, functional organs (e.g., roots in drought-deciduous species). Thus, variables that can estimate DIM risk in multiple organs are of critical interest. Consequently, it is important to evaluate the predictive power and consistency of incipient mortality thresholds among organs in different candidate variables. Differences in morphology and physiology among organs add yet another source of variation that may affect mortality thresholds and predictive power. Such variation may also affect the relationships between indicator variables and DIM risk (i.e., slope and intercept). Therefore, assessing the consistency of DIM mortality thresholds and predictive power as a function of the specific indicator variable, as well as the inter-relationships among indicator variables and DIM risk is also critical to determine which variables are good candidates for large-scale assessments of DIM risk and why (i.e. provide insight into the mechanisms of DIM).

We performed a greenhouse drought experiment based on the point of no return (i.e., no recovery after re-watering) with one-year-old ponderosa pine (*Pinus ponderosa* Douglas ex C. Lawson) seedlings to assess predictive power and incipient mortality thresholds of three DIM indicator variables (water potential, PLC, and relative water content). We focused on variability among populations and organs and we used a common garden approach with two genetically differentiated seedling provenances (North Plateau and Northern Rocky Mountain) (Potter *et al.* 2013) known to differ in responses to drought (Cregg 1994). This allowed us to assess the extent to which intraspecific variation in morphology and physiology translates into variation in incipient mortality thresholds or predictive power of water potential, PLC and RWC within species and organs. Specifically, we asked 1) do populations differ in mortality rates under drought?, 2) if so, what physiological and morphological differences contribute to differences in

mortality processes?, and 3) do water potentials, PLC, and RWC show high predictive power and incipient mortality thresholds across populations and organs?

MATERIALS AND METHODS

Study Design. We performed a greenhouse drought experiment at the University of Montana greenhouse facilities with one-year old ponderosa pine (*Pinus ponderosa* Douglas ex. C. Lawson) seedlings from two genetically differentiated populations known as the North Plateau race (NP) (42.6 N 122.8 W) and the Northern Rocky Mountain race (RM) (45.9 N 104.5 W) (Potter *et al.* 2013). We chose one-year old seedlings because of their convenient size and their biological relevance for regeneration of lower tree-line forests that are constrained by dry conditions (Simeone *et al.* 2018). On May 25th 2016 we planted 250 individuals from seed provided by the USDA Forest Service in 7.62 cm diameter x 43 cm tall pots using a homogeneous soil mixture consisting of 3:1:1 sand, peat moss, and top soil, respectively. Pots were randomly distributed on a bench at regular distances from each other. Seeds started to germinate by June 2nd and seedlings were grown at soil field capacity (i.e. soil fully saturated with water) until they were big enough to be measured (ca. 6 cm height and 2.5 cm basal diameter), which corresponded to February 24th 2017. Soil field capacity corresponded to soil volumetric water content values (VWC_s) of ca. 20%. We monitored changes in VWC_s using Meter 5TE sensors placed 10 cm above the bottom of the pots in five representative seedlings of each population. Sensors were inserted through a hole previously drilled in the side of the pots to minimize disturbance of soil structure and root system damage; which started to reach the bottom of the pot by the end of the experiment.

From February 24th 2017 to May 11th, seedlings underwent three drought pre-conditioning cycles to simulate early summer conditions. During the first two cycles, we dried pots down to 50% of their field capacity (VWC_s = 10%) after which we watered again to field capacity. On the last cycle, pots were dried down to 25% of their field capacity (VWC_s = 5%), which corresponds to a soil water potential of -0.7 MPa based on an empirical soil characteristic curve (see below), and then watered again to field capacity. This drought preconditioning provided a more realistic response to experimental severe drought since plants were able to acclimate to increasing drought as it tends to occur in natural conditions. After the drought-preconditioning, water was withheld (final drought) in all seedlings except a control group which

was kept at field capacity. Based on a preliminary drought experiment to assess symptoms of mortality as a function of soil drought and to optimize sampling times and sample size, we started measurements 29 days after the start of the drought treatment.

Sampling procedure. We assessed the degree of drought (i.e. soil water potential), seedling physiology, and mortality risk on six weekly samplings starting on day 29 of the drought treatment. At each sampling, we measured midday VWC_s in five randomly chosen seedlings from each population and we used VWC_s to estimate soil water potential based on soil water-retention curves specific for our soil type as in Sapes et al. *in review*. VWC_s sensors were installed 24h prior to measurement to reach equilibrium with soil conditions. We used the same seedlings in which VWC_s was measured to assess mid-day leaf and stem water potentials. Leaf water potential was measured in a single needle bundle using a pressure chamber (PMS Instrument Company, Corvallis, OR) following methods in (Kaufmann 1968). Stem water potentials were estimated equilibrating the water potential of a needle bundle with the stem following methods from Begg & Turner (1970) and measuring the equilibrated bundle with the pressure chamber. We also took midday measurements of stomatal conductance rates per unit leaf area in each seedling using a Licor 6400 XT using a 6400 RED LED chamber. Light conditions were set at 1,000 μmol quanta m^{-2} s^{-1} and CO2, flow, temperature, and relative humidity were set constant at 400 μmol s^{-1}, 100 mol s^{-1}, 25 ºC, and 50%, respectively. We scaled up stomatal conductance to canopy level (i.e., canopy conductance) by multiplying it by canopy area (see below). After this, seedlings were immediately harvested and kept in zip-lock bags with a moist paper towel in a cooler to prevent water loss(Garcia-Forner *et al.* 2016). Seedlings were then transported to the laboratory within two hours for hydraulic and water content measurements (see below). Because we could not assess mortality risk in plants that were harvested, we randomly chose a second independent subset of seedlings at each sampling event to assess mortality risk at any given point during the drought (see below).

Mortality assessment. We estimated the probability of mortality at the population level over time. In our study, population-level mortality is defined as the proportion of individuals from each population sampled at a given time that end up dying. At each sampling event, five groups of six seedlings (total of 30) were randomly chosen, classified as dead or alive, re-watered to field capacity, and kept well-watered until September 22nd to confirm mortality assessments. This method ensures accurate classification of both live and dead plants at every

sampling event. On that date, we classified seedlings as dead only if their canopy and phloem were completely brown and dry after a month of re-watering and no subsequent buds appeared (Cregg 1994). Then, mortality was calculated as the proportion of dead seedlings (out of 30) at a given sampling time. Notice that early re-watering groups were re-watered for longer periods of time due to the nature of the experimental design. However, seedlings removed later from the drought were completely dry and brittle with no subsequent signs of recovery. Note that in our design, physiological measurements during drought were done in individual plants, while mortality measurements were conducted at the population level. Thus, one value of probability of mortality is always associated to five individual values that reflect the variation in physiology across the population.

Organ Relative Water Content. Upon arrival to the laboratory, we separated roots, stems, and needles of each seedling to measure their Relative water content (*RWC*) based on fresh, turgid, and dry weights as: ((Fresh weight-Dry weight)/Turgid weight-Dry weight)*100 (Barrs & Weatherley 1962). Turgid weight was obtained by rehydrating needles for 5 hours in the dark at low temperatures (3 ºC). Low temperatures prevent oversaturation due to artificially low osmotic potentials resulting from catabolic conversion of starch into sugars (Boyer *et al.* 2008). We calculated whole plant *RWC* weighed by organ biomass fraction (proportion of each organ dry mass fraction multiplied by their respective *RWC*). For consistency, root *RWC* was measured before any other organ to avoid changes in *RWC* due to cleaning procedures (quick rinse and immediate blotting with paper towels) and exposure to dry air. Stems and root systems were returned to Ziploc bags and back into the cooler to prevent desiccation between measurements of fresh weight and turgid weight. Population-level pressure-volume curves were also built using midday leaf water potentials and the corresponding leaf *RWC* of each individual as in (Tyree *et al.* 2002) and Leaf RWC at turgor loss and water potential at turgor loss were extracted for each population.

Stem and Root Hydraulics. We measured stem hydraulic conductivity and root hydraulic conductance using the gravimetric method (Sperry, Donnelly & Tyree 1988) immediately after organ fresh weight measurements. We used a modification of the hydraulic apparatus described in Sperry (1988) that allowed us to measure hydraulic conductance of whole root systems in addition to stems (Sapes et al. *in review*). Stem segments previously used for *RWC* measurements were immersed in deionized water for 20 minutes to relax xylem tensions

that could artificially alter conductivity values (Trifilo *et al.* 2014). After relaxation, stems were relocated to the hydraulic apparatus and each end was recut twice at a distance of 1 mm from the tips each time (total of 2 mm per side) to remove any potential emboli resulting from previous cuts, transport, and relocation (Torres-Ruiz *et al.* 2015). Stems were then connected to the hydraulic apparatus while under water, with their terminal ends facing downstream flow. The stems were then raised out of the water and the connections were checked to ensure that there were no leaks. A solution of water with 10 mM KCl degassed at 3 kPa for at least 8 hours was used for all hydraulic measurements (Espino & Schenk 2011).

First, initial background flow was measured to account for the flow existing under no pressure, which can vary depending on the degree of dryness of the measured tissue (Hacke *et al.* 2000; Torres-Ruiz, Sperry & Fernández 2012; Blackman *et al.* 2016). Second, a pressure gradient of 5-8 kPa was applied to run water through the stem and pressurized flow was measured. This small pressure gradient prevented embolism removal from the samples while ensuring flow. Lastly, final background flow was measured, initial and final background flows were averaged, and flow was calculated as the difference between pressurized flow and average background flow. Native specific hydraulic conductivity (*K*) was estimated in stems as the flow divided by the pressure gradient used and standardized by xylem area and length. In root systems, flow was measured as above and whole root native hydraulic conductance (*k*) was estimated as the flow divided by the pressure gradient used and standardized by xylem area at the root collar.

Maximum stem hydraulic conductivity (*Kmax*) and root hydraulic conductance (*kmax*) were estimated at the population level as the average stem *K* and root *k* of the pre-conditioned control measured at day 0 since the onset of the drought. Such a population approach was necessary because 1) destructive measurements in these small seedlings prevented multiple successive measurements of *K* and water potentials on the same individuals, and 2) flushing and vacuum infiltration techniques to obtain *Kmax* from embolized tissues can generate artifacts and overestimate *Kmax* (Cochard *et al.* 2013). Percent loss of stem conductivity and percent loss of root conductance were estimated for each measured seedling as *100**(*Kmax-K)/Kmax* and *100**(*kmax-k)/kmax*, respectively. Note that negative PLC values may occur if *K* or *k* in a given sample is larger than *Kmax* estimated as the average *K* of controls. We calculated whole-plant *PLC* weighted by organ fraction. Root and stem *PLC* can be averaged together because they are

unit-less indexes that represent the *relative* loss of water transport capacity of their respective organs. Because we did not measure *PLC* in needles, whole-plant *PLC* represents the overall hydraulic integrity of the stem and root systems. We excluded negative PLC values resulting from uncertainty around population level estimates of *Kmax* (Sapes et al. *in review*). This could affect comparisons between populations if exclusion was biased towards a population or sampling time. However, exclusion of data was fairly homogeneous across the whole dataset (Table S1).

Morphological measurements. Upon harvest, we measured plant height and root system length in each seedling as the distance from the root collar to the highest needle and to the end of the longest root, respectively. We took pictures of the canopy of each seedling and estimate canopy area using ImageJ software. Organ dry weights were used to calculate whole plant biomass as the sum of needle, stem, and root dry weights. Root to shoot ratios were calculated as root dry weight divided by the sum of leaf and stem dry weights.

Statistical analyses. We tested differences in morphology between populations across the full set of measurements using two-tailed Student's t-test for independent samples. Canopy area, root to shoot ratios, organ biomass, whole-plant biomass, and plant length across all samples were used as dependent variables while population was the categorical variable in all tests. Differences in maximum stem hydraulic conductivity between populations were also tested using two tailed Student's t-tests comparing the stem hydraulic conductivity of all controls from both populations. Variables were transformed to achieve normality and homogeneity of variances when needed. We also tested potential differences in hydraulic conductivity due to plant length given that trees are known to increase hydraulic conductivity at the base of the stem as they grow tall to minimize the resistance of the hydraulic pathway (Olson *et al.* 2018). Differences in hydraulic conductivity as a function of plant length were assessed in two linear models with plant length, population and their interaction as predictors and stem hydraulic conductivity and root hydraulic conductance as response variables. Response variables were log-transformed to meet model assumptions.

We tested differences in response to drought over time between populations by splitting the drought into early drought (days 0 and 29) and late drought (days 29 to 72). This was necessary because, physiological measurements were not taken before day 29 in order to maximize sampling after the onset of mortality. Thus, analyses from day 29 to 72 reflect

responses close to and after the onset of mortality in the population (when a few individuals start to die) and characterize the processes that either prevent or ultimately cause death. Early differences in response to drought between populations were tested using two-tailed Student's t-test for independent samples at day 0 and 29. T-tests were used instead of regressions because data included only two days. Soil and plant water potentials, canopy conductance, PLC, and RWC across organs at day 0 and 29 were used as dependent variables while population was the categorical variable in all tests. Contrasts from day 0 to 29 provide information of whether observed differences after the onset of mortality originated during early stages prior to mortality. Late differences in response to drought between populations were tested using three sets of regression models with data from day 29 to 72. All models had days since the onset of drought, population, and the interaction of both factors as the predictor variables. Response variables were i) soil, leaf, or stem water potential to represent the degree of drought intensity; ii) whole-plant *PLC* or whole-plant *RWC* to represent loss of hydraulic function and degree of desiccation; and iii) population-level mortality to represent the probability of DIM. Generalized linear models (Mardia, Kent & Bibby 1979) with binomial distribution and logit link were used for models including probability of mortality. Linear models were used for all other cases as the response variables showed a linear response with time or could be transformed to meet assumptions of linearity.

We took a residuals approach to test whether differences in responses to drought between populations were driven by morphology physiology or both. We chose RWC as our response variable because desiccation is the main process leasing to DIM (Tyree *et al.* 2003, Sapes et al *in review*, Martinez-Vilalta et al. *in review*) and integrates the physiological (e.g. low stomatal conductance, maintenance of hydraulic function) and morphological (e.g. low canopy area, high root to shoot ratios, reduced growth) responses to prevent desiccation leading to DIM risk. First, we extracted the residuals from a model with RWC as the response variable and days since the onset of drought as the predictor. In this initial model, differences between populations should be expressed in the residual variation (i.e. residuals reflect population differences). Then, we built a second model for morphology with these residuals as the response variable and all the interactions between population, root to shoot ratios, and whole-plant biomass as predictive variables. In this model, a significant effect of a given morphological variable indicates an overall effect of morphology on desiccation rates. Significant interactions between a given

morphological variable and population indicate that the effects of morphology are population-specific. Thus, a significant effect of population alone or as part of an interaction indicates that morphological differences alone are not able to explain all the variation in desiccation rates existing between populations. To test the influence of physiology, we built a third model with the residuals from the model with RWC as the response variable and days since the onset of drought as the predictor (as for the morphology model) as the response variable and all the interactions between population, stomatal conductance, and whole-plant PLC as predictive variables. The interpretation of the outcomes of this model is the same as for the morphology model only that they refer to physiology rather than morphology. Morphological variables were log-transformed to meet model assumptions. Other physiological (e.g., soil and plant water potential) or morphological (e.g., plant length and canopy area) variables were excluded from these models because they were highly correlated with the selected predictors. Using whole-plant variables also allowed us to account for potential organ-specific effects without increasing the number of predictors or violating assumptions of co-linearity.

We used logistic regressions (Walker & Duncan 1967) to assess the predictive power and consistency of each mortality predictor and search for potential thresholds indicative of incipient mortality risk. For each organ within a population, logistic models included probability of mortality as the response variable and RWC, water potential, or PLC as predictors. Probability of mortality was expressed on a decimal fraction basis following requirements of models with binomial distributions. Predictive power was estimated as the proportion of variance explained (VE) by each model (i.e., [1- residual variance/ null variance] x 100) (Guisan & Zimmermann 2000). In logistic models, this model performance criterion is often discouraged because it tends to underestimate predictive power due to the lack of values between 0 and 1 in the response variable. However, population-level mortality does contain intermediate values between 0 and 1 thus overcoming this issue. We assessed predictive consistency by testing differences in slopes and intercepts of mortality relationships across populations and organs using logistic models containing the interaction between a given predictor, population, and organ. In these models, non-significant interactions were not removed because our hypothesis was explicitly directed to the interaction between population, organ, and each predictor.

RESULTS

All dates combined, Pacific Coast (NP) seedlings were longer ($t = 2.51$, $p = 0.014$; Fig. 1a) and had greater whole-plant biomass ($t = 3.58$, $p < 0.001$; Fig. 1b) than Northern Rocky Mountain (RM) seedlings. These differences were due to greater stem biomass ($t = 5.04$, $p < 0.001$; Fig. S1a) and root biomass ($t = 5.43$, $p < 0.001$; Fig. S1b) in NP seedlings. Differences in biomass allocation translated to greater root to shoot ratios in NP seedlings ($t = 4.83$, $p < 0.001$; Fig. 1c). Differences in plant length between populations were associated with greater hydraulic conductivity in NP seedlings (stem: $R^2_{adj} = 0.18$, plant length: $p < 0.001$, population: $p = 0.077$; roots: $R^2_{adj} = 0.08$, plant length: $p = 0.003$, population: $p = 0.047$; Table S2). Accordingly, NP seedlings had greater maximum hydraulic conductivity ($t = 1.94$, $p = 0.059$; Fig. S1c).
By day 29 the probability of mortality was zero in both populations (Fig. 2d). Mortality risk started to increase above zero by days 29 and 42 in NP and RM populations, respectively, based on their estimated mortality curves (Fig. 2d). After the onset of mortality in each population, mortality probabilities increased at the same rate for both populations.

At early stages of drought (day 0), populations showed no differences in any physiological variable. However, at day 29 of drought, NP seedlings had lower whole-plant RWC ($t = -4.57$, $p = 0.002$). This effect was driven by lower stem and root RWC (stem: $t = -4.70$, $p = 0.003$; roots: $t = -2.25$ $p = 0.056$). Changes from day 0 to day 29 indicate that NP seedlings experienced greater desiccation rates at some point during the early stages of the drought. While differences were not statistically significant, soil, stem, and leaf water potentials were also consistently lower in NP seedlings by day 29.

At late stages of drought (day 29 to 72), soil water potentials clearly diverged among populations and continued decreasing at similar rates ($R^2_{adj} = 0.30$, days: $p < 0.001$; population: $p = 0.029$; Fig. 2a, Table S3). The same pattern was observed in leaf and stem water potentials (needles: $R^2_{adj} = 0.77$, days: $p < 0.001$, population: $p = 0.031$; stems: $R^2_{adj} = 0.83$, days: $p < 0.001$, population: $p = 0.065$; Fig. 2a, Table S3). Declines in water potential were accompanied by increases in PLC in both populations, but NP seedlings experienced higher PLC rates ($R^2_{adj} = 0.57$, days: $p < 0.001$, days x population: $p < 0.022$; Fig. 2b, Table S3). This pattern was driven by higher PLC rates in roots ($R^2_{adj} = 0.27$, days: $p < 0.001$, population: $p = 0.044$, days x population: $p < 0.011$; Fig. 2b, Table S3), and higher PLC rates were explained by higher root to shoot ratios in NP seedlings ($R^2_{adj} = 0.60$, days: $p < 0.001$, root shoot ratio: $p = 0.035$, days x

population: p = 0.018; Fig. S2, Table S3). Consistently, NP seedlings lost RWC in needles at faster rates than RM seedlings (R^2_{adj} = 0.78, days: p < 0.001, days x population: p = 0.030; Fig. 2c, Table S3). In turn, differences in desiccation rates in needles led to marginally lower conductance rates in NP seedlings (R^2_{adj} = 0.03, days: p = 0.071, population: p = 0.055, days x population: p = 0.079; Table S3). While canopies of NP seedlings desiccated faster (i.e., different slopes between populations), this trend was not observed at the whole plant level because of the small contribution of needles to whole-plant RWC relative to other organs. However, whole-plant RWC still differed among populations (i.e. different intercepts between populations) (R^2_{adj} = 0.71, days: p < 0.001, population: p < 0.001; Fig. 2c, Table S3) as observed during early drought stages. As a result, NP seedlings started dying earlier (ca. more than two weeks) but both populations showed similar rates of mortality once mortality started (days: p < 0.001; population: p = 0.024; Fig. 2d, Table S3).

Residual analyses allowed us to determine whether differences in desiccation rates between populations were explained by differences in morphology physiology or both. Population was still significant when the leftover variation in desiccation rates was attributed to physiology (R^2_{adj} = 0.34, population: p = 0.071, population x stomatal conductance: p = 0.007, population x stomatal conductance x whole-plant PLC: p = 0.003, Table S4). This indicates that physiological differences alone cannot fully explain the differences in desiccation rates observed between populations. On the other hand, population was not significant when the leftover variation was attributed to morphology (R^2_{adj} = 0.33, log(root to shoot ratio): p = 0.013, log(plant biomass): p = 0.002, Table S4). Additionally, the morphological model explained the same amount of variation in RWC than the physiological model with less variables, thus being more parsimonious. This indicates that morphological differences in root to shoot ratios and plant size alone can fully explain the differences in desiccation rates observed between populations. That is, morphological variables absorb the variation otherwise explained by the categorical variable 'population' thus making it not significant.

The ability to predict mortality of RWC, PLC, and water potential varied among populations and organs both in terms of predictive power and degree of significance (Fig. 3, Table S5). RWC and water potential had comparably high predictive power (RWC: p-value$_{Range}$ = <0.001 - 0.002, VE$_{Average}$ = 76.35%, VE$_{Range}$: 54%-95%; water potential: p-value$_{Range}$ = <0.001 - 0.01, VE$_{Average}$ = 74.42%, VE$_{Range}$: 46%-93%). Additionally, both variables showed similar

relationships with DIM risk across organs and populations as supported by the lack of significant differences in intercepts and slopes (Fig. 4a, & c, Table S6). However, when comparing populations, water potential values leading to 50% mortality (LD50) differed more than RWC values (Fig. 4a & c). PLC had the lowest predictive power ($p\text{-value}_{Range}$ = <0.001 - 0.564, $VE_{Average}$ = 42.78%; Fig. 3) and it was highly variable among populations and organs (VE_{Range}: 1%-76%; Fig. 3 & 4b, Table S5).

Logistic regressions identified mortality thresholds in all variables (Fig. 4a, b & c). However, only RWC and water potential showed incipient mortality thresholds across all populations and organs. Importantly, all the incipient mortality thresholds found in RWC and water potential were close to the values corresponding to leaf turgor loss (Fig. 4a & c, vertical lines). In contrast to RWC and water potential, PLC only showed threshold-type responses in the NP population.

DISCUSSION

Intraspecific variation can significantly influence the predictive power and incipient mortality thresholds of indicators of DIM risk. Populations can vary in performance under drought as a result of intraspecific variation in morphology, physiology, and drought strategies. The North Plateau population (NP) showed greater biomass allocation to roots, plant size (both height and mass), and hydraulic conductivity than the rocky mountain population (RM). As a result, NP seedlings were able to absorb more water and at faster rates. Because potted conditions limit soil depth and access to water, this led to earlier desiccation and mortality in NP seedlings. While the potted conditions in this experiment are certainly artificial, these results highlight a biologically relevant point: morphological and physiological differences among populations can lead to differences in mortality rates under limited water. While plants can drastically adjust their physiology under drought, their capacity to adjust morphology under drought is often more limited (Gratani *et al.* 2003). For instance, plants can adjust stomatal conductance under water deficit but they might not be able to elongate roots to extract more water because water deficit inhibits growth (Maseda & Fernández 2015). Reducing stomatal conductance and water loss may reduce the detrimental impacts caused by the specific morphology of roots, but, like in our case, physiological adjustments might not always completely compensate morphological differences. Thus, performance under drought depends on both morphological characteristics and physiological adjustment capacity. Given that

morphology and physiology can vary among populations, drought performance may also vary across a species' range as a result of morphological and physiological variation.

Morphological variation can also lead to different drivers of mortality among populations. In our study, NP seedlings showed high PLC rates over time, high mortality at whole-plant PLC values above 50 % (consistent with thresholds reported for gymnosperms), and strong correlations between PLC and DIM risk with similar relationships across organs (Table S6). On the other hand, RM seedlings showed lower PLC rates but high mortality below 50 % whole-plant PLC and, thus, poor correlations between PLC and DIM risk across organs despite their similar relationships (Table S6). The low correlation between PLC and mortality observed in RM seedlings suggests that processes other than hydraulic failure (e.g., carbon depletion) led to mortality before they could experience lethal PLC (Mitchell *et al.* 2013). Small and young individuals within a species have small NSC pools (Sala & Mencuccini 2014 and references therein). The young age of our plants and the smaller size of RM seedlings may have led to low NSC pools thus making them highly susceptible to carbon depletion during drought. However, this hypothesis should be further explored. The high correlation between PLC and mortality observed in NP seedlings suggests that, in this case, mortality was mostly driven by hydraulic failure. Hydraulic failure might be driving NP mortality due to a more efficient but vulnerable xylem built to compensate the hydraulic resistance imposed by greater height (Olson *et al.* 2018). Tall plants may increase xylem efficiency by building both wider conduits at the base of their trunk (Carrer *et al.* 2014) and hydraulically efficient pits that impose lower resistance to water flow (Pittermann *et al.* 2010). However, these two morphological adaptations come at the cost of hydraulic safety due to both higher chances of containing faulty pits and lower torus overlap in all pits, respectively (Delzon *et al.* 2010, Roskilly et al, *in prep*). NP seedlings are likely to have more efficient but vulnerable xylem given their greater height and overall size (Fig. 1), greater maximum hydraulic conductivity (based on controls at day 0), and the observed influence of size on desiccation and PLC rates (Fig. S2). In natural conditions, NP seedlings might not need to invest in resistant xylem given their ability to avoid low water potentials through deep root systems. However, abnormally intense or frequent droughts may still lead to low water potentials, hydraulic failure, and death. Altogether, our results under greenhouse conditions suggest that the relative contribution of mechanisms leading to DIM may vary across populations as a function of morphological variation.

Depending on the type of indicator variable, mortality thresholds and predictive power can vary among populations across a species' range if the relative contribution of mechanisms leading to DIM varies among populations. Counter to expectations, NP and RM populations showed different relationships between PLC and DIM risk which led to different PLC incipient mortality thresholds and predictive power. PLC likely shows variable thresholds and predictive power because it only reflects processes linked to hydraulic failure and does not reflect other important drivers of DIM such as carbon depletion or other processes contributing to desiccation (e.g., cuticular conductance) (Blackman *et al.* 2016). This result suggests that relationships between PLC and DIM risk in a population may not be generalizable across a species' range if the drivers of DIM change across the landscape. Large-scale assessments of DIM risk might be challenging even if population-specific relationships are known and averaged to better capture the behavior of the species. For instance, we may obtain higher overall predictive power if we combined both NP and RM populations and predicted DIM risk using PLC. However, the resulting relationship would have lower predictive power in both populations and mortality thresholds would not indicate PLC values at incipient mortality in either population. Additionally, incipient mortality thresholds in PLC are also expected to vary among gymnosperms and angiosperms given their different morphology, physiology, and tolerance to embolism (Choat *et al.* 2012). Such variation among species may significantly reduce our capacity to accurately assess DIM risk across the landscape based on PLC. Instead, landscape assessments should rely on indicators that integrate multiple drivers of DIM.

Plant water potentials showed consistent mortality thresholds associated to turgor loss and high predictive power across both populations and organs. Low water potentials are responsible for both formation of emboli and stomatal closure (Tyree & Sperry 1989; Meinzer *et al.* 2016), which can lead to hydraulic failure and carbon depletion (McDowell *et al.* 2008), respectively. Given that low water potentials drive both processes, water potentials may reflect both hydraulic failure and carbon depletion to a certain extent. Additionally, plant water potential also indicates turgor loss (Ψ_{TLP}) thus explaining the observed thresholds associated to turgor loss. The consistent water potential thresholds and high predictive power found in both populations suggest that there is little variability in lethal water potentials among individuals and populations. This is very promising because water potential is widely used in modeling and can be used to connect the soil-plant-atmosphere continuum. Thus, water potentials could accurately predict

incipient mortality and DIM risk across populations regardless of existing differences in morphology, physiology, and drought strategies. However, plant water potential is likely to show different incipient mortality thresholds across species given the enormous variation in minimum water potential (Choat *et al.* 2012) and in Ψ_{TLP} (Bartlett *et al.* 2012) across species and biomes. Thus, large-scale assessments of DIM based on water potential might be challenging in diverse forests. However, this may be resolved by including the Ψ_{TLP} of each species in DIM models and monitoring approaches.

Relative water content (RWC) integrates drivers of DIM, reduces variation in thresholds and predictive power, and predicts DIM risk from any organ. While the contribution of hydraulic failure -and perhaps carbon depletion or other processes- to desiccation and DIM varied between populations, results for water potential and RWC indicate that desiccation was the common driver of DIM. Water content variables such as RWC are direct measures of desiccation and integrate the two physiological processes leading to DIM (Sapes et al. *in review*). Accordingly, we found that RWC showed similar thresholds and high predictive power among populations and organs. Additionally, RWC represents plant water status and can thus be linked to turgor loss (using RWC_{TLP}), the ultimate cause of cellular death under drought (Guadagno *et al.* 2017). Hence, we found that incipient mortality occurred at RWC values indicative of turgor loss and increased with further declines as cellular damage likely increased (membrane people here). Given that turgor loss and cellular damage is ubiquitous across organs under drought, the consistent thresholds and relationships between DIM risk and RWC across plant organs are expected. This is of critical importance given that some organs such as leaves may not be present in species that discard their canopy under drought (Daubenmire 1972). Thus, using integrative indicators such as RWC, which can also assess DIM risk from any organ available, are preferable for large scale assessments.

RWC is a good candidate for large-scale assessments of DIM risk because it can be remotely sensed and absorbs variation in morphology, physiology, and drought strategies. Unfortunately to date, PLC cannot be measured at large scales because measurements are complex, time consuming, and we lack remote sensing techniques to estimate it. Water potentials can be estimated using remote sensing techniques (Cohen *et al.* 2005). However, variation in morphology, physiology, and drought strategies among species is likely to be reflected in water potential measurements taken at large scales. For instance, the average water potential of a pixel

containing a mixture of drought-avoidant and tolerant species is more likely to reflect the diversity in drought-strategies existing in that pixel than the degree of DIM risk (Martinez-Vilalta et al. *in review*). On the other hand, plant water content can be remotely sensed across the landscape using hyperspectral and thermal techniques (Ceccato *et al.* 2001; Elsayed *et al.* 2017; Konings *et al.* 2017). RWC also standardizes differences in water content due to morphological and physiological variation among populations and species, integrates the different drivers of DIM (Sapes et al. *in review*), and shows consistent RWC_{TLP} across organs, species, and biomes (Bartlett *et al.* 2012). Thus the average RWC of a pixel is likely to accurately reflect the expected degree of DIM at a given point in time regardless of differences among populations or species. For these reasons, RWC stands out as a good candidate for large-scale assessments of DIM risk with potential to allow monitoring of DIM even across species and biomes.

Overall, our results suggest that intraspecific variation can significantly influence mortality risk under drought across a species' range and our ability to monitor and predict DIM risk. Large-scale indicators of DIM risk should accurately assess DIM risk across plants regardless of such variation and should be chosen based on the consistency of their mortality thresholds and predictive power among populations and species. Variables related to plant water pools (e.g., RWC) are good candidates because they reflect the ultimate causes of mortality under drought, integrate physiological drivers of DIM, show consistent thresholds, and have high predictive power. While our results support RWC as a good candidate for large-scale monitoring of DIM risk based on its consistency and predictive capacity across populations, future research should test the consistency of incipient mortality thresholds and the predictive power of RWC across species. Until tested, the consistency of RWC across species remains unknown. However, this avenue is promising given that RWC accounts for differences in anatomy among species and integrates differences in drivers of DIM resulting from varying morphology and physiology. Similarly, remote sensing techniques measure VWC rather than RWC (Yilmaz, Hunt & Jackson 2008; Mirzaie *et al.* 2014; Veysi *et al.* 2017). However proxies of remotely sensed RWC have been recently developed (Rao et al. in review) and are likely to become more abundant in the near future. Despite, the work that still lays ahead, the results shown here will help increase the accuracy of current monitoring efforts and may open a path of research towards global scale assessments of DIM risk (Martinez-Vilalta et al. *in review*).

ACKNOWLEDGEMENTS

This work was supported by a National Science Foundation grant to AS (BCS 1461576). GS received funding from the NSF Experimental Program to Stimulate Competitive Research (EPSCoR) Track-1 EPS-1101342 (INSTEP 3). The authors thank P. Demaree for his help collecting data and S. Dobrowski, A. Woods, and B.Roskilly for comments in early versions of this manuscript. We also want to thank all the trees in this experiment that sacrificed their young lives for the greater good of their kind.

REFERENCES

Anderegg, W.R.L., Berry, J.A. & Field, C.B. (2012) Linking definitions, mechanisms, and modeling of drought-induced tree death. *Trends in Plant Science*, **17**, 693–700.

Asner, G.P., Brodrick, P.G., Anderson, C.B., Vaughn, N., Knapp, D.E. & Martin, R.E. (2015) Progressive forest canopy water loss during the 2012–2015 California drought. *Proceedings of the National Academy of Sciences*, **2015**, 201523397.

Barigah, T.S., Charrier, O., Douris, M., Bonhomme, M., Herbette, S., Améglio, T., Fichot, R., Brignolas, F. & Cochard, H. (2013) Water stress-induced xylem hydraulic failure is a causal factor of tree mortality in beech and poplar. *Annals of Botany*, **112**, 1431–1437.

Barrs, H.D. & Weatherley, P.E. (1962) A Re-Examination of the Relative Turgidity Technique for Estimating Water Deficits in Leaves. *Australian Journal of Biological Sciences*, **15**, 413–428.

Bartlett, M.K., Scoffoni, C. & Sack, L. (2012) The determinants of leaf turgor loss point and prediction of drought tolerance of species and biomes: a global meta-analysis. *Ecology Letters*, **15**, 393–405.

Begg, J.E. & Turner, N.C. (1970) Water Potential Gradients in Field Tobacco. *PLANT PHYSIOLOGY*.

Blackman, C.J., Pfautsch, S., Choat, B., Delzon, S., Gleason, S.M. & Duursma, R.A. (2016) Toward an index of desiccation time to tree mortality under drought. *Plant Cell and Environment*, **39**, 2342–2345.

Boyer, J.S., James, R.A., Munns, R., Condon, T. & Passioura, J.B. (2008) Osmotic adjustment leads to anomalously low estimates of relative water content in wheat and barley. *Functional Plant Biology*, **35**, 1172–1182.

Carrer, M., Von Arx, G., Castagneri, D. & Petit, G. (2014) Distilling allometric and environmental information from time series of conduit size: The standardization issue and its relationship to tree hydraulic architecture. *Tree Physiology*, **35**, 27–33.

Ceccato, P., Flasse, S., Tarantola, S., Jacquemoud, S. & Grégoire, J.M. (2001) Detecting vegetation leaf water content using reflectance in the optical domain. *Remote Sensing of Environment*, **77**, 22–33.

Choat, B., Jansen, S., Brodribb, T.J., Cochard, H., Delzon, S., Bhaskar, R., Bucci, S.J., Feild, T.S., Gleason, S.M., Hacke, U.G., Jacobsen, A.L., Lens, F., Maherali, H., Martínez-Vilalta, J., Mayr, S., Mencuccini, M., Mitchell, P.J., Nardini, A., Pittermann, J., Pratt, R.B., Sperry, J.S., Westoby, M., Wright, I.J. & Zanne, A.E. (2012) Global convergence in the vulnerability of forests to drought. *Nature*, **491**, 752–755.

Cochard, H., Badel, E., Herbette, S., Delzon, S., Choat, B. & Jansen, S. (2013) Methods for measuring plant vulnerability to cavitation: a critical review. *Journal of Experimental Botany*, **64**, 4779–4791.

Cohen, Y., Alchanatis, V., Meron, M., Saranga, Y. & Tsipris, J. (2005) Estimation of leaf water potential by thermal imagery and spatial analysis. *Journal of Experimental Botany*, **56**, 1843–1852.

Cregg, B.M. (1994) Carbon allocation, gas exchange, and needle morphology of Pinus ponderosa genotypes known to differ in growth and survival under imposed drought. *Tree Physiology*, **14**, 883–898.

Dai, A. (2013) Increasing drought under global warming in observations and models. *Nature Climate Change*, **3**, 52–58.

Daubenmire, R.F. (1972) Phenology and other characteristics of tropical semi-deciduous forest in north-western Costa Rica. *The Journal of Ecology*, **60**, 147–170.

Delzon, S., Douthe, C., Sala, A. & Cochard, H. (2010) Mechanism of water-stress induced cavitation in conifers: bordered pit structure and function support the hypothesis of seal capillary-seeding. *Plant, Cell & Environment*, **33**, 2101–2111.

Elsayed, S., Darwish, W., Elsayed, S. & Darwish, W. (2017) Hyperspectral remote sensing to assess water status, biomass and yield ofmaize cultivars under salinity and water stress. , **76**, 62–7262.

Espino, S. & Schenk, H.J. (2011) Mind the bubbles: Achieving stable measurements of maximum hydraulic conductivity through woody plant samples. *Journal of Experimental Botany*, **62**, 1119–1132.

Garcia-Forner, N., Sala, A., Biel, C., Savé, R. & Martínez-Vilalta, J. (2016) Individual traits as determinants of time to death under extreme drought in Pinus sylvestris L. (ed D Whitehead). *Tree Physiology*, **36**, 1196–1209.

Gratani, L., Meneghini, M., Pesoli, P. & Crescente, M.F. (2003) Structural and functional plasticity of Quercus ilex seedlings of different provenances in Italy. *Trees - Structure and Function*, **17**, 515–521.

Greenwood, S., Ruiz-Benito, P., Martínez-Vilalta, J., Lloret, F., Kitzberger, T., Allen, C.D., Fensham, R., Laughlin, D.C., Kattge, J., Bönisch, G., Kraft, N.J.B. & Jump, A.S. (2017) Tree mortality across biomes is promoted by drought intensity, lower wood density and higher specific leaf area. *Ecology Letters*, **20**, 539–553.

Guadagno, C.R., Ewers, B.E., Speckman, H.N., Aston, T.L., Huhn, B.J., DeVore, S.B., Ladwig, J.T., Strawn, R.N. & Weinig, C. (2017) Dead or alive? Using membrane failure and chlorophyll fluorescence to predict mortality from drought. *Plant Physiology*, **175**, 223–234.

Guisan, A. & Zimmermann, N.E. (2000) Predictive habitat distribution models in ecology. *Ecological Modelling*.

Hacke, U.G., Sperry, J.S., Ewers, B.E., Ellsworth, D.S., Schäfer, K.V.R. & Oren, R. (2000) Influence of soil porosity on water use in Pinus taeda. *Oecologia*, **124**, 495–505.

Hartmann, H., Adams, H.D., Anderegg, W.R.L., Jansen, S. & Zeppel, M.J.B. (2015) Research frontiers in drought-induced tree mortality: Crossing scales and disciplines. *New Phytologist*, **205**, 965–969.

Hastings, S., Oechel, W. & Sionit, N. (1989) *Water Relations and Photosynthesis of Chap- Arral Resprouts and Seedlings Following Fire and Hand Clearing* (ed K SC). Natural History Museum of Los Angeles County, Los Angeles.

Kaufmann, M. (1968) Evaluation of the Pressure Chamber Technique for Estimating Plant Water Potential of Forest Tree Species. *Forest Science*, **14**, 369–374.
Konings, A.G., Yu, Y., Xu, L., Yang, Y., Schimel, D.S. & Saatchi, S.S. (2017) Active microwave observations of diurnal and seasonal variations of canopy water content across the humid African tropical forests. *Geophysical Research Letters*, **44**, 2290–2299.
Maherali, H. & Pockman, W.T. (2004) Adaptive Variation in the Vulnerability of Woody Plants To Xylem Cavitation. *Ecology*, **85**, 2184–2199.
Mardia, K. V., Kent, J.T. & Bibby, J.M. (1979) *Multivariate Analysis*. Academic Press.
Maseda, P.H. & Fernández, R.J. (2015) Growth potential limits drought morphological plasticity in seedlings from six Eucalyptus provenances. *Tree Physiology*, **36**, 243–251.
Matías, L., González-Díaz, P. & Jump, A.S. (2014) Larger investment in roots in southern range-edge populations of Scots pine is associated with increased growth and seedling resistance to extreme drought in response to simulated climate change. *Environmental and Experimental Botany*, **105**, 32–38.
Mcculloh, K.A., Johnson, D.M., Meinzer, F.C. & Woodruff, D.R. (2014) The dynamic pipeline: Hydraulic capacitance and xylem hydraulic safety in four tall conifer species. *Plant, Cell and Environment*, **37**, 1171–1183.
McDowell, N., Pockman, W.T., Allen, C.D., Breshears, D.D., Cobb, N., Kolb, T., Plaut, J., Sperry, J., West, A., Williams, D.G. & Yepez, E. a. (2008) Mechanisms of plant survival and mortality during drought: why do some plants survive while others succumb to drought? *The New phytologist*, **178**, 719–39.
Meinzer, F.C., Woodruff, D.R., Marias, D.E., Smith, D.D., McCulloh, K.A., Howard, A.R. & Magedman, A.L. (2016) Mapping 'hydroscapes' along the iso- to anisohydric continuum of stomatal regulation of plant water status. *Ecology Letters*.
Mencuccini, M., Minunno, F., Salmon, Y., Martínez-Vilalta, J. & Hölttä, T. (2015) Coordination of physiological traits involved in drought-induced mortality of woody plants. *New Phytologist*, **208**, 396–409.
Mirzaie, M., Darvishzadeh, R., Shakiba, A., Matkan, A.A., Atzberger, C. & Skidmore, A. (2014) Comparative analysis of different uni- and multi-variate methods for estimation of vegetation water content using hyper-spectral measurements. *International Journal of Applied Earth Observation and Geoinformation*, **26**, 1–11.
Mitchell, P.J., O'Grady, A.P., Tissue, D.T., White, D. a., Ottenschlaeger, M.L. & Pinkard, E. a. (2013) Drought response strategies define the relative contributions of hydraulic dysfunction and carbohydrate depletion during tree mortality. *New Phytologist*, **197**, 862–872.
Olson, M.E., Soriano, D., Rosell, J.A., Anfodillo, T., Donoghue, M.J., Edwards, E.J., León-Gómez, C., Dawson, T., Camarero Martínez, J.J., Castorena, M., Echeverría, A., Espinosa, C.I., Fajardo, A., Gazol, A., Isnard, S., Lima, R.S., Marcati, C.R. & Méndez-Alonzo, R. (2018) Plant height and hydraulic vulnerability to drought and cold. *Proceedings of the National Academy of Sciences*, **115**, 7551–7556.
Pittermann, J., Choat, B., Jansen, S., Stuart, S.A., Lynn, L. & Dawson, T.E. (2010) The Relationships between Xylem Safety and Hydraulic Efficiency in the Cupressaceae: The Evolution of Pit Membrane Form and Function. *Plant Physiology*, **153**, 1919–1931.
Potter, K.M., Hipkins, V.D., Mahalovich, M.F. & Means, R.E. (2013) Mitochondrial DNA haplotype distribution patterns in Pinus ponderosa (Pinaceae): Range-wide evolutionary history and implications for conservation. *American Journal of Botany*, **100**, 1562–1579.

Saatchi, S., Asefi-Najafabady, S., Malhi, Y., E. O. C. Aragão, L., Anderson, L.O., Myneni, R.B. & Nemani, R. (2013) Persistent effects of a severe drought on Amazonian forest canopy. *Proceedings of the National Academy of Sciences*, **110**, 565–570.

Sala, A. & Mencuccini, M. (2014) Plump trees win under drought. *Nature Climate Change*, **4**, 666–667.

Sergent, A.-S., Bréda, N., Sanchez, L., Bastein, J.-C. & Rozenberg, P. (2014) North Plateau and interior Douglas-fir provenances differ in growth performance and response to drought episodes at adult age. *Annals of Forest Science*, **71**, 709–720.

Simeone, C., Maneta, M.P., Holden, Z.A., Sapes, G., Sala, A. & Dobrowski, S.Z. (2018) *Coupled Ecohydrology and Plant Hydraulics Modeling Predicts Ponderosa Pine Seedling Mortality and Lower Treeline in the US Northern Rocky Mountains*.

Sperry, J.S., Donnelly, J.R. & Tyree, M.T. (1988) A method for measuring hydraulic conductivity and embolism in xylem. *Plant, Cell & Environment*, **11**, 35–40.

Sperry, J.S. & Love, D.M. (2015) What plant hydraulics can tell us about responses to climate-change droughts. *New Phytologist*, **207**, 14–27.

Stocker, T.F., Qin, D., Plattner, G.-K., Tignor, M., Allen, S.K., Boschung, J., Nauels, A., Xia, Y., Bex, V. & Midgley, P.M. (2013) IPCC, 2013: Climate Change 2013: The Physical Science Basis. Contribution of Working Group I to the Fifth Assessment Report of the Intergovernmental Panel on Climate Change. *IPCC*, **AR5**, 1535.

Subbarao, G.V., Nam, N.H., Chauhan, Y.S. & Johansen, C. (2000) Osmotic adjustment, water relations and carbohydrate remobilization in pigeonpea under water deficits. *Journal of Plant Physiology*, **157**, 651–659.

Tognetti, R., Michelozzi, M. & Giovannelli, a. (1997) Geographical variation in water relations, hydraulic architecture and terpene composition of Aleppo pine seedlings from Italian provenances. *Tree Physiology*, **17**, 241–250.

Torres-Ruiz, J.M., Jansen, S., Choat, B., McElrone, A.J., Cochard, H., Brodribb, T.J., Badel, E., Burlett, R., Bouche, P.S., Brodersen, C.R., Li, S., Morris, H. & Delzon, S. (2015) Direct X-Ray Microtomography Observation Confirms the Induction of Embolism upon Xylem Cutting under Tension. *Plant Physiology*, **167**, 40–43.

Torres-Ruiz, J.M., Sperry, J.S. & Fernández, J.E. (2012) Improving xylem hydraulic conductivity measurements by correcting the error caused by passive water uptake. *Physiologia Plantarum*, **146**, 129–135.

Trenberth, K.E., Dai, A., Van Der Schrier, G., Jones, P.D., Barichivich, J., Briffa, K.R. & Sheffield, J. (2014) Global warming and changes in drought. *Nature Climate Change*, **4**, 17–22.

Trifilo, P., Barbera, P.M., Raimondo, F., Nardini, A. & Gullo, M. a. L. (2014) Coping with drought-induced xylem cavitation: coordination of embolism repair and ionic effects in three Mediterranean evergreens. *Tree Physiology*, **34**, 109–122.

Tyree, M.T., Engelbrecht, B.M.J., Vargas, G., Kursar, T. a, States, U., Forest, A., Box, P.O. & Vermont, M.T.T. (2003) Desiccation Tolerance of Five Tropical Seedlings in Panama. Relationship to a Field Assessment of Drought Performance. *Plant physiology*, **132**, 1439–1447.

Tyree, M.T. & Sperry, J.S. (1989) Vulnerability of Xylem to Cavitation and Embolism. *Ann. Rev. Plant. Phys. Mol. Bio.*, **40**, 19–38.

Tyree, M.T., Vargas, G., Engelbrecht, B.M.J. & Kursar, T. a. (2002) Drought until death do us part: a case study of the desiccation-tolerance of a tropical moist forest seedling-tree,

Licania platypus (Hemsl.) Fritsch. *Journal of experimental botany*, **53**, 2239–2247.
Ullah, S., Skidmore, A.K., Naeem, M. & Schlerf, M. (2012) An accurate retrieval of leaf water content from mid to thermal infrared spectra using continuous wavelet analysis. *Science of the Total Environment*, **437**, 145–152.
Venturas, M.D., Sperry, J.S., Love, D.M., Frehner, E.H., Allred, M.G., Wang, Y. & Anderegg, W.R.L. (2018) A stomatal control model based on optimization of carbon gain versus hydraulic risk predicts aspen sapling responses to drought. *New Phytologist*.
Veysi, S., Naseri, A.A., Hamzeh, S. & Bartholomeus, H. (2017) A satellite based crop water stress index for irrigation scheduling in sugarcane fields. *Agricultural Water Management*, **189**, 70–86.
Walker, S.H. & Duncan, D.B. (1967) Estimation of the probability of an event as a function of several independent variables. *Biometrika*.
Wang, Q. & Li, P. (2012) Identification of robust hyperspectral indices on forest leaf water content using PROSPECT simulated dataset and field reflectance measurements. *Hydrological Processes*, **26**, 1230–1241.
Wright, I.J., Reich, P.B., Westoby, M., Ackerly, D.D., Baruch, Z., Bongers, F., Cavender-Bares, J., Chapin, T., Cornelissen, J.H.C., Diemer, M., Flexas, J., Garnier, E., Groom, P.K., Gulias, J., Hikosaka, K., Lamont, B.B., Lee, T., Lee, W., Lusk, C., Midgley, J.J., Navas, M.-L., Niinemets, U., Oleksyn, J., Osada, N., Poorter, H., Poot, P., Prior, L., Pyankov, V.I., Roumet, C., Thomas, S.C., Tjoelker, M.G., Veneklaas, E.J. & Villar, R. (2004) The worldwide leaf economics spectrum. *Nature*, **428**, 821–7.
Yilmaz, M.T., Hunt, E.R. & Jackson, T.J. (2008) Remote sensing of vegetation water content from equivalent water thickness using satellite imagery. *Remote Sensing of Environment*, **112**, 2514–2522.

FIGURES

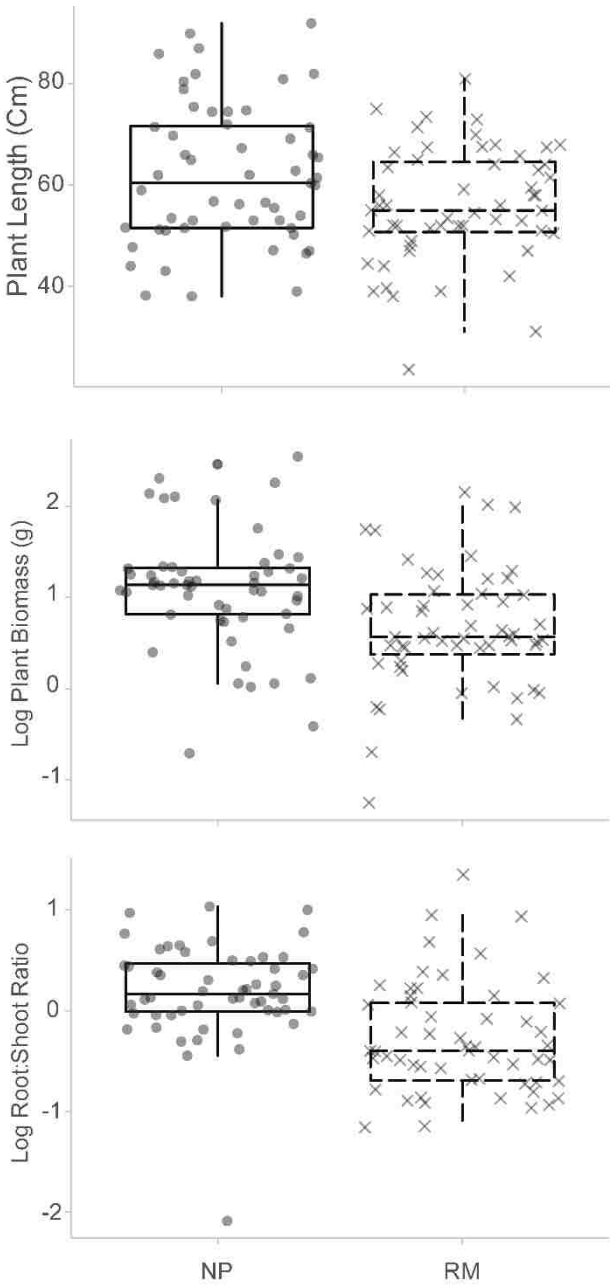

Fig. 1. Morphological differences between North Plateau (NP) and Rocky Mountain (RM) seedlings. NP seedlings were consistently bigger in size and biomass and allocated greater biomass to below ground organs. Differences among populations are significant across all panels.

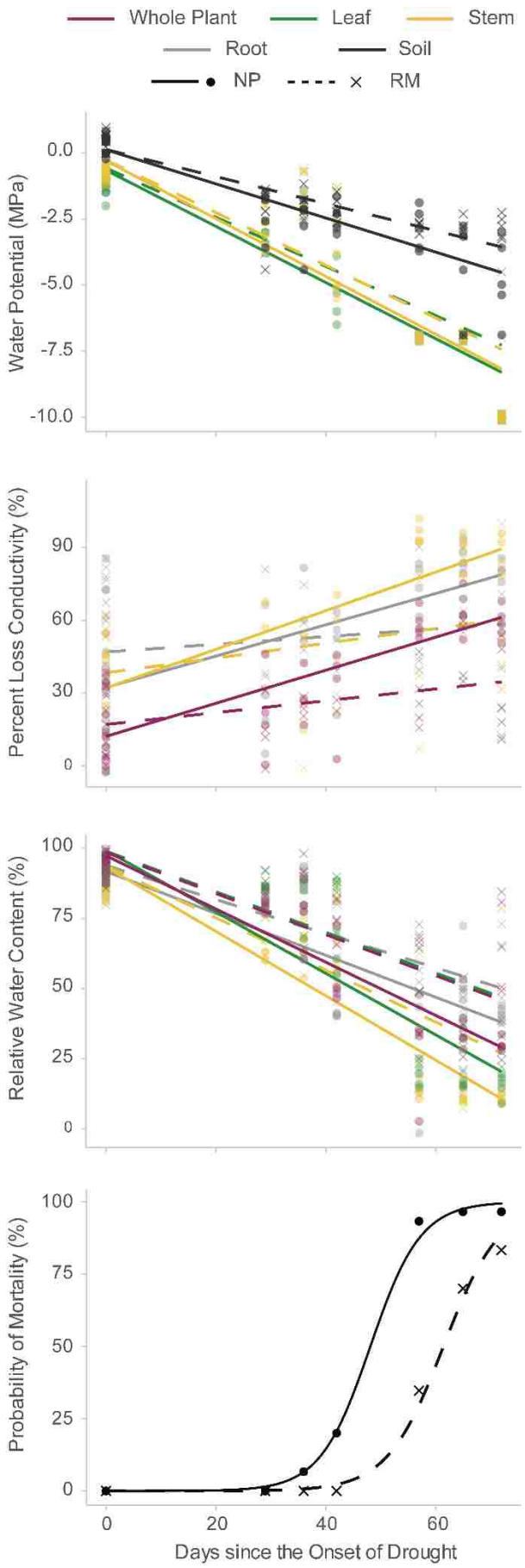
Whole Plant
Leaf
Stem
Root
Soil
NP
RM
Water Potential (MPa)
0.0
-2.5
-5.0
-7.5
-10.0
Percent Loss Conductivity (%)
90
60
30
0
Relative Water Content (%)
100
75
50
25
0
Probability of Mortality (%)
100
75
50
25
0
0
20
40
60
Days since the Onset of Drought

Fig. 2. Dynamics of population-level mortality, drought intensity, and whole-plant physiological state over time. Panel A: Probability of mortality increased after day 29 and 42 of drought in North Plateau (NP, open circles and corresponding solid line) and Rocky Mountain (RM, closed circles and corresponding dashed line) seedlings, respectively. Panel B: Water potentials decreased over time in soil (gray), stem (orange) and leaves (green) but NP seedlings experienced greater decline rates. Panel C: Both populations experienced loss of conductivity over time in both stems and roots (brown) and at the plant level (blue), but NP seedlings lost hydraulic conductivity at faster rates in all organs. Panel D: Relative water content declined over time at similar rates in all organs but NP seedlings desiccated faster than RM seedlings.

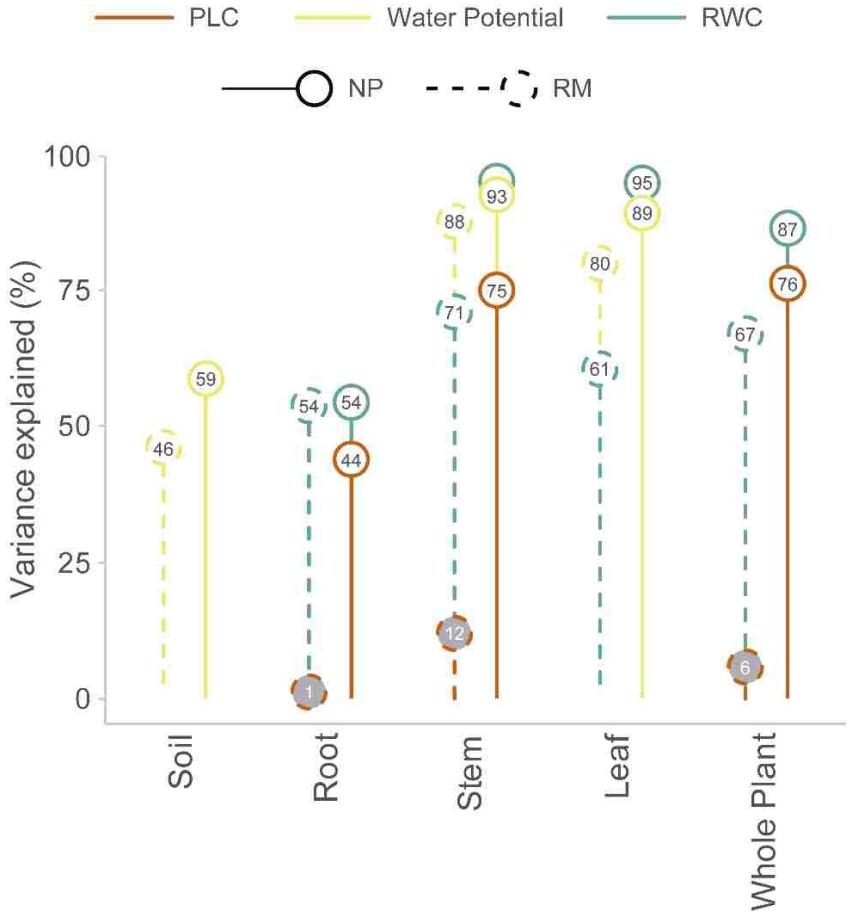

Fig. 3. Percentage of variation in DIM risk explained by each predictor of mortality in each organ and population. Relative water content (RWC) (green) and water potential (yellow) predicted DIM risk in all organs and populations and had a similar average predictive power (i.e. variance explained). In contrast, loss of conductivity (PLC) (purple) only predicted DIM risk in NP seedlings and had lower average predictive power even after excluding non-significant models (gray circles).

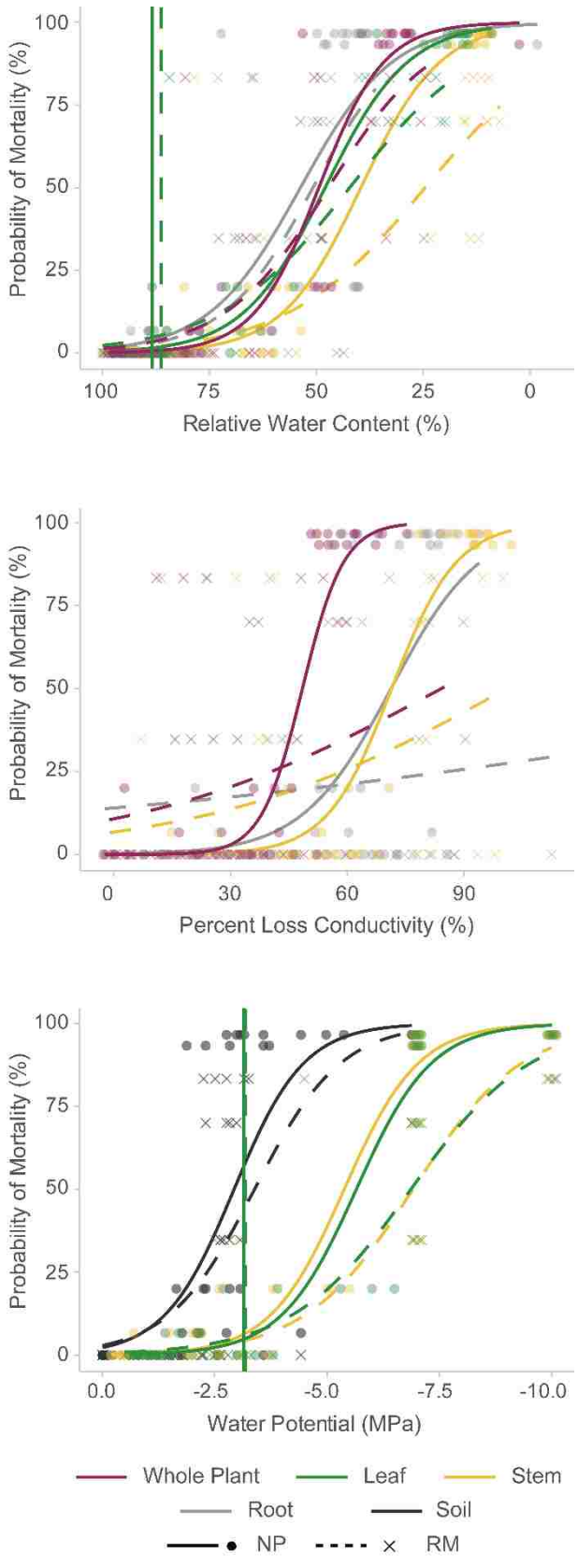
Probability of Mortality (%)
100
75
50
25
0
100
75
50
25
0
Relative Water Content (%)
Probability of Mortality (%)
0
30
60
90
Percent Loss Conductivity (%)
Probability of Mortality (%)
0.0
-2.5
-5.0
-7.5
-10.0
Water Potential (MPa)
Whole Plant
Leaf
Stem
Root
Soil
NP
RM

Fig. 4. Relationships between mortality risk and each DIM predictor. Percent loss conductivity (PLC) showed different mortality functions between NP and RM seedlings and no incipient mortality thresholds in RM seedlings. Both relative water content (RWC) and water potential showed similar mortality functions with incipient mortality thresholds at turgor loss (vertical lines) across organs and populations. However, values leading to 50% mortality risk across organs and populations were less variable in RWC than in water potential or in PLC.

SUPPORTING INFORMATION

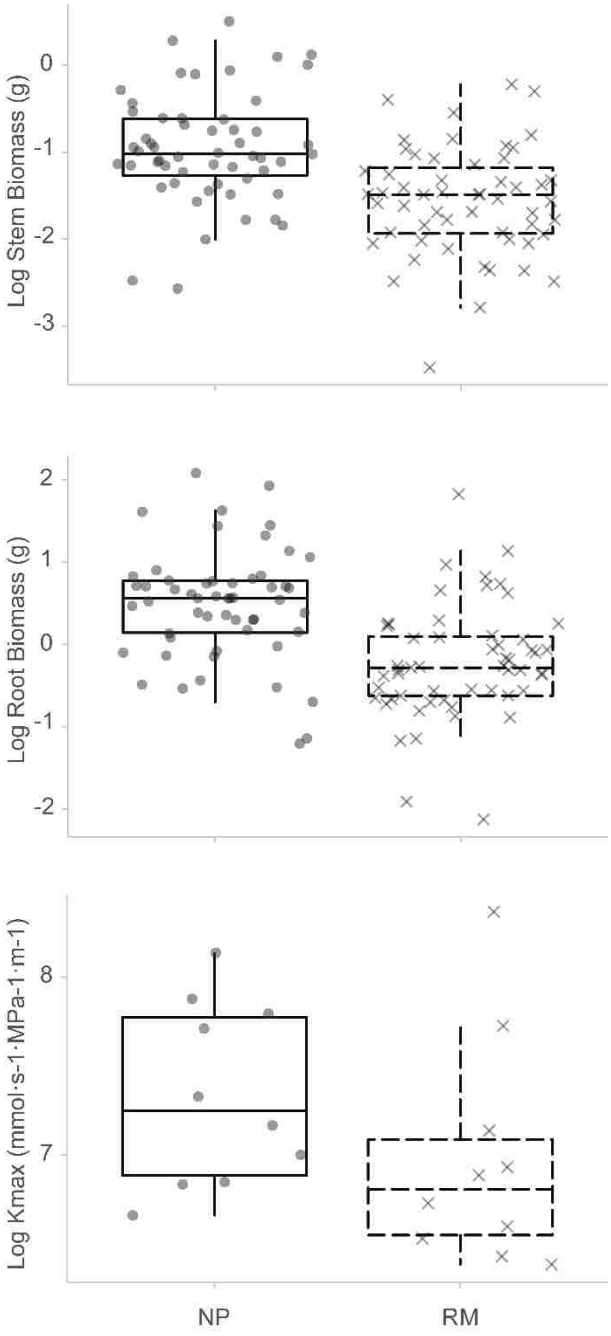

Fig. S1. Differences in stem and root biomass and hydraulic conductivity between North Plateau (NP) and Rocky Mountain (RM) seedlings. NP seedlings were consistently bigger and had greater hydraulic conductivity. Differences among populations are significant across all panels.

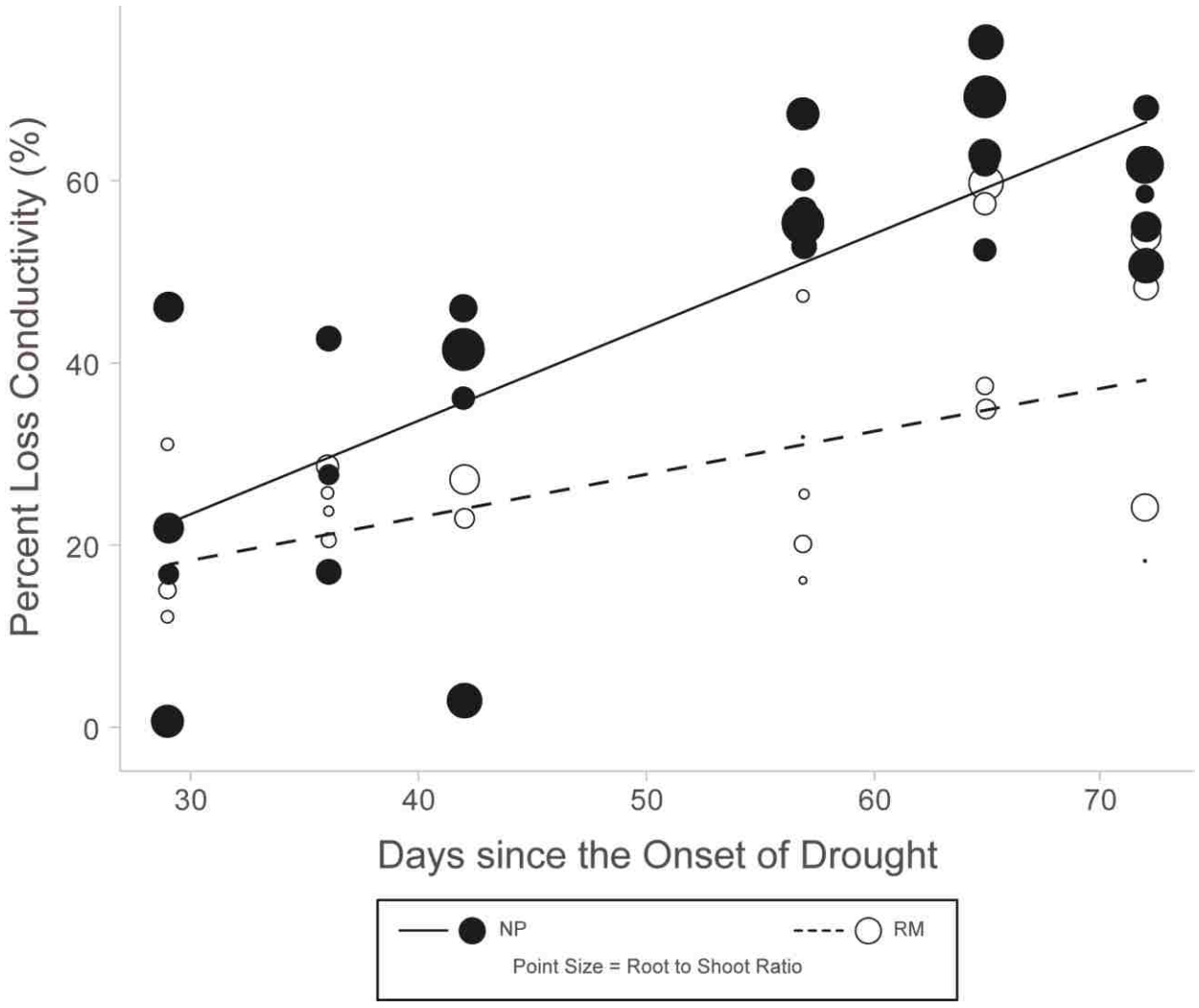

Fig. S2. North Plateau seedlings (NP, black points and solid line) lost hydraulic conductivity at faster rates than Rocky Mountain seedlings (RM, white points and dashed line) due to differences in biomass allocation. NP seedlings allocated more biomass to roots and consumed water in the soil at faster rates.

Table S1. Number of PLC data points removed by population, organ and sampling group. The number of points removed was similar in each population and organ. The highest number of points removed in each organ corresponds to Controls. Removed data within this group correspond to two groups of well-watered control seedlings (preconditioned and non-preconditioned) that were measured at the end of the experiment. These seedlings grew over time which resulted in greater hydraulic conductivity than in the preconditioned controls used to calculate population-level Kmax at day 0. Removal of these data is unlikely to drive patterns found in PLC between populations given that observed differences between populations appeared at late stages of drought.

Group	Stem			Root			Whole Plant		
	Coastal	Rocky Mountain	Difference	Coastal	Rocky Mountain	Difference	Coastal	Rocky Mountain	Difference
Controls	9	5	4	6	3	3	9	4	5
Drought - Day 29	2	5	-3	1	2	-1	1	2	-1
Drought - Day 36	2	1	1	2	1	1	2	1	1
Drought - Day 42	2	3	-1	1	3	-2	1	3	-2
Drought - Day 57	0	0	0	0	0	0	0	0	0
Drought - Day 65	0	1	-1	0	0	0	0	1	-1
Drought - Day 72	0	0	0	0	0	0	0	0	0
TOTAL	**15**	**15**		**10**	**9**		**13**	**11**	

Table S2. Linear models used to standardize RWC by morphology and physiology and residual models testing independent effects of morphology and physiology on population differences in desiccation rates.

Model and Factors	Estimate	95% C.I. Estimates		*p-value*	d.f. (res.)	Adjusted R square
		2.5%	97.5%			
Log(Stem Hydraulic Conductivity) = Plant length x Population				**<0.001**	102	0.18
Intercept	1.830401	1.37624098	2.28456091	**<0.001**	-	-
Plant Length	0.017699	0.01068521	0.02471359	**<0.001**	-	-
Population - RMR	0.162318	-0.01802708	0.34266243	0.077	-	-
Log(Root Hydraulic Conductance) = Plant length x Population				**<0.001**	105	0.08
Intercept	3.626437	3.265981513	3.98689211	**<0.001**	-	-
Plant Length	0.008438	0.002852591	0.01402426	**0.003**	-	-
Population - RMR	0.148013	0.001958142	0.29406819	**0.047**	-	-

Table S3. Models assessing changes in drought intensity, whole-plant hydraulic function and degree of desiccation, population-level mortality and canopy activity levels over time starting at day 29 since the onset of drought. Only significant factors are shown. A logistic model was used for probability of mortality because it could not be transformed to meet linear model assumptions. Probability of mortality was also transformed to per unit basis following requirements of models with binomial distributions.

Model and Factors	**Model type**	**Estimate**	**95% C.I. Estimates**		***p-value***	**d.f. (res.)**	**Adjusted R square**
			2.5%	**97.5%**			
Soil Water Potential = Days since Onset of Drought x Population					**<0.001**	57	0.30
Intercept	LM	-1.075160	-0.239196239	0.48603325	**0.031**	-	-
Days since Onset of Drought		-0.041689	-0.073496211	-0.05567413	**<0.001**	-	-
Population-RMR		0.620238	-0.503905295	0.52172409	**0.029**	-	-
Leaf Water Potential = Days since Onset of Drought x Population					**<0.001**	53	0.77
Intercept	LM	2.22232	0.95229030	3.4923595	**<0.001**	-	-
Days since Onset of Drought		-0.15796	-0.18092399	-0.1350017	**<0.001**	-	-
Population-RMR		0.79490	0.07352279	1.5162857	**0.031**	-	-
Stem Water Potential = Days since Onset of Drought x Population					**<0.001**	54	0.83
Intercept	LM	3.15997	2.04923568	4.2706960	**<0.001**	-	-
Days since Onset of Drought		-0.17223	-0.19250203	-0.1519484	**<0.001**	-	-
Population-RMR		0.59747	-0.03882642	1.2337579	0.065	-	-

Model and Factors	Model type	Estimate	95% C.I. Estimates		*p-value*	d.f. (res.)	Adjusted R square
			2.5%	97.5%			
Plant PLC = Days since Onset of Drought x Population	LM				**<0.001**	44	0.57
Intercept		-7.5348	-25.9228774	10.87328814	0.414	-	-
Days since Onset of Drought		1.0279	0.6910973	1.36463821	**<0.001**	-	-
Population-RMR		11.9945	-14.0948133	38.08376569	0.360	-	-
Days since Onset of Drought x Population-RMR		-0.5622	-1.0405618	-0.08380609	**0.022**	-	-
Plant PLC = Days since Onset of Drought x Population x Root Shoot Ratio	LM				**<0.001**	43	0.60
Intercept		-17.6897	-37.7473072	2.36782551	0.082	-	-
Days since Onset of Drought		0.9740	0.6460260	1.30191448	**<0.001**	-	-
Population-RMR		17.6961	-7.9630927	43.35522894	0.172	-	-
Root Shoot Ratio		8.3719	0.6118301	16.13193591	**0.035**	-	-
Days since Onset of Drought x Population-RMR		-0.5591	-1.0194898	-0.09866543	**0.018**	-	-
Stem PLC = Days since Onset of Drought x Population	LM				**<0.001**	40	0.49
Intercept		8.1380	-15.6972775	31.973188	0.495	-	-
Days since Onset of Drought		1.2206	0.7976874	1.643427	**<0.001**	-	-
Population-RMR		-24.8821	-37.5015720	-12.262635	**<0.001**	-	-
Root PLC = Days since Onset of Drought x Population	LM				**<0.001**	45	0.27
Intercept		9.1774	-17.7046217	36.059357	0.496	-	-
Days since Onset of Drought		1.0530	0.5609697	1.545101	**<0.001**	-	-
Population-RMR		39.2267	1.1932278	77.260242	**0.044**	-	-
Days since Onset of Drought x Population-RMR		-0.9189	-1.6133898	-0.224493	**0.011**	-	-

Model and Factors	Model type	Estimate	95% C.I. Estimates		*p-value*	d.f. (res.)	Adjusted R square
			2.5%	97.5%			
Plant RWC = Days since Onset of Drought x Population	LM				**<0.001**	54	0.71
Intercept		110.9513	99.456181	122.4465168	**<0.001**	-	-
Days since Onset of Drought		-1.1934	-1.403436	-0.9833056	**<0.001**	-	-
Population-RMR		12.6950	6.098499	19.2915497	**<0.001**	-	-
Leaf RWC = Days since Onset of Drought x Population	LM				**<0.001**	54	0.78
Intercept		141.8941	124.20776335	159.580410	**<0.001**	-	-
Days since Onset of Drought		-1.8720	-2.20868295	-1.535356	**<0.001**	-	-
Population-RMR		-8.9838	-33.99603021	16.028446	0.475	-	-
Days since Onset of Drought x Population-RMR		0.5308	0.05469984	1.006928	**0.030**	-	-
Stem RWC = Days since Onset of Drought x Population	LM				**<0.001**	55	0.73
Intercept		118.3478	104.167577	132.528118	**<0.001**	-	-
Days since Onset of Drought		-1.6074	-1.866141	-1.348607	**<0.001**	-	-
Population-RMR		12.9269	4.857052	20.996774	**0.002**	-	-
Root RWC = Days since Onset of Drought x Population	LM				**<0.001**	54	0.51
Intercept		97.7960	85.046141	110.5459402	**<0.001**	-	-
Days since Onset of Drought		-0.8574	-1.09040	-0.6244183	**<0.001**	-	-
Population-RMR		9.7382	2.421658	17.0547688	**0.010**	-	-

Model and Factors	Model type	Estimate	95% C.I. Estimates		*p-value*	d.f. (res.)	Adjusted R square
			2.5%	97.5%			
Total Conductance = Days since Onset of Drought x Population	LM				0.219	54	0.03
Intercept		1.710e-05	2.844115e-06	3.136323e-05	**0.020**	-	-
Days since Onset of Drought		-2.493e-07	-5.207803e-07	2.208813e-08	0.071	-	-
Population-RMR		-1.971e-05	-3.987444e-05	4.576837e-07	0.055	-	-
Days since Onset of Drought x Population-RMR		3.430e-07	-4.088858e-08	7.268434e-07	0.079	-	-
Probability of Mortality/100 = Days since Onset of Drought x Population	GLM				**<0.001**	57	NA
Intercept		-10.04974	-16.279168	-5.8607657	**<0.001**	-	-
Days since Onset of Drought		0.20847	0.123628	0.3383138	**<0.001**	-	-
Population-RMR		-2.76760	-5.752685	-0.7046645	**0.024**	-	-

Table S4. Linear models used to predict changes in RWC over time and residual models testing effects of morphology and physiology on population differences in desiccation rates. Data used corresponds to values starting at day 29 since the onset of drought to the end of the drought.

Model and Factors	Estimate	95% C.I. Estimates		*p-value*	d.f. (res.)	Adjusted R square	AICc
		2.5%	97.5%				
Plant RWC = Days since Onset of Drought				**<0.001**	45	0.59	-
Intercept	112.2879	97.627177	126.9487100	**<0.001**	-	-	-
Days since Onset of Drought	-1.1199	-1.388956	-0.8508492	**<0.001**	-	-	-
Residuals Plant RWC = Population x Plant PLC x Stomatal Conductance				**<0.001**	39	0.34	396.00
Intercept	-2.583e+00	-15.5342417	10.3680573	0.689	-	-	-
Population-RMR	1.556e+01	-1.3856152	32.5083621	0.071	-	-	-
Plant PLC	-7.542e-02	-0.3247718	0.1739392	0.545	-	-	-
Stomatal Conductance	-1.459e+03	-5117.8146684	2199.5811954	0.425	-	-	-
Population-RMR x Stomatal Conductance	7.118e+03	2074.9238767	12160.4019900	**0.007**	-	-	-
Population-RMR x Plant PLC	-1.392e-01	-0.5553165	0.2769169	0.503	-	-	-
Plant PLC x Stomatal Conductance	3.520e+01	-44.1219635	114.5237150	0.375	-	-	-
Population-RMR x Plant PLC x Stomatal Conductance	-2.424e+02	-396.5837658	-88.2785224	**0.003**	-	-	-
Residuals Plant RWC = Population x log(Root to shoot ratio) x log(Plant biomass)				**<0.001**	44	0.33	389.02
Intercept	11.704	4.340938	19.066895	**0.002**	-	-	-
log(Plant biomass)	-9.078	-16.156395	-1.999588	**0.013**	-	-	-
log(Root to shoot ratio)	-13.090	-20.922028	-5.257927	**0.002**	-	-	-

Table S5. Logistic models assessing the ability to predict mortality of *RWC*, *PLC* and water potential in each organ within a population.

Model and Factors	Estimate	95% C.I. Estimates 2.5%	97.5%	*p-value*	d.f. (res.)	V.E.	AIC
Coastal Pine							
Probability of Mortality/100 = Root RWC				**0.001**	34	0.54	31.80
Intercept	4.98366	2.2091939	8.678722	**0.002**	-	-	-
Root RWC	-0.09276	-0.1639429	-0.044972	**0.001**	-	-	-
Probability of Mortality/100 = Stem RWC				**< 0.001**	50	0.95	8.47
Intercept	4.26961	2.0814809	8.46725910	**0.003**	-	-	-
Stem RWC	-0.10784	-0.1846087	-0.06349933	**< 0.001**	-	-	-
Probability of Mortality/100 = Leaf RWC				**< 0.001**	48	0.95	8.88
Intercept	4.95464	2.4975909	9.43711623	**0.002**	-	-	-
Leaf RWC	-0.10333	-0.1772533	-0.06096504	**< 0.001**	-	-	-
Probability of Mortality/100 = Plant RWC				**0.002**	39	0.87	15.42
Intercept	6.47419	3.2503647	12.0944653	**0.002**	-	-	-
Plant RWC	-0.13098	-0.2491567	-0.0686114	**0.002**	-	-	-
Rocky Mountain							
Probability of Mortality/100 = Root RWC				**0.005**	35	0.54	28.08
Intercept	4.78117	1.3645408	9.33191421	**0.015**	-	-	-
Root RWC	-0.09411	-0.1745279	-0.03855422	**0.005**	-	-	-
Probability of Mortality/100 = Stem RWC				**< 0.001**	49	0.71	26.29
Intercept	1.51439	0.09518901	3.15167840	**0.046**	-	-	-
Stem RWC	-0.06163	-0.10373380	-0.03298452	**< 0.001**	-	-	-
Probability of Mortality/100 = Leaf RWC				**< 0.001**	50	0.61	29.67
Intercept	2.74463	0.6939106	5.2292095	**0.015**	-	-	-
Leaf RWC	-0.06500	-0.1064305	-0.0337169	**< 0.001**	-	-	-
Probability of Mortality/100 = Plant RWC				**< 0.001**	43	0.67	26.43
Intercept	3.84161	1.2997532	7.12454758	**0.008**	-	-	-
Plant RWC	-0.08141	-0.1396342	-0.04074093	**< 0.001**	-	-	-

Model and Factors	Estimate	95% C.I. Estimates 2.5%	97.5%	*p-value*	d.f. (res.)	V.E.	AIC
Coastal Pine							
Probability of Mortality/100 = Root PLC				**0.003**	43	0.44	37.06
Intercept	-6.21832	-11.16383724	-2.9931479	**0.002**	-	-	-
Root PLC	0.08727	0.04087564	0.1558133	**0.003**	-	-	-
Probability of Mortality/100 = Stem PLC				**< 0.001**	35	0.75	17.02
Intercept	-8.58459	-14.88912583	-4.5411667	**< 0.001**	-	-	-
Stem PLC	0.12022	0.06412035	0.2083284	**< 0.001**	-	-	-
Probability of Mortality/100 = Plant PLC				**0.003**	39	0.76	15.60
Intercept	-9.16749	-17.2236736	-4.4382974	**0.004**	-	-	-
Plant PLC	0.18904	0.0934005	0.3492716	**0.003**	-	-	-
Rocky Mountain							
Probability of Mortality/100 = Root PLC				0.564	44	0.01	51.76
Intercept	-1.813737	-3.79172600	-0.2196395	**0.042**	-	-	-
Root PLC	0.008344	-0.01954568	0.0384584	0.564	-	-	-
Probability of Mortality/100 = Stem PLC				0.114	33	0.12	38.75
Intercept	-2.62256	-5.152451247	-0.7063709	**0.018**	-	-	-
Stem PLC	0.02598	-0.004303739	0.0616459	0.114	-	-	-
Probability of Mortality/100 = Plant PLC				0.211	40	0.06	44.82
Intercept	-2.11749	-3.81842509	-0.73632606	**0.006**	-	-	-
Plant PLC	0.02514	-0.01423102	0.06756254	0.211	-	-	-

Model and Factors	Estimate	95% C.I. Estimates 2.5%	97.5%	*p-value*	d.f. (res.)	V.E.	AIC
Coastal Pine							
Probability of Mortality/100 = Soil Water Potential				**<0.001**	53	0.59	35.66
Intercept	-3.9644	-6.842051	-2.2048206	**<0.001**	-	-	-
Soil Water Potential	-1.3502	-2.366627	-0.7167899	**<0.001**	-	-	-
Probability of Mortality/100 = Stem Water Potential				**<0.001**	53	0.93	11.46
Intercept	-6.5164	-12.347141	-3.5992918	**0.002**	-	-	-
Stem Water Potential	-1.2105	-2.188772	-0.6825154	**<0.001**	-	-	-
Probability of Mortality/100 = Leaf Water Potential				**<0.001**	52	0.89	14.34
Intercept	-6.758	-13.420706	-3.6954542	**0.002**	-	-	-
Leaf Water Potential	-1.195	-2.227083	-0.6702828	**<0.001**	-	-	-
Rocky Mountain							
Probability of Mortality/100 = Soil Water Potential				**0.010**	53	0.46	37.00
Intercept	-3.8623	-6.974155	-2.1278054	**<0.001**	-	-	-
Soil Water Potential	-1.1648	-2.345810	-0.4730897	**0.010**	-	-	-
Probability of Mortality/100 = Stem Water Potential				**0.002**	52	0.88	19.37
Intercept	-5.7081	-11.295333	-3.193501	**0.002**	-	-	-
Stem Water Potential	-0.8257	-1.624107	-0.435619	**0.002**	-	-	-
Probability of Mortality/100 = Leaf Water Potential				**<0.001**	52	0.80	22.78
Intercept	-5.1561	-9.064376	-3.0238930	**<0.001**	-	-	-
Leaf Water Potential	-0.7508	-1.325623	-0.4035579	**<0.001**	-	-	-

Table S6. Logistic models assessing the consistency of the relationships between probability of Mortality and water potential, *PLC* and *RWC* among populations and organs.

Model and Factors	Estimate	95% C.I. Estimates		*p-value*	d.f. (res.)	AIC
		2.5%	97.5%			
*Probability of Mortality = RWC * Population * Organ*				**< 0.001**	348	175.1
Intercept	4.954645	2.49759289	9.43711507	**0.002**	-	-
RWC	-0.103329	-0.17725331	-0.06096500	**< 0.001**	-	-
Population-RMR	-2.210012	-7.06192957	1.34636292	0.262	-	-
Organ-Plant	1.519549	-3.97511538	7.68110342	0.566	-	-
Organ-Roots	0.029017	-5.15107061	4.53011361	0.990	-	-
Organ-Stem	-0.685038	-5.68687207	4.16151679	0.753	-	-
*RWC * Population-RMR*	0.038328	-0.02155419	0.11789299	0.243	-	-
*RWC * Organ-Plant*	-0.027653	-0.15367542	0.06955652	0.588	-	-
*RWC * Organ-Roots*	0.010569	-0.07288420	0.09767735	0.791	-	-
*RWC * Organ-Stem*	-0.004513	-0.09221156	0.08169024	0.910	-	-
*Population-RMR * Organ-Plant*	-0.422577	-7.37617276	6.07617875	0.895	-	-
*Population-RMR * Organ-Roots*	2.007525	-4.13144001	8.82999003	0.531	-	-
*Population-RMR * Organ-Stem*	-0.545209	-5.98431389	4.99210991	0.831	-	-
*RWC * Population-RMR * Organ-Plant*	0.011241	-0.10293724	0.14764083	0.849	-	-
*RWC * Population-RMR * Organ-Roots*	-0.039680	-0.15626517	0.06767046	0.471	-	-
*RWC * Population-RMR * Organ-Stem*	0.007881	-0.08965499	0.10636449	0.866	-	-

Model and Factors	Estimate	95% C.I. Estimates		*p-value*	d.f. (res.)	AIC
		2.5%	97.5%			
*Probability of Mortality = PLC * Population * Organ*				< **0.001**	234	205.01
Intercept	-9.16749	-17.22367359	-4.43829743	**0.004**	-	-
PLC	0.18904	0.09340050	0.34927158	0.003	-	-
Population-RMR	7.05000	1.98881145	15.21450305	**0.030**	-	-
Organ-Roots	2.94917	-4.01424362	11.67861929	0.433	-	-
Organ-Stem	0.58290	-7.40475793	9.62889084	0.885	-	-
*PLC * Population-RMR*	-0.16390	-0.32793433	-0.05796376	**0.013**	-	-
*PLC * Organ-Roots*	-0.10176	-0.26910035	0.01718508	0.142	-	-
*PLC * Organ-Stem*	-0.06882	-0.23922148	0.06199070	0.340	-	-
*Population-RMR * Organ-Roots*	-2.64542	-11.62832907	4.68665170	0.502	-	-
*Population-RMR * Organ-Stem*	-1.08798	-10.46760595	7.28388241	0.798	-	-
*PLC * Population-RMR * Organ-Roots*	0.08497	-0.04440641	0.25798939	0.248	-	-
*PLC * Population-RMR * Organ-Stem*	0.06966	-0.07075485	0.24630373	0.363	-	-

Model and Factors	Estimate	95% C.I. Estimates		*p-value*	d.f. (res.)	AIC
		2.5%	97.5%			
*Probability of Mortality = Water potential * Population * Organ*				< **0.001**	315	140.62
Intercept	-6.75760	-13.4207055	-3.6954542	**0.002**	-	-
Water potential	-1.19521	-2.2270832	-0.6702828	< **0.001**	-	-
Population-RMR	1.60149	-3.4211186	8.6136058	0.543	-	-
Organ-Soil	2.79325	-1.4895129	9.6921907	0.263	-	-
Organ-Stem	0.24124	-6.4449649	7.5774654	0.937	-	-
*Water potential * Population-RMR*	0.44437	-0.3366592	1.5321003	0.291	-	-
*Water potential * Organ-Soil*	-0.15503	-1.3158572	1.0504650	0.775	-	-
*Water potential * Organ-Stem*	-0.01526	-1.1356876	1.1495089	0.976	-	-
*Population-RMR * Organ-Soil*	-1.49940	-9.0635572	4.4072637	0.628	-	-
*Population-RMR * Organ-Stem*	-0.79325	-9.4144049	7.0472438	0.835	-	-
*Water Potential * Population-RMR * Organ-Soil*	-0.25894	-1.8746480	1.1901370	0.726	-	-
*Water Potential * Population-RMR * Organ-Stem*	-0.05958	-1.4018790	1.2175489	0.923	-	-

CHAPTER 3: ECTOMYCORRHIZAL NETWORKS IMPAIR CARBON AND WATER RELATIONS OF PLANT HOSTS DURING PERIODS OF CARBON DEPLETION

ABSTRACT

Ectomycorrhizal networks can transfer nutrients from plants with abundant resources to resource-limited individuals. Among the resources that fungal networks can transfer, carbon has been particularly debated. During periods of carbon limitation, networks could relocate carbon from carbon-rich hosts to carbon-limited plants (plant-centric view). Alternatively, carbon-limited hosts may induce carbon deficit on ectomycorrhizal fungi, which then may increase carbon demand from hosts with abundant carbon (fungal-centric view). Given that carbon may play an important role in plant water relations, movement of carbon through ectomycorrhizal networks may also affect host water relations. Using a greenhouse experiment with *Pinus ponderosa* seedlings, we tested the extent to which ectomycorrhizal networks operate under plant-centric or fungal-centric views during periods of carbon limitation. We also assessed whether changes in host carbon pools affected host water relations. Ectomycorrhizal networks depleted carbon-rich hosts in response to carbon-limited hosts. Hosts with low carbon showed low water retention, loss of turgor, and desiccation symptoms despite being well-watered throughout the experiment. Symbiotic ectomycorrhizal networks can become parasitic in response to disturbances that cause differential host carbon availability. The observed effects of carbon depletion on host water relations suggest that networks may increase plant vulnerability to drought under future climates.

INTRODUCTION

Associations between plants and fungi have been incredibly successful and are found across the whole plant kingdom. In exchange for plant carbon, ectomycorrhizal associations increase resource uptake (Lapeyrie & Chilvers 1985), enhance growth (Thomson *et al.* 1994), help recruit seedlings (Bingham & Simard 2012) and, ultimately, can influence forest composition. Ectomycorrhizae also form underground networks that connect several plants through the same fungi. These networks can transfer resources from

hosts with abundant resources to hosts in need of them (Warren *et al.* 2008; He *et al.* 2009; Song *et al.* 2015). While several nutrients can be transferred, it is unclear whether non-structural carbohydrates (NSC) can be also transferred from carbon-rich to carbon-limited plants (e.g., seedlings with low assimilation) (Simard & Perry 1997; Wu *et al.* 2001).

Some suggest that hosts with abundant NSC may transfer them to stressed, carbon-limited seedlings via ectomycorrhizal networks (Simard & Perry 1997; Song *et al.* 2015) (i.e., plant-centric view). Stressed seedlings could benefit from such transfer because higher NSC increases survival (Poorter & Kitajima 2007; O'Brien *et al.* 2014). In the long term, both hosts and fungi may also benefit because surviving seedlings could recover and share the carbon costs of the network. However, this hypothesis has two major critiques. First, carbon-rich hosts and fungi must pay a performance cost to sustain stressed seedlings (Ellström *et al.* 2015) and may not be favored by natural selection. Second, surviving hosts may compete for resources later and offset the long-term benefits of carbon transfer. Others suggest that fungi can switch demand from carbon-depleted to carbon rich hosts to meet the carbon needs of their fungal biomass (Fungi-centric view). This hypothesis suggests that hosts cannot regulate how much NSC are transferred to fungi which is not consistent with recent studies (Nehls *et al.* 2007 and references therein; Kiers *et al.* 2011). Clearly, there is controversy on whether carbon transfer is regulated by plant or fungal members of the network.

Carbon transfer through fungal networks can influence drought stress at fine scales and affect host physiology. Drought stress causes stomatal closure, reduces assimilation, and often leads to carbon depletion (McDowell *et al.* 2008; Sperry & Love 2015). Seedlings are especially susceptible to carbon depletion because they have small carbon pools (Sala & Mencuccini 2014 and references therein) but high carbon demands to grow and establish. Under drought, neighboring seedlings and adults may become carbon-depleted to different extents because drought stress varies across space and time (Simeone *et al.* 2018), and across plants with different traits (Lloret *et al.* 2018). Consequently, drought-stressed seedlings may provide less NSC to the network than non-stressed seedlings and both seedlings and fungi may lack sufficient carbon to cover all their needs. If plant hosts regulate carbon movement, there may be a redistribution of carbon from carbon-rich hosts to carbon-poor hosts. This redistribution may increase overall survival by

preventing severe carbon deficit on both hosts and fungi until drought eventually subsides. If fungi regulate carbon movement, they may reassign de symbiotic costs of carbon-poor hosts to carbon-rich hosts and draw more carbon from them. In turn, this increase in carbon costs may lead to carbon deficit and reduce overall survival. It is critical to determine whether networks are plant- or fungi-centric because they have contrasting implications. If networks transfer carbon from carbon rich to carbon poor hosts and reduce physiological stress, forests may be resistant to more intense and frequent droughts under future climates. However, if networks steal carbon from hosts and increase stress, forests may be vulnerable under future drought (Oliva *et al.* 2014). We need to know how fungal networks influence host physiology under variable stress to understand how forests will respond to future droughts. However, studies rarely assess the effects of fungal networks on host physiology under variable stress.

By drawing carbohydrates, fungal networks could affect the water relations of hosts during periods of carbon limitation. A global synthesis by Martinez-Vilalta *et al.* (2016) showed that plants rarely consume NSC below certain levels and suggested that basal levels of NSC are critical for survival. Other studies have shown that NSC could be used as osmolytes to maintain turgor in living cells (Sevanto *et al.* 2014), or to enhance water transport (McDowell *et al.* 2011; O'Brien *et al.* 2014). Together, these findings suggest that stored NSC cannot be consumed below a minimum threshold without impairing plant water relations. If stored NSC are important for water relations, carbon depletion by fungi could impair water relations and exacerbate drought stress. The effects of carbon depletion on water relations could be especially damaging for seedlings because of their already small NSC storage and their strong carbon needs. However, seedlings may avoid this problem if they receive NSC from non-stressed plants through fungal networks. If fungal networks do not decrease carbon demand during periods of carbon limitation (e.g., via mortality of fungi associated with carbon-poor hosts), the water relations of seedlings -including non-stressed ones- may eventually be impaired by their own symbionts. Some studies have shown that networks increase plant performance and seedling survival (Bingham & Simard 2012). However, these studies do not consider fluctuating conditions that can create carbon deficit between plant hosts and fungi and rarely study plant water relations in depth (but see Nardini *et al.* 2000). Additionally, these studies often focus on networks with large hub

trees which likely have sufficiently high NSC pools to feed small seedlings or their fungi (Beiler *et al.* 2015). However, plant-fungal networks may not always contain large trees and, in some instances such as in forest boundaries, they may be largely composed by recruiting seedlings.

We must decouple carbon depletion from drought stress to fully understand the role of fungal networks in water relations. Drought kills plants by impairing their water relations (Adams *et al.* 2017). However, carbon depletion is involved in the process because NSC interacts with water (O'Brien *et al.* 2014; Sevanto *et al.* 2014; Secchi & Zwieniecki 2016, Sapes et al. in review). However, we do not fully understand the nature of this interaction, in part, because drought stress affects both plant water and plant carbon status. Thus, it is difficult to tease apart the sole effects of carbon depletion on water relations from those of water deficit. For the same reason, it is difficult to assess whether fungal networks affect host water relations with water deficit confounding the observed results. Thus, before adding drought to the equation, we must study how networks influence water relations through carbon without water deficit. By excluding drought, we can find how much carbon can be consumed without compromising plant water relations and whether networks ameliorate or amplify these effects. We can ask these questions using experimental designs that deplete stored NSC under well-watered conditions.

We performed a greenhouse experiment with two-year-old ponderosa pine (*Pinus ponderosa* Douglas ex C. Lawson) seedlings connected through ectomycorrhizal networks. We applied a carbon depletion treatment under well-watered conditions to assess whether ectomycorrhizal networks move carbon among hosts following gradients of carbon and influence host physiology. Specifically, we asked 1) do networks transfer carbon from non-depleted to carbon-depleted hosts or do they increase carbon demand from non-depleted hosts without benefit to depleted hosts?; and 2) does network movement of carbon under differential stress affects host water relations?

MATERIALS AND METHODS

Experimental Design. In the spring of 2016, we planted eighty one-year-old ponderosa pine seedlings (source: Zone IV-V block of the Missoula Ponderosa Pine Seed Orchard, Department of Natural Resources) in forty 19 L pots at the University of Montana

greenhouse facilities. Each pot contained two seedlings. Half of the pots contained a stainless-steel mesh (139.7 µm wire diameter and 177.8 µm pore diameter) penetrable by fungal hyphae that separated seedlings and prevented root contacts. The remaining pots did not contain this mesh and allowed both root and mycorrhizal interactions between seedlings. The purpose of these barriers was to distinguish whether treatment effects were caused by mycorrhizal connections or root connections among plants and examine if the effects varied in the presence of roots. We observed the same patterns in both categories for all variables measured. For the sake of simplicity and sample size, we merged these two categories from here on. Seedlings were planted in a soil mixture consisting of 40% sand, 30% topsoil, and 30% peat moss; and were kept at field capacity (saturated soil) throughout the duration of the experiment. We inoculated the rhizosphere of each seedling with both a commercial mixture of *Rhizopogon* spores (Mycorrhizal Applications**.** Grants Pass, OR) and spores gathered from *Pezizales* already present in seedling root systems. Both *Rhizopogon* and members of the order *Pezizales* can form structures capable of redistributing resources among plants (Beiler *et al.* 2010; Song *et al.* 2015). After inoculation, seedlings grew unperturbed for 47 weeks to allow establishment of mature ectomycorrhizal associations between seedlings.

In the fall of 2017, we split all pots into two groups and applied a 3-week NSC depletion treatment to one group using light-blocking covers (Fig. 1). This procedure generated control (light) and NSC-depleted treatments. In each pot within the NSC-depleted treatment, we placed a cover over one of the two seedlings (dark) to reduce stored NSCs through photosynthetic inhibition and metabolic consumption while the other seedling (light paired with dark) was left undisturbed. Each cover consisted of a wire scaffolding (20 x 40 cm) overlaid with aluminum foil that blocked incoming light while keeping air temperatures similar to those in non-covered neighbor seedlings (ca. 24 ºC). We pierced 5 mm diameter holes evenly across the cover walls to facilitate air flow, keep the atmosphere around the plant unsaturated (i.e., relative humidity < 50%), and allow canopy transpiration. We maximized the number of holes while keeping minimum levels of light inside the covers (Photosynthetic Active Radiation < 0.40 µmol quanta m^{-2} s^{-1}). After three weeks of depletion, we harvested ten pots from both control an NSC-depleted treatments to assess the physiological status (see below) of light seedling pairs (LL), light paired with

dark (LD), and dark (D) seedlings. This harvest was also used to establish base-line $^{13}C/^{12}C$ ratios ($\Delta^{13}C$) in all organs across treatments. Note that sample size in light seedlings is twice as big as in dark and light neighbor seedlings because both plants in light pots qualify as light seedlings. Immediately after the harvest, the remaining light paired with dark seedlings within the carbon-depletion treatment were subjected to isotopic labeling with ^{13}C (see below) to assess potential transfer of carbon between individuals in the presence of carbon-limiting conditions. We also performed an identical labeling process in the remaining control pots to assess potential transfer among non-stressed plants. In this case, the labeled seedling was chosen at random between the two seedlings. Comparing carbon transfer between control and NSC-depleted pots provided information of the dynamics of carbon transfer in response to stress. After one week of labeling, we harvested the remaining pots in both treatments to measure changes in $^{13}C/^{12}C$ ratios.

Isotopic Labeling and Carbon Transfer Variables. Labeling was performed following similar methods to Song *et al.* (2015). We introduced ^{13}C into labeled seedlings by enclosing the entire canopy of each plant in a clear 2 L plastic bag. Each bag was subsequently injected with 20 mL of Carbon-^{13}C dioxide (99 atom % 13C, <3 atom % 18O, Sigma Aldrich. St. Louis, MO. USA) for a ratio of 10 mL of ^{13}C per 1 L of air and was left undisturbed for 2 hours. ^{13}C injections were performed at midday over two consecutive days. After each labeling event, enriched air was removed from bags and directed outside the greenhouse facilities using an industrial vacuum thus preventing contamination of neighboring seedlings. Ground samples of dry needles, stems, and roots were sent to the Stable Isotope Facility at University of California, Davis and analyzed to obtain $\Delta^{13}C$ values. We also collected a representative sample of fungal material from roots in seedlings across treatments and analyzed $\Delta^{13}C$ in them. Fungal samples were collected to ensure that ^{13}C traveled from needles in labeled seedlings to mycorrhizae on the labeled side and also to the mycorrhizae of paired non-labeled plants through the mycorrhizal network. Thus, it served us to validate the existence of a mycorrhizal network between seedling pairs. Additionally, extra seedlings were randomly interspersed throughout the treatments and used to assess possible contamination of the greenhouse environment during labeling. We collected needles from these seedlings after each labeling to compare the concentration of

^{13}C to that in seedlings measured prior to labeling. No signs of excess $\Delta^{13}C$ were observed in these seedlings.

Sampling Procedure. We measured midday leaf and stem water potentials in each seedling using a pressure chamber (PMS Instrument Company, Corvallis, OR) following methods in (Kaufmann 1968). Stem water potential was estimated equilibrating the water potential of a needle bundle with that in the stem following methods from Begg & Turner (1970) and measuring the equilibrated bundle with the pressure chamber. Subsequently, we harvested seedlings and collected tissue samples (needles, stem, and roots) for osmotic potential measurements. Tissue samples were wrapped in aluminum foil to prevent artificial declines in osmotic potential due to water loss. Then, they were placed in small Ziploc bags and stored in a cooler with dry ice for transport to the lab within the following 2 hours. The rest of the seedling was placed in a Ziploc bag containing a wet paper towel partially covered in tin foil to prevent desiccation without introducing external moisture into the tissues in contact with the towel (Garcia-Forner *et al.* 2016). Bags were placed in a cooler and transported to the lab to measure both hydraulic function (i.e., water content, hydraulic conductivity, and pressure-volume curves) and NSC pools (see below).

Upon arrival to the lab, samples collected for osmotic potential were crushed to extract cellular liquid contents and the extruded solution was used to saturate 28 mm^2 filter paper disks. Disks were then placed in a C-52 sample chamber attached to a Psypro data logger (Wescor, Inc. Logan, Utah. USA) to measure osmotic potentials. Finally, pressure potential was calculated in stems and needles as the difference between their respective water potentials and osmotic potentials. Pressure potential was not calculated in roots because we lacked root water potentials.

Pressure-Volume Curves. We used pressure-volume curves to estimate turgor loss point, osmotic potential at full turgor, modulus of elasticity, and capacitance; following the methods outlined in (Bartlett *et al.* 2012). For each seedling, water potential was recurrently measured in a needle bundle as described above. Bundles were placed on a bench to air-dry between consecutive water potential measurements. During water potential measurements, care was taken to increase and decrease pressure within the sample chamber at an equal rate

(< 0.01 MPa s^{-1}). PV-curves were considered complete when 4 – 8 data points on the apparent linear portion of the curve were obtained. After completion, each bundle was placed in a drying oven at 70ºC for a minimum of 48 hours to obtain individual dry mass. Turgor loss point was estimated as the point of transition between curved and linear portions in each p-v curve. The osmotic potential at full turgor was estimated as the intercept of a linear fit to the linear portion of the p-v curve. The modulus of elasticity was estimated as the change in osmotic water potential across the portion of the p-v curve before turgor loss point, divided by the change in RWC across the same span. Finally, capacitance was estimated by taking the slope of a regression of RWC and leaf water potential.

Relative Water Content. We used a sample of roots, stems, and needles of each seedling to measure their relative water content (RWC). First, samples were weighted to obtain fresh weight and returned to Ziploc bags in the cooler to avoid changes in hydraulic conductivity due to exposure to dry air. For consistency, root fresh weight was measured before any other tissue to avoid changes in RWC or hydraulic conductivity due to exposure to dry air. After hydraulic conductivity measurements (see below), stem, needle, and root samples were hydrated to full turgidity for 5 hours in a water bath at 10 °C. After hydration, we blotted each sample to remove surface moisture using a paper towel and weighed them to determine weight at full turgor. Samples were then oven dried at 70ºC, until a constant mass was achieved and weighed to determine dry weight. RWC was calculated as: ((Fresh weight - Dry weight)/(Turgid weight - Dry weight))*100 following methods from (Barrs & Weatherley 1962). The rest of the seedling was dried, separated by organ, and weighed. These weights were later combined with sample dry weights to calculate whole plant RWC by multiplying the dry mass of each tissue relative to whole-plant dry mass (i.e., tissue fraction) by their respective RWC. Whole-plant dry mass for each seedling was calculated by combining the dry mass of all samples and the remaining biomass.

Hydraulic Conductivity. We measured stem hydraulic conductivity and root hydraulic conductance using the gravimetric method (Sperry *et al.* 1988), after fresh weight measurements. We used the same hydraulic apparatus described in Sapes et al. (in review)

capable of measuring hydraulic conductance of both whole root systems and stems. After measuring fresh weight, stem segments were immersed in deionized water for 20 minutes to relax xylem tensions that could artificially alter conductivity values (Trifilò *et al.* 2014). After relaxation, stems were relocated to the hydraulic apparatus and each end was recut twice at a distance of 1 mm from the tips each time (total of 2 mm per side) to remove any potential emboli resulting from transport, previous cuts, and relocation (Torres-Ruiz *et al.* 2015). Stems were then connected to the hydraulic apparatus while under water, with their terminal ends facing downstream flow. The stems were then raised out of the water and the connections were checked to ensure that there were no leaks. A solution of water with 10 mM KCl degassed at 3 kPa for at least 8 hours was then used for all hydraulic measurements (Espino & Schenk 2011). First, initial background flow was measured to account for the flow existing under no pressure, which can vary depending on the degree of dryness of the measured tissue (Hacke *et al.* 2000; Torres-Ruiz *et al.* 2012; Blackman *et al.* 2016). Second, a pressure gradient of 5-8 kPa was applied to run water through the stem and pressurized flow was measured. This small pressure gradient prevented embolism removal from the samples while ensuring flow. Lastly, final background flow was measured, initial and final background flows were averaged, and flow was calculated as the difference between pressurized flow and average background flow. Native specific hydraulic conductivity (K) was estimated in stems as the flow divided by the pressure gradient used and standardized by xylem area and length. Stem segments where then removed from the apparatus and placed in a water bath for measurements of RWC (see above). The configuration of the apparatus was then changed to measure whole root system hydraulic conductance using the same gravimetric principle as explained in Sapes et al., (in review). Flow, including initial and final background flow, was measured as above and whole root native hydraulic conductance (k) was estimated as the flow divided by the pressure gradient used and standardized by xylem area at the root collar. We used the R code published in Sapes et al., (in review, see Methods S1 in Supporting Information) to calculate pressurized and background flows once flow stabilizes. Once flow rates were measured, root samples were placed in a water bath to be used in measurements of RWC.

Non-structural Carbohydrates. Non-structural carbohydrates were analyzed in all organs and at the whole plant level. A sample of each tissue was immediately collected upon arrival to the laboratory, microwaved for 180 seconds at 900 Watts in three cycles of 60 seconds to stop metabolic activity (i.e., consumption of NSC pools), and then placed in a drying oven at 70 ^{o}C. Samples were dried to a constant mass and then finely ground into a homogenous powder. We used 11 mg of needle tissue and 13 mg of stem or root tissue to analyze NSC concentrations following the enzymatic digestion method (McCleary *et al.* 1997). We calculated the total pool of NSCs, starch, soluble sugars, and glucose or fructose in each tissue by multiplying the corresponding concentration of each tissue by its dry weight. Concentrations (total NSC and each individual component) were later scaled up to whole-plant level as explained in the RWC section.

Statistical Analyses. We tested differences among treatments in all variables using Wilcoxon tests for independent samples followed by Tukey's HSD post-hoc tests. We chose Wilcoxon rank tests because variables did not met assumptions of normality across all groups. To test the effectiveness of the NSC-depletion, we compared NSC pools and each NSC component (i.e., starch, sucrose, and glucose and fructose together) among treatments for each organ and at the whole-plant level. We also tested potential artificial effects of covers on stomatal conductance. To test the effectiveness of the labeling process, we compared Δ^{13}C values in labeled seedlings to values in seedlings from the same treatment harvested prior to labeling. Note that dark seedlings were excluded because they were never labeled. These comparisons were done for each organ type to ensure that ^{13}C reached all organs of the labeled plant. Changes in Δ^{13}C in mycorrhizae were descriptive because, while we have values from non-labeled seedlings harvested after labeling, only a few samples were collected from labeled seedlings and from seedlings harvested prior to labeling. To assess potential carbon transfer to non-labeled seedlings, we compared Δ^{13}C values in non-labeled seedlings harvested after labeling to values in seedlings from the same treatment harvested prior to labeling. Note that light neighbor seedlings were excluded because they were all labeled. These comparisons were done for each organ type to assess the extent to which transferred ^{13}C was able to reach different organs. We tested differences in water relations among treatments. Variables tested included hydraulic

conductivity, water potential, osmotic potential, pressure potential, relative water content, and parameters extracted from pressure-volume curves (i.e., turgor loss point, osmotic potential at full turgor, modulus of elasticity, and capacitance). These comparisons were done for each organ available and at the whole-plant level when possible.

Additionally, we assessed whether osmotic potential and pressure potential change in response to carbon depletion. We used two linear regressions with NSC concentrations in needles as predictor and either leaf osmotic potential or leaf pressure potential as response variables. For these analyses, response variables were normalized using log transformations. We focused on needles because they are the most exposed organ to dry conditions and because they showed the most striking patterns in these variables. Finally, we assessed whether NSC storage influences turgor loss as water potentials decrease using linear regressions. Leaf pressure potential was the response variable and the interaction between leaf water potential and whole-plant NSC concentrations was given as a predictor.

RESULTS

NSC pools significantly differed among treatments (Fig. 2). As expected, light deprivation extremely reduced NSC pools in dark (D) seedlings ($p < 0.001$) because stored NSC were used to maintain metabolism. Light seedlings paired with dark (LD) plants also experienced NSC depletion and showed intermediate NSC pools relative to light (LL) and dark seedlings ($p < 0.001$, and $p = 0.009$, respectively). When broken down to each NSC compound, we found that starch was significantly lower in dark seedlings ($p < 0.001$) relative to LL seedlings and LD plants had marginally higher levels than dark seedlings ($p < 0.079$). However, starch levels did not differ between dark seedlings and their respective light pairs. Both sucrose and glucose + fructose were lower in dark seedlings than in light and LD seedlings (sucrose: light: $p < 0.001$, light paired with dark: $p = 0.040$; glucose and fructose: light: $p < 0.001$, light paired with dark: $p = 0.018$). However, no differences were detected between LL and LD seedlings. Patterns within each organ were consistent with those observed at the whole-plant level (Fig S1).These results indicate that carbon-depleted seedlings converted stored starch into free sugars to minimize their depletion. Dark seedlings depleted stored starch to a point were consumed free sugars could not be replaced anymore thus incurring carbon limitation.

Labeled seedlings showed high levels of $\Delta^{13}C$ relative to pre-labeling base-line values (Fig. 3) indicating that seedlings had successfully incorporated the labeling isotope. ^{13}C of labeled seedlings increased in all organs and followed a gradient with the highest values in needles and the lowest in roots ($p < 0.001$ in all seedling types and organs, Fig. 3a-c). High levels of ^{13}C were also present in the mycorrhizae associated to labeled seedlings and, to a lesser extent, in mycorrhizae associated to non-labeled LL plants paired with labeled seedlings (Fig. 3d). The presence of ^{13}C in fungi from non-labeled LL plants confirmed the existence of a mycorrhizal network between seedlings. However, ^{13}C did not travel from mycorrhizae associated to labeled LD seedlings to fungi from non-labeled D plants. In all cases, ^{13}C levels in non-labeled seedlings were similar to base-line values regardless of organ or treatment (Fig. 3e-g). Thus, ^{13}C traveled from needles to both sides of the fungal network in non-depleted conditions but stayed in the side of the labeled seedling in carbon-depleted conditions. In both cases, mycorrhizae did not transfer carbon to non-labeled plants.

Hydraulic conductivity did not significantly differed among treatments in any organ (Fig S2). However, osmotic potentials were significantly lower in light seedlings than in LD and D seedlings (Fig. 4a-c). These differences were observed in needles ($p < 0.001$ in all treatments), stems (dark: $p = 0.002$, light paired with dark: $p < 0.001$), and roots (dark: $p < 0.001$, light paired with dark: $p = 0.001$). High osmotic potentials were associated to low pressure potentials in needles (dark: $p < 0.001$, light paired with dark: $p < 0.001$, Fig. 4d) and stems (dark: $p = 0.012$, light paired with dark: $p < 0.001$, Fig. 4e). Pressure potentials in stems were low enough to bring stems to turgor loss (i.e., pressure potential lower than 0). As a result, we observed lower stem RWC in depleted seedlings than in non-depleted plants (dark: $p < 0.001$, light paired with dark: $p = 0.047$, Fig. 5).

The patterns observed through direct measurements of osmotic potential were corroborated by indirect estimations of osmotic potentials at turgor loss point from pressure-volume curves. However, because of the greater uncertainty inherent from this method, only dark seedlings showed lower osmotic potentials at turgor loss point than light seedlings ($p = 0.032$, Fig. 6a). Pressure-volume curves also detected significant differences in saturated water content in dark seedlings relative to their counterparts (light: $p < 0.007$,

light paired with dark: $p < 0.008$, Fig. 6b). No differences were detected in osmotic potential at full turgor, capacitance, and elasticity.

Low leaf osmotic potentials were associated to high leaf NSC concentrations ($p < 0.001$, $R^2_{Adj} = 0.69$, Table S1, Fig. 7a). This relationship was linear at low NSC and reached a plateau at values close to the average NSC from control pots. Increases in NSC beyond this value had a minimal effect on leaf osmotic potentials. The effects of NSC were mirrored in pressure potential ($p < 0.001$, $R^2_{Adj} = 0.40$, Table S1, Fig. 7b). In this case, turgor increased linearly until NSC values were close to the average NSC from control pots. Beyond that point, turgor plateaued around a maximum value of 1.5 MPa.

Stored NSC also influenced the relationship between leaf pressure potential and leaf water potential ($p < 0.001$, $R^2_{Adj} = 0.60$, Table S1). Plants with low NSC showed lower pressure at any given water potential and higher water potentials at turgor loss (Fig. 8, red vertical line and black horizontal line, respectively). Additionally, plants with low NSC lost more turgor than plants with high NSC given the same decline in water potential (Fig. 8, slopes).

DISCUSSION

Carbon gradients among plant hosts did not elicit transfer of carbon through fungal networks. We did not observe carbon transfer despite the differences in carbon pools among plant hosts. Light seedlings paired with dark plants became carbon-depleted relative to controls, indicating that they incurred a carbon cost imposed by dark seedlings. However, dark seedlings exhibited even lower carbon pools yet no increase in ^{13}C, indicating that they did not receive any carbon from their neighbors in the light. Instead, fungi retained the ^{13}C received from light seedlings paired to dark plants and the same occurred in light seedlings paired to light plants. These results suggest that plants cannot control carbon once it reaches the fungal network. Thus, in the case of carbon-based resources, we did not find supporting evidence for the plant-centric view. These results also suggest that fungi may have mechanisms to retain carbon in their system and prevent loss of carbon towards carbon-depleted hosts. Other studies have found that fungi convert plant carbon into fungi-specific sugars and alcohols (Nehls *et al.* 2007 and references therein). These studies suggest that fungi convert plant NSC to i) maximize plant-derived sugar concentrations gradients from hosts to fungi and facilitate passive carbon transfer and ii)

prevent transfer back to hosts by storing carbon in forms that are not compatible with plant sugar-transport proteins. Other studies also failed to find evidence of significant carbon transfer among plant hosts. For instance, Newman (1988) provides an extensive review of carbon-labeling studies showing that carbon is unlikely to move among plant hosts. In most instances, labeled carbon in fungi did not re-enter plant tissues. In the cases where carbon re-entered hosts, the amounts were likely too small to significantly increase host NSC storage (Simard & Perry 1997). Recent studies suggest that these small quantities of carbon may re-enter hosts as amino acids or stress-signaling compounds such as jasmonate (Teste *et al.* 2010; Song *et al.* 2015). While the indirect transfer of carbon via these compounds may be relevant on its own, it is unlikely to have a significant effect on plant carbon pools. Thus, carbon transfer among plant hosts likely occurs as a byproduct of other functions rather than as a mechanism to counter carbon depletion.

Covers served to simulate carbon-limiting conditions that occur during drought or shading. When we applied covers, fungal networks received less carbon from their darkened hosts. As a result, fungal networks draw carbon from seedlings in the light and depleted their NSC storage. We did not observe these effects in networks without covers. Thus, carbon limitation turned the symbiotic relationship between plants and fungal networks into a parasitic relationship. Shifts in plant-fungal relationships are common and often occur when environmental conditions change the cost-benefit of the relationship between both organisms. For instance, under nutrient limitation, mycorrhizae are known to provide extra nutrients for plants and enhance their growth despite the carbon costs imposed by the fungi (Thomson *et al.* 1994). In contrast, if limiting nutrients become abundant (e.g., fertilization), the carbon cost of mycorrhizae offsets its benefits and can reduce potential growth (Newton & Pigott 1991; Alberton *et al.* 2007; van der Heijden & Horton 2009). Some plants can reduce these negative effects by regulating how much carbon is transferred to mycorrhizae (Nehls *et al.* 2007 and references therein). Accordingly, we observed lower ^{13}C in fungi of carbon-depleted plants (Fig. 3d) relative to non-depleted plants. While these mechanisms may have existed in our case, they were not able to fully stop carbon transfer to fungi. This pattern could also be explained if fungi purposely reduced their live biomass using digestive enzymes (Ellström *et al.* 2015). This would be consistent with the differences in ^{13}C observed between carbon-depleted and non-

depleted treatments. First, fungal networks may have drawn more carbon from seedlings paired with darkened hosts during early stages of carbon depletion. As a result, these seedlings depleted their NSC pools. Then, as carbon deficit persisted, networks selectively killed fungi from darkened hosts that were not providing plant carbon to maximize their survival. This strategy may have reduced carbon demand in seedlings paired with darkened hosts due to lower live fungal biomass. Thus, it would explain why their fungal ^{13}C levels were lower than labeled light seedlings and why this ^{13}C did not travel to (dead) fungi from darkened hosts. Importantly, we would have not identified a shift towards a parasitic relationship if we had measured typical indicators of plant performance such as growth rather than plant carbon. Thus, we must assess host physiology to get a full view of the potential long-term effects of fungal networks on plants and, ultimately, forest vulnerability to drought. Given that seedlings are highly sensitive to carbon depletion, dry areas with forest boundaries that rely on seedling recruitment may be especially vulnerable to relationship shifts between plants and fungi.

Carbon depletion impairs host water relations and may predispose plants to early stress under drought. When stored NSC were consumed in hosts in the dark or drawn from seedlings by fungi, osmotic potentials increased indicating insufficient solutes (Fig. 7). Water potentials in these tissues likely became greater than the xylem water potential and tissues started losing water towards the vascular system. As a result, tissues of carbon-depleted plants had lower pressure potential relative to light controls and often reached turgor loss, which can cause loss of cell function and lead to death (Guadagno *et al.* 2017, Sapes & Sala, in prep). However, plants did not lose turgor due to loss of water transport (similar conductivity regardless of carbon status, Fig. S2). More likely, high osmotic potentials were unable to match xylem water potentials, and water simply traveled through the xylem and to the atmosphere without entering living cells. Other water-related traits were also affected by the increase in osmotic potentials associated to carbon depletion. Plants with high osmotic potentials also lost turgor at high water potentials (i.e., higher turgor loss point) and had lower pressure at full turgor (i.e., water potential close to 0) (Fig. 8) which makes them more vulnerable to drought (Bartlett *et al.* 2012). Interestingly, carbon-depleted plants also had higher saturated water content which has been related to capacitance (Ogburn & Edwards 2012). It is possible that cells consumed many starch

granules and water filled the volume previously occupied by starch. This would increase the saturated water content of the tissues by increasing the amount of water relative to their dry biomass. However, we lack direct evidence for this hypothesis and it should be further tested.

Plants may experience resource-allocation tradeoffs as a result of carbon depletion. Our results suggest that seedlings use most of their stored carbon for water retention (Fig. 7). Plants reduced their water retention and turgor when NSC storage decreased below the average values observed in controls. Only plants with NSC pools above average the control values seemed to have enough carbon to spend in other functions without risk of impairing their water relations. Plants use stored NSC to provide a source of energy for metabolic needs, produce defenses, grow, and reproduce, in addition to retain water in living tissues. Given that stored NSC are used for all these functions, seedlings may have to continuously choose which functions to prioritize, thus facing significant resource-allocation tradeoffs. These tradeoffs may easily compromise seedlings if they become carbon-limited by fungal networks or drought stress, thus making them more vulnerable than adult trees. However, these detrimental effects may have a lesser impact in plant-fungal networks with carbon-rich trees that can cover the carbon deficit of neighboring seedlings (Bingham & Simard 2012; Beiler *et al.* 2015). Yet, we lack studies on the effects of plant and network size on host water relations.

Our results add to existing evidence showing how critical stored NSC are to maintain water relations (Anderegg & Callaway 2012; Sevanto *et al.* 2014; Secchi & Zwieniecki 2016) and to elongate survival under drought (O'Brien *et al.* 2014). The patterns found in this experiment are also consistent with hypotheses from a recent framework of drought-induced mortality that integrates carbon depletion, water deficit, and biotic agents (Oliva *et al.* 2014). This framework suggests that biotrophic parasites that attack trees before drought should deplete plant NSC pools and impair water relations such that, once drought starts, plants die at faster rates. While we did not explicitly assess the effects of fungal-driven carbon depletion under drought, we observed higher osmotic potential and turgor loss point, and lower turgor and relative water content in carbon-depleted seedlings. Additionally, we observed stronger declines of turgor per unit of water potential in depleted seedlings. Finally, we did not observe loss of water transport.

However, depleted plants may have lost conductivity under drought at faster rates given their greater loss of turgor per unit water potential. These results strongly suggest that depleted plants would have experienced early mortality under drought as suggested by Oliva *et al.* (2014).

Overall, we found that relationships between plant and fungi are highly responsive to disturbances that affect carbon balance. Studying the effects of fungal networks on host physiology rather than just growth or survival may help us better understand the responses of plant-fungi relationships to stress. In the case of drought, changes in carbon balance between plant hosts and fungi due to drought may influence plant water relations and ultimately forest vulnerability to drought. Future research should develop similar experiments that explicitly test how hosts respond to carbon depletion in combination with water deficit and assess the role of host and network size on host physiology.

ACKNOWLEDGEMENTS

This work was supported by a National Science Foundation grant to AS (BCS 1461576). GS received funding from the NSF Experimental Program to Stimulate Competitive Research (EPSCoR) Track-1 EPS-1101342 (INSTEP 3). PD received funding from NSF EPSCoR RII Track 1 award number IIA-1443108. The authors thank Laura Thornton and Maria Pilar de Moreta for their help collecting data, and Mauri Valett and Lila Fishman for letting us use their facilities.

REFERENCES

Adams, H.D., Zeppel, M.J.B., Anderegg, W.R.L., Hartmann, H., Landhäusser, S.M., Tissue, D.T., *et al.* (2017). A multi-species synthesis of physiological mechanisms in drought-induced tree mortality. *Nat. Ecol. Evol.*, 1, 1285–1291.

Alberton, O., Kuyper, T.W. & Gorissen, A. (2007). Competition for nitrogen between Pinus sylvestris and ectomycorrhizal fungi generates potential for negative feedback under elevated CO2. *Plant Soil*, 296, 159–172.

Anderegg, W.R.L. & Callaway, E.S. (2012). Infestation and hydraulic consequences of induced carbon starvation. *Plant Physiol.*, 159, 1866–74.

Barrs, H.D. & Weatherley, P.E. (1962). A Re-Examination of the Relative Turgidity Technique for Estimating Water Deficits in Leaves. *Aust. J. Biol. Sci.*, 15, 413–428.

Bartlett, M.K., Scoffoni, C. & Sack, L. (2012). The determinants of leaf turgor loss point and prediction of drought tolerance of species and biomes: a global meta-analysis. *Ecol. Lett.*, 15, 393–405.

Begg, J.E. & Turner, N.C. (1970). Water Potential Gradients in Field Tobacco. *PLANT*

Physiol.
Beiler, K.J., Durall, D.M., Simard, S.W., Maxwell, S.A. & Kretzer, A.M. (2010). Architecture of the wood-wide web: Rhizopogon spp. genets link multiple Douglas-fir cohorts. *New Phytol.*, 185, 543–553.
Beiler, K.J., Simard, S.W. & Durall, D.M. (2015). Topology of tree–mycorrhizal fungus interaction networks in xeric and mesic Douglas-fir forests. *J. Ecol.*, 103, 616–628.
Bingham, M. a. & Simard, S. (2012). Ectomycorrhizal Networks of Pseudotsuga menziesii var. glauca Trees Facilitate Establishment of Conspecific Seedlings Under Drought. *Ecosystems*, 15, 188–199.
Blackman, C.J., Pfautsch, S., Choat, B., Delzon, S., Gleason, S.M. & Duursma, R.A. (2016). Toward an index of desiccation time to tree mortality under drought. *Plant Cell Environ.*, 39, 2342–2345.
Ellström, M., Shah, F., Johansson, T., Ahrén, D., Persson, P. & Tunlid, A. (2015). The carbon starvation response of the ectomycorrhizal fungus Paxillus involutus. *FEMS Microbiol. Ecol.*, 91, 1–11.
Espino, S. & Schenk, H.J. (2011). Mind the bubbles: Achieving stable measurements of maximum hydraulic conductivity through woody plant samples. *J. Exp. Bot.*, 62, 1119–1132.
Garcia-Forner, N., Sala, A., Biel, C., Savé, R. & Martínez-Vilalta, J. (2016). Individual traits as determinants of time to death under extreme drought in Pinus sylvestris L. *Tree Physiol.*, 36, 1196–1209.
Guadagno, C.R., Ewers, B.E., Speckman, H.N., Aston, T.L., Huhn, B.J., DeVore, S.B., *et al.* (2017). Dead or alive? Using membrane failure and chlorophyll fluorescence to predict mortality from drought. *Plant Physiol.*, 175, 223–234.
Hacke, U.G., Sperry, J.S., Ewers, B.E., Ellsworth, D.S., Schäfer, K.V.R. & Oren, R. (2000). Influence of soil porosity on water use in Pinus taeda. *Oecologia*, 124, 495–505.
He, X., Xu, M., Qiu, G.Y. & Zhou, J. (2009). Use of15N stable isotope to quantify nitrogen transfer between mycorrhizal plants. *J. Plant Ecol.*, 2, 107–118.
van der Heijden, M.G. & Horton, T.R. (2009). Socialism in Soil? the Importance of Mycorrhizal Fungal Networks for Facilitation in Natural Ecosystems. *J. Ecol.*, 97, 1139–1150.
Kaufmann, M. (1968). Evaluation of the Pressure Chamber Technique for Estimating Plant Water Potential of Forest Tree Species. *For. Sci.*, 14, 369–374.
Kiers, E.T., Duhamel, M., Beesetty, Y., Mensah, J.A., Franken, O., Verbruggen, E., *et al.* (2011). Reciprocal Rewards Stabilize Cooperation in the Mycorrhizal Symbiosis. *Science (80-.).*, 333, 880–882.
Lapeyrie, F. & Chilvers, G.A. (1985). An Endomycorrhiza-Ectomycorrhiza Succession Associated With Enhanced Growth of Eucalyptus Dumosa Seedlings Planted in a Calcareous Soil. *New Phytol.*, 100, 93–104.
Lloret, F., Sapes, G., Rosas, T., Galiano, L., Saura-Mas, S., Sala, A., *et al.* (2018). Non-structural carbohydrate dynamics associated with drought-induced die-off in woody species of a shrubland community. *Ann. Bot.*, 00, 1–14.
Martinez-Vilalta, J., Sala, A., Asensio, D., Galiano, L., Hoch, G., Palacio, S., *et al.* (2016). Dynamics of non-structural carbohydrates in terrestrial plants: A global synthesis. *Ecol. Monogr.*, 86, 495–516.
McCleary, B. V., Gibson, T.S. & Mugford, D.C. (1997). Measurement of Total Starch in Cereal Products by Amyloglucosidase-α-Amylase Method: Collaborative Study. *J.*

AOAC Int., 80, 571–579.
McDowell, N., Pockman, W.T., Allen, C.D., Breshears, D.D., Cobb, N., Kolb, T., *et al.* (2008). Mechanisms of plant survival and mortality during drought: why do some plants survive while others succumb to drought? *New Phytol.*, 178, 719–39.
McDowell, N.G., Beerling, D.J., Breshears, D.D., Fisher, R.A., Raffa, K.F. & Stitt, M. (2011). The interdependence of mechanisms underlying climate-driven vegetation mortality. *Trends Ecol. Evol.*, 26, 523–532.
Nardini, A., Salleo, S., Tyree, M.T. & Vertovec, M. (2000). Influence of the ectomycorrhizas formed by Tuber melanosporum Vitt . on hydraulic conductance and water relations of Quercus ilex L . seedlings. *Ann. For. Sci.*, 57, 305–312.
Nehls, U., Grunze, N., Willmann, M., Reich, M. & Küster, H. (2007). Sugar for my honey: Carbohydrate partitioning in ectomycorrhizal symbiosis. *Phytochemistry*, 68, 82–91.
Newman, E.I. (1988). Mycorrhizal Links Between Plants: Their Functioning and Ecological Significance. *Adv. Ecol. Res.*, 18, 243–270.
Newton, A. & Pigott, C. (1991). Mineral nutrition and mycorrhizal infection of seedling oak and birch. *New Phytol.*, 117, 45–52.
O'Brien, M.J., Leuzinger, S., Philipson, C.D., Tay, J. & Hector, A. (2014). Drought survival of tropical tree seedlings enhanced by non-structural carbohydrate levels. *Nat. Clim. Chang.*, 4, 1–5.
Ogburn, R.M. & Edwards, E.J. (2012). Quantifying succulence : a rapid , physiologically meaningful metric of plant water storage. *Plant Cell Environ.*, 35, 1533–1542.
Oliva, J., Stenlid, J. & Martinez-Vilalta, J. (2014). The effect of fungal pathogens on the water and carbon economy of trees: implications for drought-induced mortality. *New Phytol.*, 203, 1028–1035.
Poorter, L. & Kitajima, K. (2007). Carbohydrate Storage and Light Requirements of Tropical Moist and Dry Forest Tree Species. *Ecology*, 88, 1000–1011.
Sala, A. & Mencuccini, M. (2014). Plump trees win under drought. *Nat. Clim. Chang.*, 4, 666–667.
Secchi, F. & Zwieniecki, M.A. (2016). Accumulation of sugars in the xylem apoplast observed under water stress conditions is controlled by xylem pH. *Plant Cell Environ.*, 39, 2350–2360.
Sevanto, S., McDowell, N.G., Dickman, L.T., Pangle, R. & Pockman, W.T. (2014). How do trees die? A test of the hydraulic failure and carbon starvation hypotheses. *Plant. Cell Environ.*, 37, 153–61.
Simard, S.W. & Perry, D. a. (1997). Net transfer of carbon between ectomycorrhizal tree species in the field. *Nature*, 388, 579.
Simeone, C., Maneta, M.P., Holden, Z.A., Sapes, G., Sala, A. & Dobrowski, S.Z. (2018). *Coupled ecohydrology and plant hydraulics modeling predicts ponderosa pine seedling mortality and lower treeline in the US Northern Rocky Mountains*. *New Phytol.*
Song, Y.Y., Simard, S.W., Carroll, A., Mohn, W.W. & Zeng, R. Sen. (2015). Defoliation of interior Douglas-fir elicits carbon transfer and stress signalling to ponderosa pine neighbors through ectomycorrhizal networks. *Sci. Rep.*, 5, 8495.
Sperry, J.S., Donnelly, J.R. & Tyree, M.T. (1988). A method for measuring hydraulic conductivity and embolism in xylem. *Plant. Cell Environ.*, 11, 35–40.
Sperry, J.S. & Love, D.M. (2015). What plant hydraulics can tell us about responses to climate-change droughts. *New Phytol.*, 207, 14–27.

Teste, F.P., Simard, S.W., Durall, D.M., Guy, R.D. & Berch, S.M. (2010). Net carbon transfer between Pseudotsuga menziesii var. Glauca seedlings in the field is influenced by soil disturbance. *J. Ecol.*, 98, 429–439.

Thomson, B.D., Grove, T.S., Malajczuk, N. & Hardy, G. (1994). The Effectiveness of Ectomycorrhizal Fungi in Increasing the Growth of Eucalyptus-Globulus Labill in Relation To Root Colonization and Hyphal Development in Soil. *New Phytol.*, 126, 517–524.

Torres-Ruiz, J.M., Jansen, S., Choat, B., McElrone, A.J., Cochard, H., Brodribb, T.J., *et al.* (2015). Direct X-Ray Microtomography Observation Confirms the Induction of Embolism upon Xylem Cutting under Tension. *Plant Physiol.*, 167, 40–43.

Torres-Ruiz, J.M., Sperry, J.S. & Fernández, J.E. (2012). Improving xylem hydraulic conductivity measurements by correcting the error caused by passive water uptake. *Physiol. Plant.*, 146, 129–135.

Trifilò, P., Barbera, P.M., Raimondo, F., Nardini, A., Gullo, M.A. Lo & Meinzer, F. (2014). Coping with drought-induced xylem cavitation: Coordination of embolism repair and ionic effects in three Mediterranean evergreens. *Tree Physiol.*, 34, 109–122.

Warren, J.M., Brooks, J.R., Meinzer, F.C. & Eberhart, J.L. (2008). Hydraulic redistribution of water from Pinus ponderosa trees to seedlings: evidence for an ectomycorrhizal pathway. *New Phytol.*, 178, 382–394.

Wu, B., Nara, K. & Hogetsu, T. (2001). Can 14C-labeled photosynthetic products move be Pinus densiflora seedlings linked by ectomycorrhiza mycelia? *New Phytol.*, 149, 137–146.

FIGURES

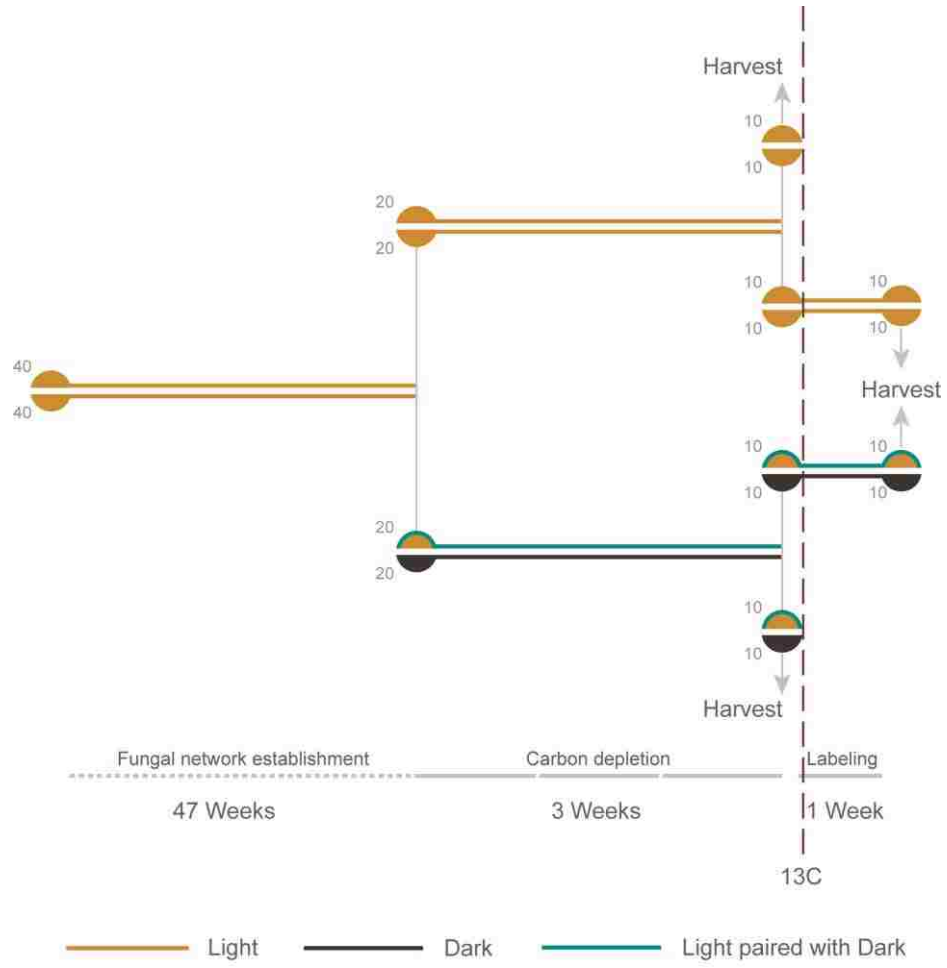

Fig. 1. Experimental design. Circles represent pots divided with barriers and a seedling on each side. Colors represent plants exposed to natural light (golden), plants with light-blocking covers (black), and plants exposed to natural light paired with plants with covers (teal). Numbers in the side of each circle indicate the sample size of the treatment represented in that side of the circle at a given point on time. Dashed red line indicates the time of ^{13}C labeling. Arrows indicate harvesting events.

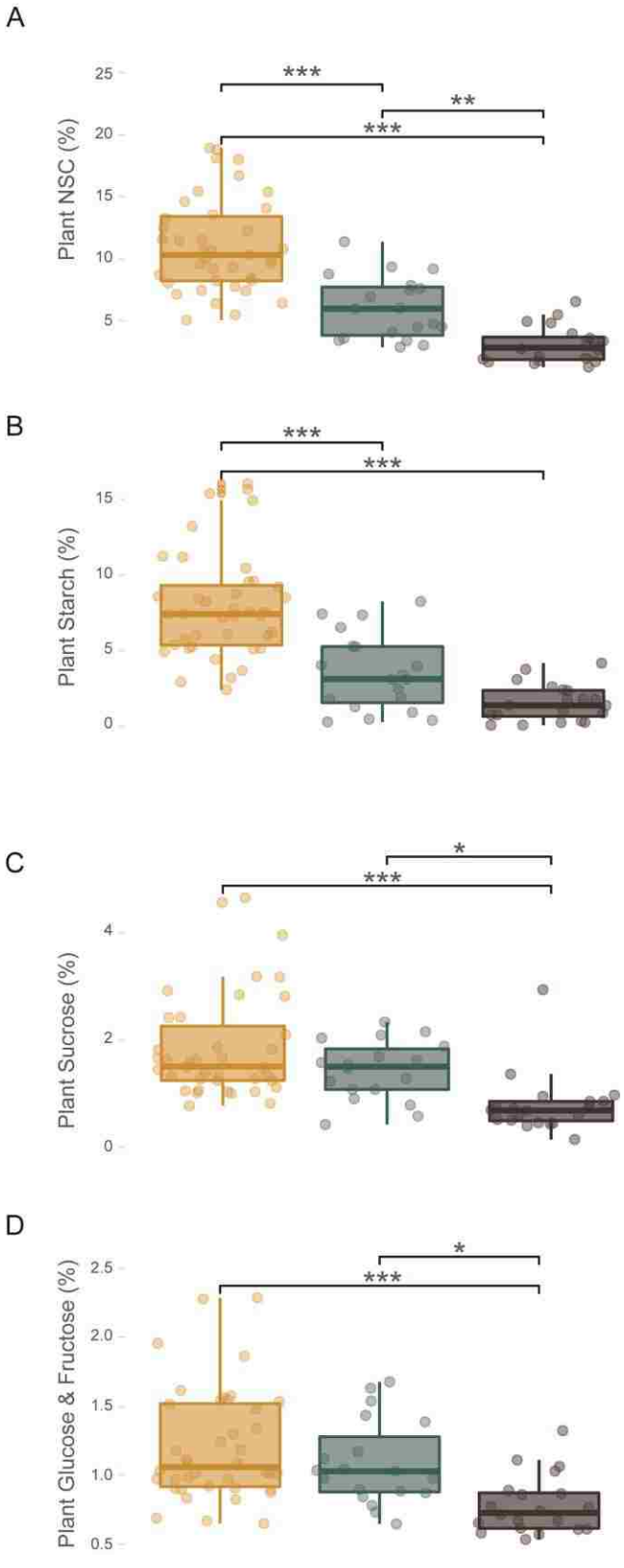
A
Plant NSC (%)
25
20
15
10
5
***
**
***
B
Plant Starch (%)
15
10
5
0
***
***
C
Plant Sucrose (%)
4
2
0
*
***
D
Plant Glucose & Fructose (%)
2.5
2.0
1.5
1.0
0.5
*
***

Fig. 2. All seedlings in carbon-depleted pots showed low carbohydrate levels in all NSC components. Panels correspond to whole-plant A) NSC storage, B) Starch, C) Sucrose, and D) Glucose & Fructose concentrations. Colors represent plants exposed to natural light (golden), plants with light-blocking covers (black), and plants exposed to natural light paired with plants with covers (teal). Lines within boxes represent the median and top and bottom hinges represent 25th and 75th percentiles. Whiskers indicate highest and lowest value no further than 1.5 times the inter-quartile range represented by the hinges. Dots represent the distribution of the data. Asterisks indicate the degree of significance between groups (* = 0.05, ** = 0.01, *** = < 0.001).

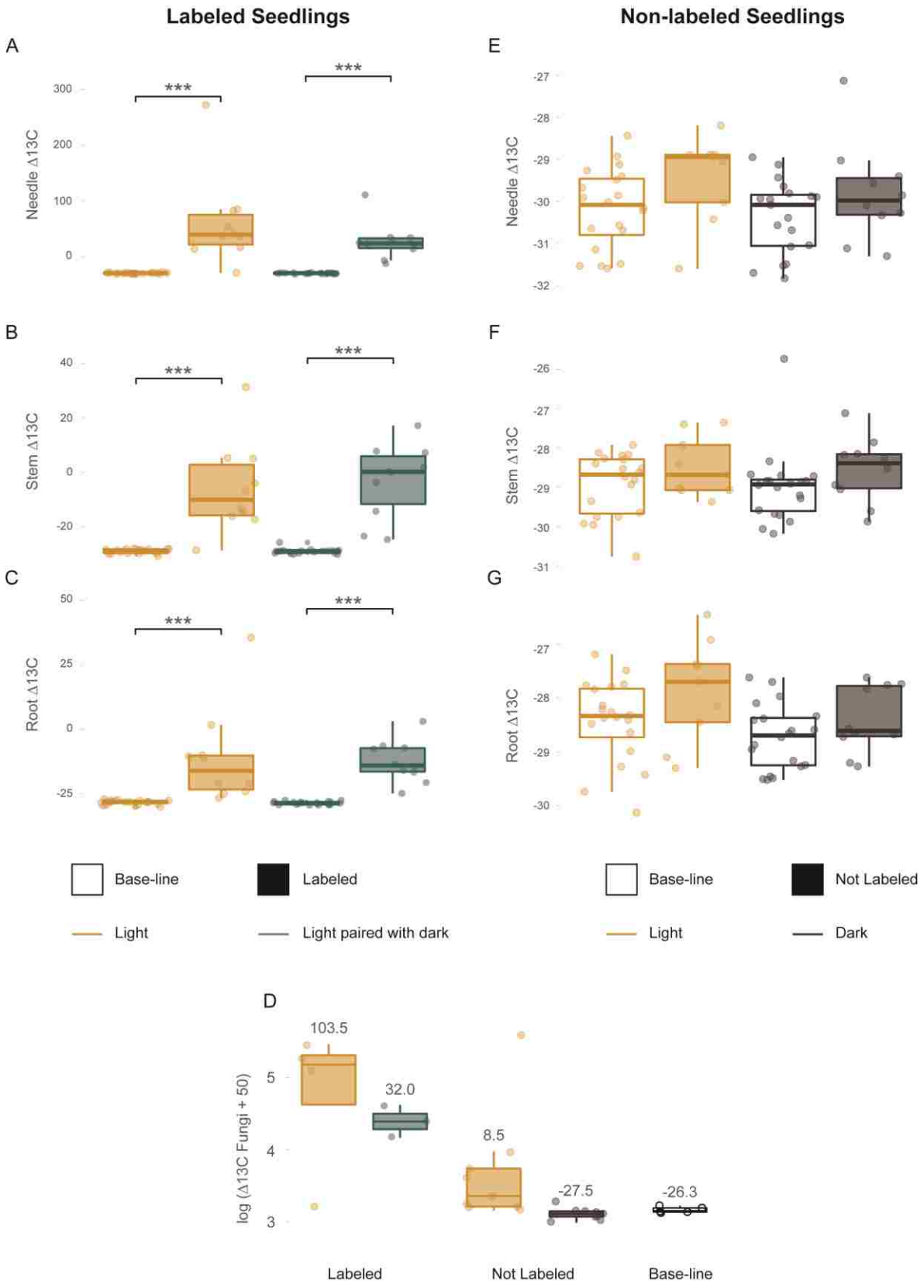
Labeled Seedlings
Non-labeled Seedlings
A
B
C
D
E
F
G
Needle Δ13C
Stem Δ13C
Root Δ13C
***
Base-line
Labeled
Light
Light paired with dark
Not Labeled
Dark
log (Δ13C Fungi + 50)
103.5
32.0
8.5
-27.5
-26.3
Labeled
Not Labeled
Base-line

Fig. 3. ^{13}C isotope reached all organs in labeled plants and the fungal network but was not transferred to carbon-depleted hosts. Panels on the left correspond to $^{13}C/^{12}C$ ratios ($\Delta^{13}C$) in A) needles, B) stems, and C) roots, from labeled plants. Panel D corresponds to the fungal network. Numbers on boxplots in panel D indicate average values of $\Delta^{13}C$ for that group. Panels on the right correspond to $\Delta^{13}C$ in A) needles, B) stems, and C) roots, from non-labeled plants. Open boxes indicate values before labeling (i.e., base-line) and solid boxes indicate values after labeling. Colors represent plants exposed to natural light (golden), plants with light-blocking covers (black), and plants exposed to natural light paired with plants with covers (teal). Lines within boxes represent the median and top and bottom hinges represent 25th and 75th percentiles. Whiskers indicate highest and lowest value no further than 1.5 times the inter-quartile range represented by the hinges. Dots represent the distribution of the data. Asterisks indicate the degree of significance between groups (* = 0.05, ** = 0.01, *** = < 0.001).

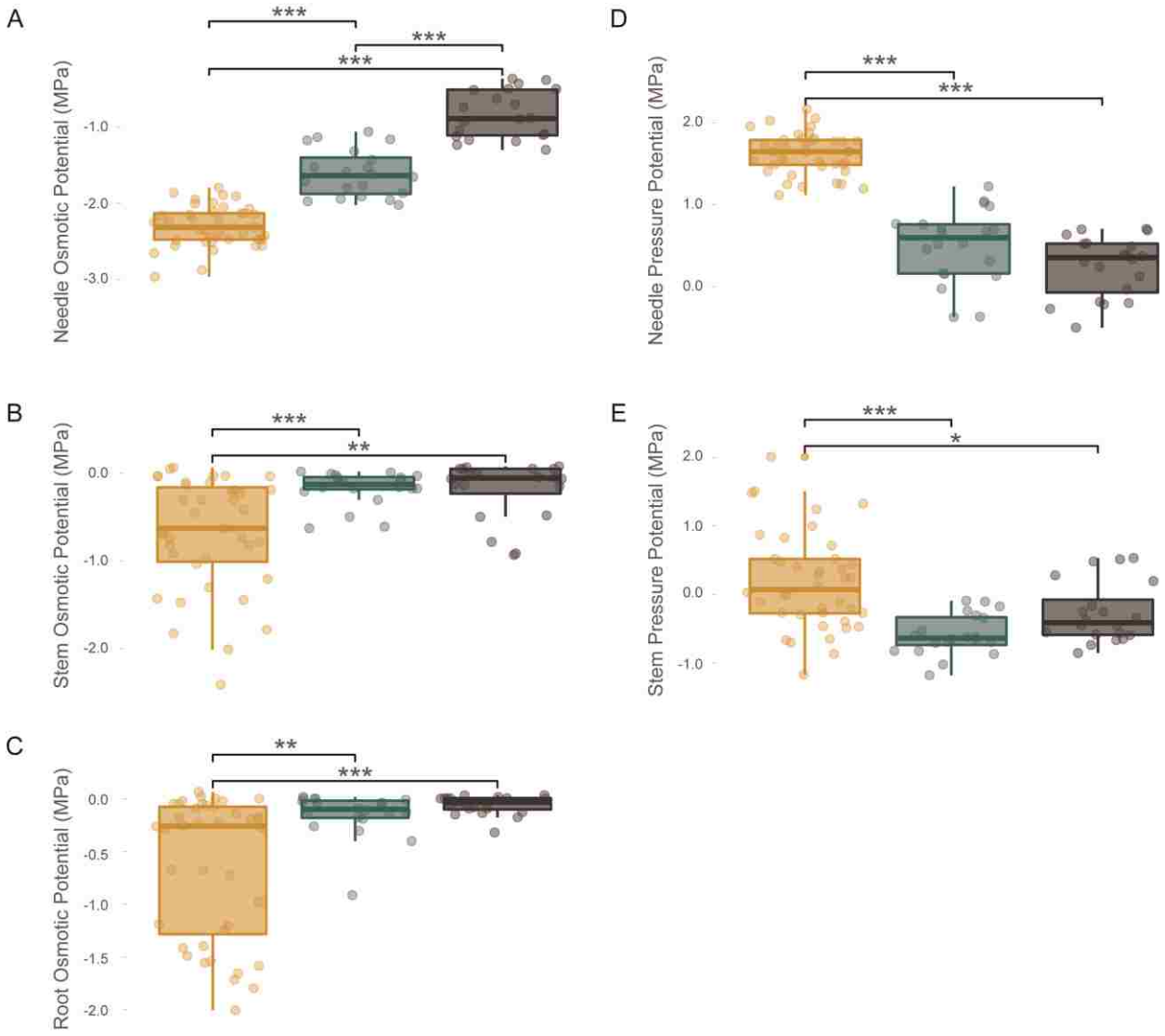

Fig. 4. All tissues in carbon-depleted treatments lost water retention and turgor. Panels on the left correspond to osmotic potentials of A) needles, B) stems, and C) roots. Panels on the right correspond to pressure potentials of D) needles and E) stems. Colors represent plants exposed to natural light (golden), plants with light-blocking covers (black), and plants exposed to natural light paired with plants with covers (teal). Lines within boxes represent the median and top and bottom hinges represent 25th and 75th percentiles. Whiskers indicate highest and lowest value no further than 1.5 times the inter-quartile range represented by the hinges. Dots represent the distribution of the data. Asterisks indicate the degree of significance between groups (* = 0.05, ** = 0.01, *** = < 0.001).

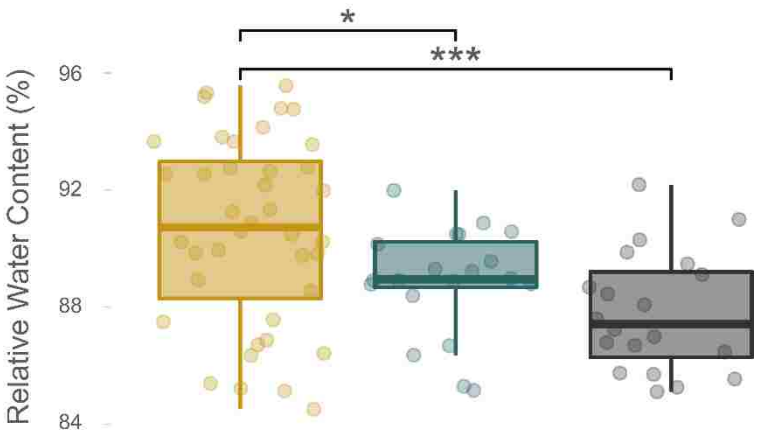

Fig. 5. Carbon-depleted plants lose water content under well-watered conditions. Colors represent plants exposed to natural light (golden), plants with light-blocking covers (black), and plants exposed to natural light paired with plants with covers (teal). Lines within boxes represent the median and top and bottom hinges represent 25th and 75th percentiles. Whiskers indicate highest and lowest value no further than 1.5 times the inter-quartile range represented by the hinges. Dots represent the distribution of the data. Asterisks indicate the degree of significance between groups (* = 0.05, ** = 0.01, *** = < 0.001).

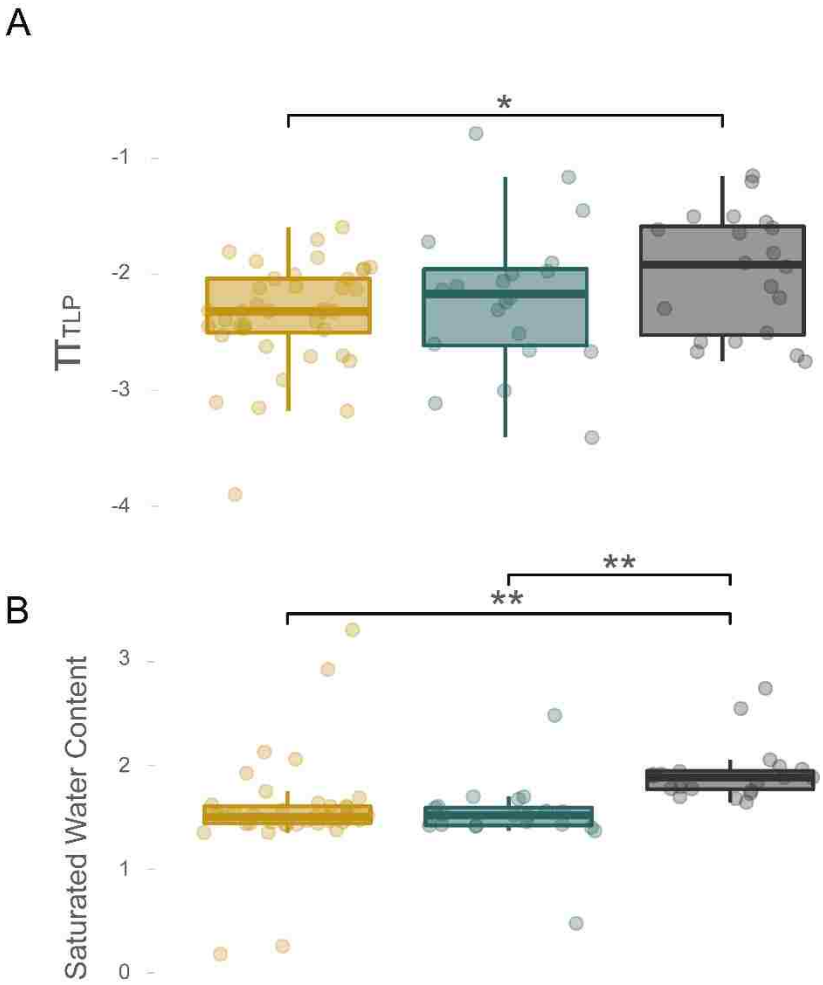

Fig. 6. Water potential at turgor loss point and capacitance increase in carbon depleted plants. Panels correspond to A) turgor loss point and B) saturated water content. Colors represent plants exposed to natural light (golden), plants with light-blocking covers (black), and plants exposed to natural light paired with plants with covers (teal). Lines within boxes represent the median and top and bottom hinges represent 25th and 75th percentiles. Whiskers indicate highest and lowest value no further than 1.5 times the inter-quartile range represented by the hinges. Dots represent the distribution of the data. Asterisks indicate the degree of significance between groups (* = 0.05, ** = 0.01, *** = < 0.001).

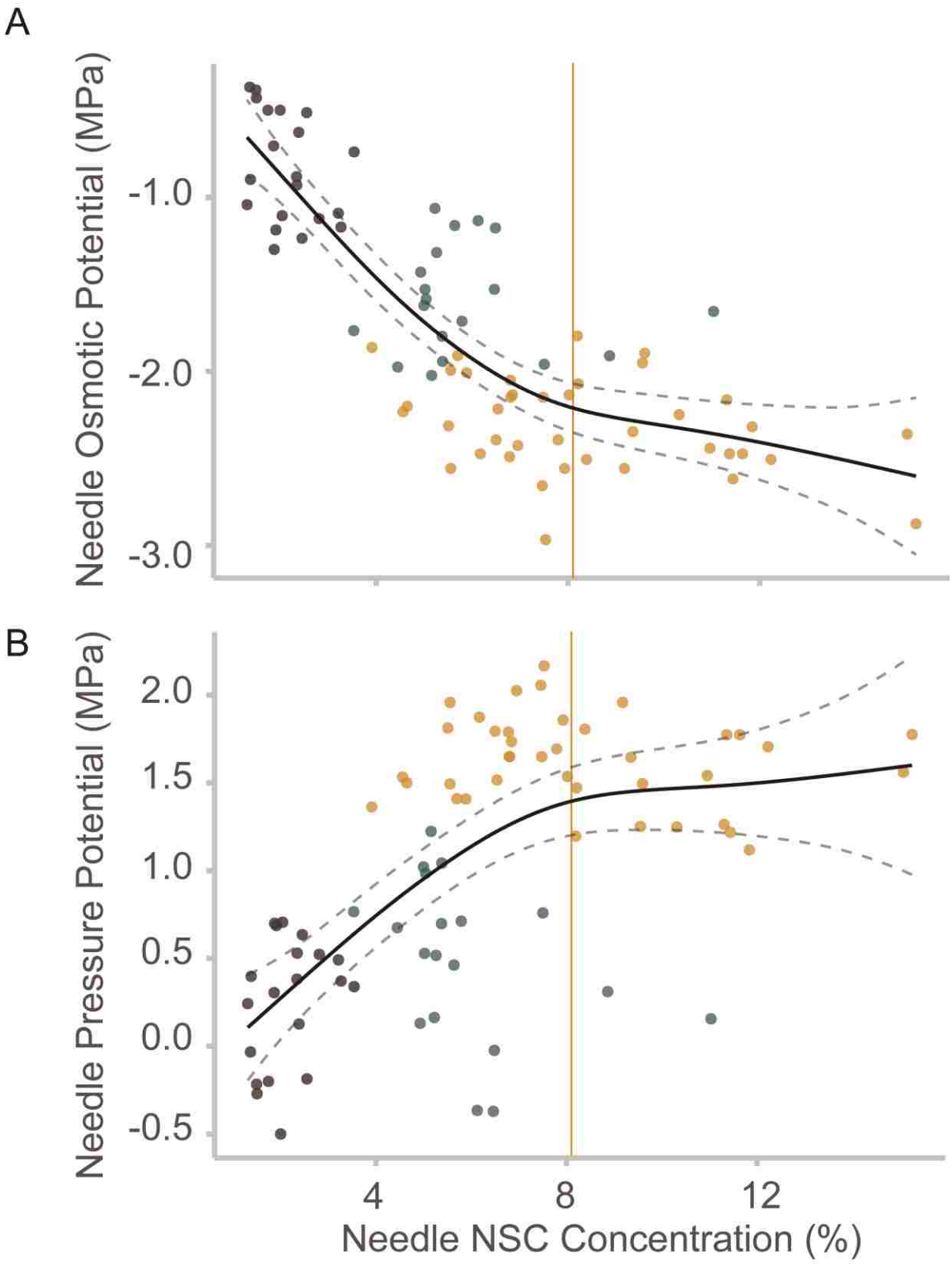
A
Needle Osmotic Potential (MPa)
-1.0
-2.0
-3.0
B
Needle Pressure Potential (MPa)
2.0
1.5
1.0
0.5
0.0
-0.5
4
8
12
Needle NSC Concentration (%)

Fig. 7. Water relations are impaired when NSC drop below control values. Panels correspond to A) osmotic potential and B) turgor pressure. All treatments are merged for this analysis. Vertical golden lines indicate average leaf NSC content in control pots (i.e., light plants). A loess function was fit to the data to best represent the relationship between variables. Dashed lines indicate 95% confidence interval of the regression lines.

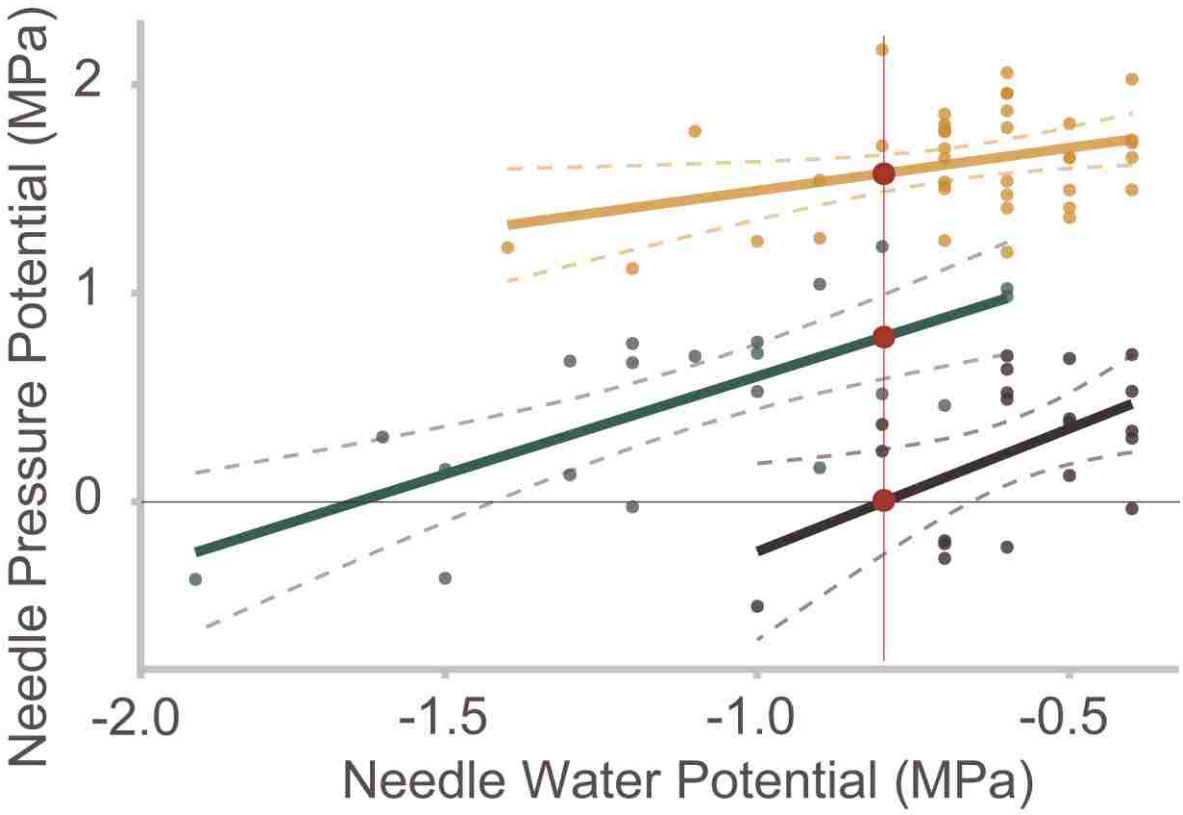

Fig. 8. Carbon depletion is associated to turgor loss at high water potentials. Colors represent plants exposed to natural light (golden), plants with light-blocking covers (black), and plants exposed to natural light paired with plants with covers (teal). Vertical red line and points indicate differences in turgor at a given water potential. Horizontal line indicates turgor loss point. Dashed lines indicate 95% confidence interval of the regression lines.

SUPPORTING INFORMATION

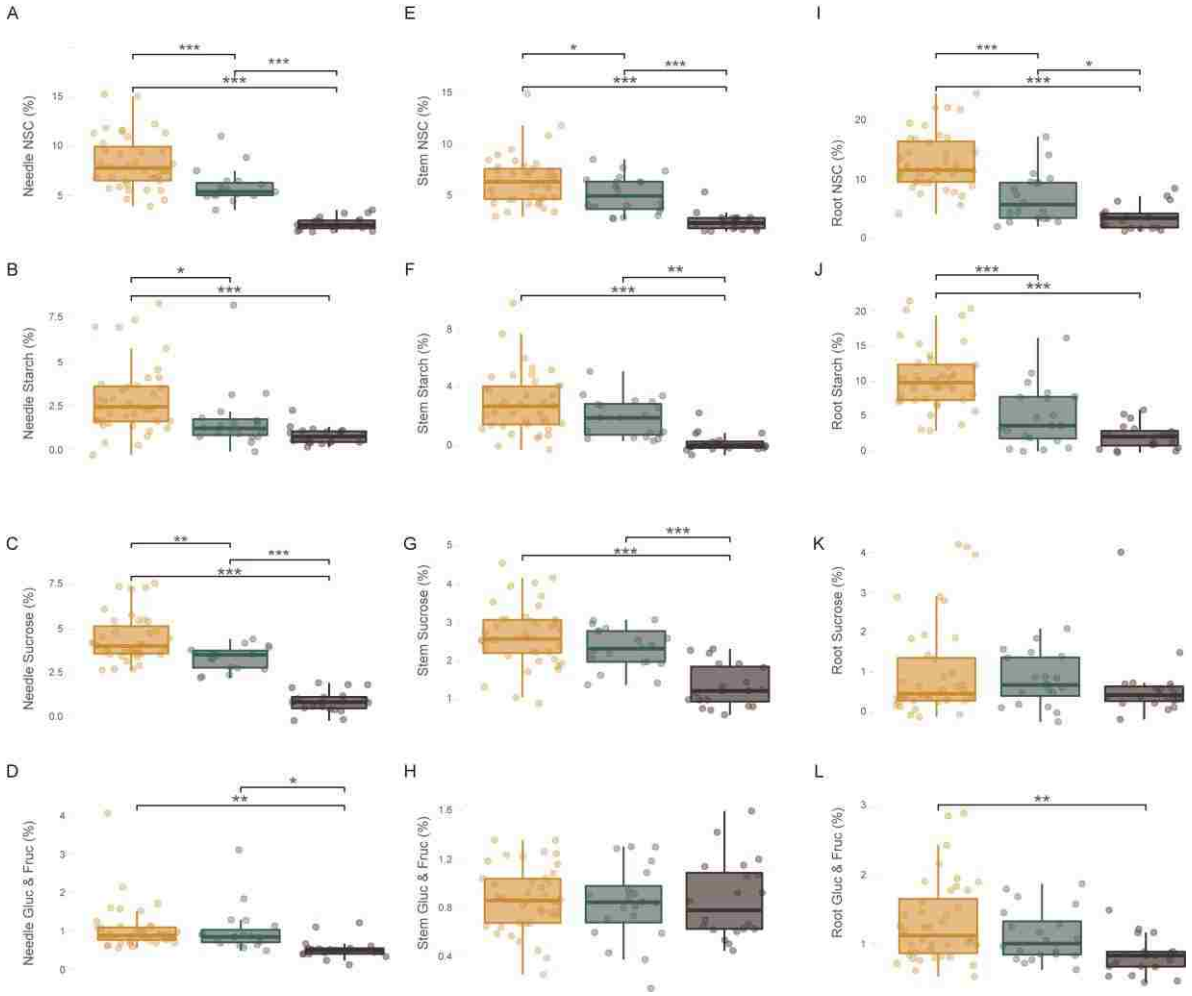

Fig. S1. All seedlings in carbon-depleted pots showed low carbohydrate levels in all NSC components and organs. Panels correspond to NSC storage, Starch, Sucrose, and Glucose & Fructose concentrations in needles (left), stems (middle), and roots (right). Colors represent plants exposed to natural light (golden), plants with light-blocking covers (black), and plants exposed to natural light paired with plants with covers (teal). Lines within boxes represent the median and top and bottom hinges represent 25th and 75th percentiles. Whiskers indicate highest and lowest value no further than 1.5 times the inter-quartile range represented by the hinges. Dots represent the distribution of the data. Asterisks indicate the degree of significance between groups (* = 0.05, ** = 0.01, *** = < 0.001).

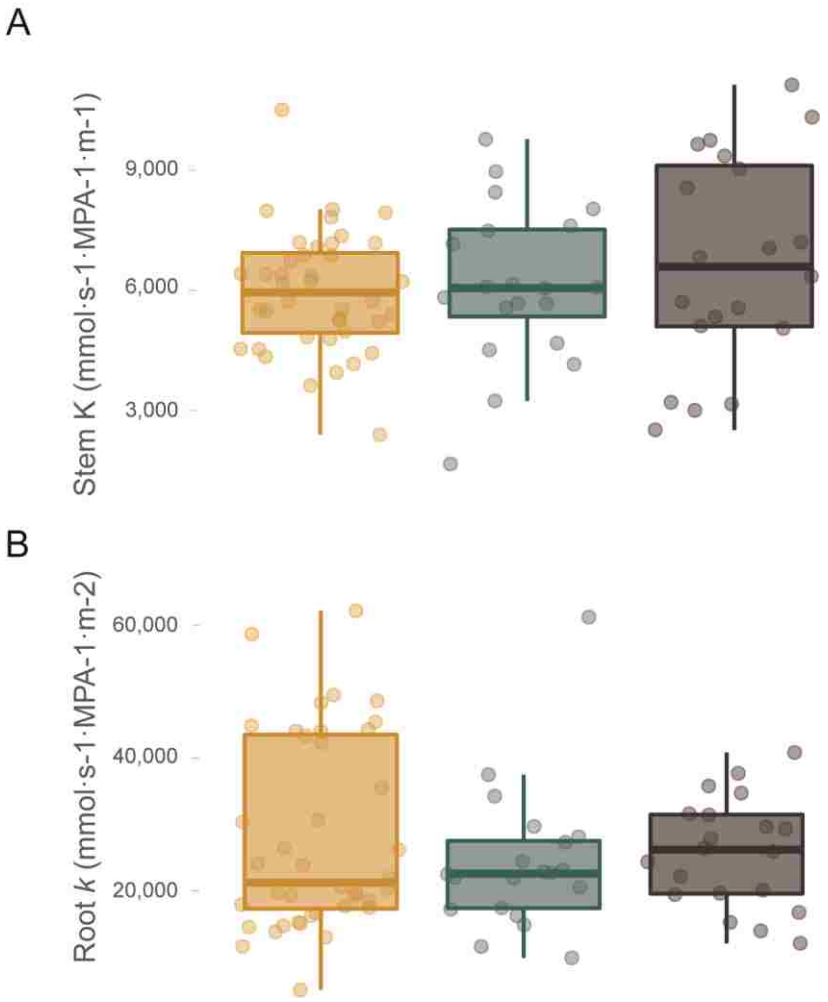

Fig. S2. Depletion of NSC did not affect water transport in plants. Panels correspond to A) stem hydraulic conductivity and B) root hydraulic conductance. Colors represent plants exposed to natural light (golden), plants with light-blocking covers (black), and plants exposed to natural light paired with plants with covers (teal). Lines within boxes represent the median and top and bottom hinges represent 25th and 75th percentiles. Whiskers indicate highest and lowest value no further than 1.5 times the inter-quartile range represented by the hinges. Dots represent the distribution of the data. No significant differences were observed among groups.

Table S1. Linear models showing the influence of non-structural carbohydrates on pressure and osmotic potentials.

Model and Factors	Estimate	95% C.I. Estimates		*p-value*	d.f. (res.)	Adjusted R square
		2.5%	97.5%			
Leaf Osmotic Potential = log(Leaf NSC Concentrations)				**<0.001**	75	0.69
Intercept	-0.28307	-0.524066	-0.0420816	**0.022**	-	-
log(Leaf NSC Concentrations)	-0.89378	-1.030518	-0.7570468	**<0.001**	-	-
Leaf Pressure Potential = Leaf NSC Concentrations				**<0.001**	75	0.40
Intercept	-0.2105	-0.5626360	0.1416684	0.238	-	-
log(Leaf NSC Concentrations)	0.7326	0.5328177	0.9324307	**<0.001**	-	-
Leaf Pressure Potential = Leaf Water Potential x Plant NSC Concentrations				**<0.001**	71	0.60
Intercept	0.15526	-0.4363549	0.7468661	0.602	-	-
Leaf Water Potential	-0.02210	-0.7650880	0.7208887	0.953	-	-
Plant NSC Concentrations	0.20671	0.1319697	0.2814489	**<0.001**	-	-
Leaf Water Potential x Plant NSC Concentrations	0.13082	0.0382965	0.2233412	**0.006**	-	-